MATHEMATICAL MODELS OF AIRBORNE INFECTION CONTROL IN AN OUTPATIENT DEPARTMENT WITH VENTILATION SYSTEM

WASU TIMPITAK

A THESIS SUBMITTED IN PARTIAL FULFILLMENT OF THE REQUIREMENT
FOR THE DEGREE OF DOCTOR OF PHILOSOPHY IN APPLIED MATHEMATICS
DEPARTMENT OF MATHEMATICS SCHOOL OF SCIENCE
KING MONGKUT'S INSTITUTE OF TECHNOLOGY LADKRABANG
2023

KMITL-2023-SC-D-001-013

Thesis Title	Mathematical Models of Airborne Infection Control in an Outpatient Department with Ventilation System
Student Name	Mr.Wasu Timpitak
Student ID	63605004
Degree	Doctor of Philosophy (Applied Mathematics)
Department	Mathematics
Year	2023
Thesis Advisor	Assoc.Prof.Dr.Nopparat Pochai

Abstract

The airborne infection spreads through the air, especially in indoor spaces. Indoor spaces present a significant infection risk, although this may be reduced by employing all methodologies to prevent infection via aerosols. TB, COVID-19, MERS, and SARS are dangerous infectious diseases of diseases that spread from person to person through air or aerosol in a variety of ways, including coughing, spitting, sneezing, speaking, or through wounds. Every day, people of all ages come to obtain a wide range of services, which puts them at risk of airborne transmission. Air quality control in outpatient departments is thus critical. Good air quality reduces the risk of infection among service users. The number of users, the ventilation system, and the size of the outpatient department all also to be factors that contribute to air quality issues in the outpatient department. We should indeed be informed on the treatment and control of these diseases. As a result, effective air quality monitoring, such as carbon dioxide (CO2) concentrations, is essential to monitor and limit the risk of infected air. It is difficult to assess and monitor carbon dioxide in a room with a ventilation system where the number of people in each room changes frequently. We will propose a numerical model for estimating the concentration of exhaled air in a zero-dimensional and a two-dimensional with an outlet ventilation system, as well as the risk of infection. There are many scenarios for improving air quality in the suggested simulations. The proposed strategy represents the balance in the air quality management process between the number of people allowed to stay in the room and the performance of the air ventilation system.

Keywords : Airborne, Infectious, Diseases, Ventilation system.

Acknowledgements

I would like to thank the many people who helped me reach this point. My advisor Assoc. Prof. Dr. Nopparat Pochai, for taking me on as a student, introducing me to mathematics and methodology knowledge and enduring my frequent tardiness. Assoc. Prof. Dr. Nopparat Pochai, for give me a scholarship. My family no matter where I have gone, home has always been with you. My classmate for our friendship, supportiveness and helping me find my way through graduate.

Wasu Timpitak

Table of Contents

List of Tables

Table **Page**

List of Figures

Figure **Page**

Chapter 1

Introduction

1.1 Research Motivation

Many people have died from infectious diseases throughout history. Because medical science was not as advanced as it is now, humans lacked the knowledge and skills to deal with the occurrence of sickness. As a result, the disease epidemic is strong and swiftly infects others. There are infectious diseases that can spread to both people and animals. A variety of germs cause the disease. These can be transmitted through infected wounds caused by animal bites or scratches, consuming pathogen-contaminated food, infection by breathing as the infection spreads through the air, and contact with the patient's secretions. Although bacteria can spread and cause infectious diseases. However, humans can avoid this by changing their daily habits and living surroundings.

The most common cause of respiratory tract diseases is infections caused by viruses and bacteria, such as temple disease, influenza, avian influenza, SARS, pneumonia, TB, and COVID-19. Infectious diseases can affect both children and adults. If not treated appropriately and soon, it can result in severe sickness and death. Dangerous infection diseases such as tuberculosis, COVID-19, MERS, and SARS are infectious and transmitted from person to person by the air droplets in different ways such as coughing, saliva, sneezing, talking, or through wounds. The infection risk can reduce by keeping the living environment clean, including ventilation in the home to ensure efficient air movement, avoiding traveling to busy places, and before you eat washing your hands. Presently, several vaccines are available that actively prevent respiratory infections.

At the end of 2019, the world experienced an emerging disease caused by the most recently discovered coronavirus. The COVID-19 pandemic is a worldwide epidemic impacting a lot of individuals. It affects global public health and the economy. Many people have died as a result of early coronavirus infection. Since this type of virus and new disease are unclear. Global public health defenders have taken steps to reduce tourism and travel, as well as to cancel large-scale events and close schools. Many nations prohibit people from leaving their homes at night, conduct screening at airports and train stations, and prevent the country from accepting international visitors, which may affect the domestic economy.

COVID-19 is spread from person to person via droplets of spit or snot produced by COVID-19 patients coughing, sneezing, or speaking. Droplets can land on items and surfaces like phones, tables, doorknobs, railings, etc. When a person's hand comes

into contact with the device and touches its eyes, nose, or mouth, it can introduce pathogens into the body. The treatment tried to control the patient's symptoms because there was no vaccine or antiviral medicine in the early phases. Preventive methods recommended by public health include a 1-meter social distancing, wearing masks, washing hands with alcohol, and quarantining sick individuals for 14 days.

Many patients will visit outpatient rooms every day, causing a significant air pollution issue that may pose a risk of exposure to respiratory infectious diseases in outpatient rooms and harm human health. COVID-19, TB, MERS, and SARS are risks, and the chances of success toward lethal infection make more patients ill in the hospital. We should be notified of the care and control of these diseases. As a result, effective air quality monitoring is required to monitor and reduce the potential for infected air, such as carbon dioxide (CO2) concentrations. Carbon dioxide measurement and control at a hospital with a ventilation system where the number of patients in each room varies. While normally persons are allowed to stay in the same room as infectors, this study will use a mathematical model to estimate the concentration of exhaled air in a space with an outlet ventilation system along with the risk of infection.

Figure 1.1: The outpatient department of Maharaj Nakorn Chiang Mai Hospital [1]

1.2 Literature Reviews

In [9], they proposed the Wells-Riley mathematical model for predicting the risk of influenza infection during train transportation. The marginal incidence of infection rises as the number of people using public transportation rises. Improving ventilation is an efficient method of preventing influenza infection. In [11], they proposed the risk of inhalation of indoor airborne infection by using the probability transmission dynamic modeling method. Three examples were estimated using Wells-Riley mathematical models: (1) CO2 exposure concentrations in indoor settings based on epidemiological data, (2) baseline reproduction numbers, and (3) local air variability. The risk of infection in susceptible populations under a variety of scenarios of exposure. Improved

indoor ventilation has been demonstrated to minimize the risk of infection in studies. In [8], and [13], they proposed carbon dioxide(CO_2) be used as an indicator of air quality indoor, built on the notion that people release CO_2 at a rate dictated by their body weight and bodily movement, and that levels of CO_2 indoor are measured by fresh air clearance.

In [15], [19], they proposed the concentration of inhaled air increases the risk of airborne infection among susceptible people increases. Exhaled air from an infected individual contains airborne infectious particles within the nucleus that can stay in the air for a long period. This causes infection in those who are susceptible.

In [5], they developed a mathematical model to estimate the risk of infectious diseases in the air. The calculations revealed that the probability of infection increased as the number of sick people and airborne infectious diseases increased. In [14], they proposed an assessment of the feasibility of using natural ventilation to control infection in naturally ventilated hospital wards in Hong Kong. A high rate of natural ventilation can reduce cross-infection of airborne diseases.

In [17], they proposed to develop multilevel IAQ control strategies to reduce the risk of infection in buildings and transport areas. A multi-level IAQ control technique is evaluated for indoor environments, including long-term care facilities such as schools, universities, retail stores, hospitals, and transport areas. Assessing the effectiveness of IAQ control strategies can be used to help address the current challenges of COVID-19. In [20], they propose a subjective questionnaire survey and field test of hospital facility indoor air quality. Temperature, indoor air velocity, humidity, carbon dioxide, and total volatile organic compound concentration are one of the field test parameters. First employs questionnaire survey and field test methods, then creates the model based on test data. The influence law of parameters under different air distributions uses the computational fluid dynamics method to examine based on the model, in terms of improving the air quality in hospital consulting rooms. According to the results, a small number of people are dissatisfied with the air quality in the hospital consulting room, and the concentration of carbon dioxide in some locations is high, which is harmful to health.

In [7], they propose assessing IAQ at a huge university hospital in Al-Khobar City, Saudi Arabia's Eastern Province. Inadequate hospital IAQ can lead to epidemics of building-related diseases such as headaches, weariness, eye and skin irritations, and other symptoms. Furthermore, several factors were investigated to determine which were most likely to influence IAQ values. Outdoor levels of all air pollutant levels, except volatile organic compounds (VOCs), were higher than indoor levels, indicating that IAQ inside healthcare facilities (HCFs) was strongly influenced by outdoor sources, notably traffic.

1.3 Objectives of the Study

1) We will propose a computational model that is used to estimate the carbon dioxide concentration in a room with an open ventilation system.

2) We will propose that the classical fourth-order Runge-Kutta method be used to estimate the model solution.

3) We will propose that the actual concentration level, the number of people, and the rate of ventilation are factors in the concentration of carbon dioxide in a room with an open ventilation system.

4) We will propose a mathematical model that can be analyzed to simulate the exhaled air concentration in a space with an outlet ventilation system and the risk of infection while normal people and vaccinated people remain in the same room as infectors.

5) We will propose that the actual concentration level, the number of people, and the rate of ventilation are factors in the concentration of the exhaled air concentration in a space with an outlet ventilation system and infection risk.

6) We will propose the adaptive Runge-Kutta method be used to estimate the model solution.

7) We will propose that the number of people in the room is represented using the Lagrange interpolating polynomial and the cubic splines interpolation since the number of people who stay there varies over time.

8) We will propose a two-dimensional mathematical model of airborne infection in an outpatient room with an outlet ventilation system.

9) We will propose a two-dimensional Gaussian function used to determine the initial conditions so that the initial carbon dioxide value corresponds to the individual seated in each location within the enclosed area.

10) We will propose the initial concentration level, the distance between persons in the room, the number of users, and the ventilation rate all impact the exhaled air concentration and infection risk.

1.4 Scopes of the Study

1) We will study a zero-dimensional mathematical risk assessment model for airborne infection in a room with an open ventilation system and an outlet ventilation system.

2) We will study a two-dimensional mathematical model of airborne infection in an outpatient room with an outlet ventilation system.

3) We will generate a zero-dimensional mathematical risk assessment model for airborne infection in a room with an open ventilation system and an outlet ventilation system.

4) We will generate a two-dimensional mathematical model of airborne infection in an outpatient room with an outlet ventilation system.

5) We will define initial conditions, boundary conditions, and parameters consistent with the problem of a mathematical risk assessment model for airborne infection in a room with an outlet ventilation system.

6) We will use numerical methods to simulate a zero-dimensional mathematical model of airborne infection in a room with an open ventilation system and an outlet ventilation system.

7) We will use numerical methods to simulate a two-dimensional mathematical model of airborne infection in an outpatient room with an outlet ventilation system.

8) We will define the simulation under various situations to control the level of airborne infection in the outpatient department.

1.5 Benefits of the Study

1) We can use a zero-dimensional mathematical model to predict the concentration of exhaled air in a room with an open ventilation system and an outlet ventilation system.

2) We can use a two-dimensional mathematical model to predict the concentration of exhaled air in a room with an outlet ventilation system.

3) We can use a zero-dimensional mathematical model to predict the risk of infection when healthy people remain in the same room as infected people.

4) We can use a two-dimensional mathematical model to predict the risk of infection when healthy people remain in the same room as infected people.

5) We can use the interpolation method for converting field data of a number of people to a function.

1.6 Research Methodology

1) We will study a zero-dimensional mathematical model of risk assessment for airborne infection in a room with an open ventilation system and an outlet ventilation system.

2) We will study a two-dimensional mathematical model of risk assessment for airborne infection in a room with an outlet ventilation system.

3) We will generate a zero-dimensional mathematical model of risk assessment for airborne infection in a room with an open ventilation system and an outlet ventilation system.

4) We will generate a two-dimensional mathematical model of risk assessment for airborne infection in a room with an outlet ventilation system.

5) We will define initial conditions and parameters consistent with the problem of a zero-dimensional mathematical model of risk assessment for airborne infection in a room with an open ventilation system and an outlet ventilation system.

6) We will define initial conditions, boundary conditions, and parameters consistent with the problem of a two-dimensional mathematical model of risk assessment for airborne infection in a room with an outlet ventilation system.

7) We will use numerical methods to simulate a zero-dimensional mathematical model of risk assessment for airborne infection in a room with an open ventilation system and an outlet ventilation system.

8) We will use numerical methods to simulate a two-dimensional mathematical model of risk assessment for airborne infection in a room with an outlet ventilation system.

9) We will define the simulation under various situations to control the level of airborne infection in the outpatient department.

Chapter 2

Governing equations

The outpatient department is an agency that provides services to users and is a hospital outpost. Outpatient department tasks begin with a historical inquiry. Diagnose the cause of the disease, give treatment, and monitor the symptoms of various diseases. During treatment, the patient will be classified and assigned to the appropriate examination room based on the kind of disease, such as the general examination room, hearing room, obstetrics, and gynecology room, among others.

Every day, people of all ages come to obtain a wide range of services, which puts them at risk of airborne transmission. Air quality control in outpatient departments is thus critical. Good air quality reduces the risk of infection among service users. The number of users, the ventilation system, and the size of the outpatient department all also to be factors that contribute to air quality issues in the outpatient department. We should indeed be informed on the treatment and control of these diseases. As a result, effective air quality monitoring, such as carbon dioxide (CO2) concentrations, is essential to monitor and limit the risk of infected air. In this research, we propose mathematical models of airborne infection control in an outpatient department with a ventilation system.

2.1 Inhaled quantity of rebreathed air in the room required to instigate infection

The room's environmental carbon dioxide concentration (CE) is around 400 ppm. When there are individuals within, the concentration of exhaled air rises. Increased exhaled air concentration is determined by the rate of ventilation per person, the room size, and the number of people in the room [8], [13], and [12].

Considering that a room of size (V) has an initial environmental carbon dioxide (CE) concentration of about 400 ppm and it becomes occupied by the number of people(n). In the room, the concentration of exhaled air containing infectious particles increases. This is determined by the ventilation rate and the number of people in the room. We assume that people in the room contribute significantly to the generation of carbon dioxide, which acts as a mark of exhaled air. The fundamental equation of the accumulation rate exhaled air concentration in a room with the environmental carbon dioxide, is equal to the exhaled air rate created by inhabitants plus the rate of environmental carbon dioxide, minus ventilation rate removes exhaled air. The fundamental equation for the exhaled air accumulation rate is as follows [5]:

$$V\frac{dC}{dt} = npC_a + QC_E - QC, \tag{2.1}$$

where C is the concentration of air exhaled indoor (ppm), p is the rate of respiration in the room (L/s) for each person and C_a is a fraction of the CO_2 contained in inbreathed air. t is the duration time and T is the stationery simulation time. Initial condition $C(0) = C_0$ where C_0 is the latent CO_2 concentration.

The model of carbon dioxide concentration measurement in a room with an opened ventilation system

If the value of Q assumed by Q_{in} and Q_{out}, then these values are named the inlet ventilation rate and the outlet ventilation respectively and in a simple scenario, a number of people are unstable then a number of people depend on the time assumed by $n(t)$, and $n(t)$ is a continuous function. In this study preferred to use Eq.(2.1) as follow:

$$V\frac{dC}{dt} = n(t)pC_a + Q_{in}C_E - Q_{out}C, \tag{2.2}$$

for all $0 \leq t \leq T$.

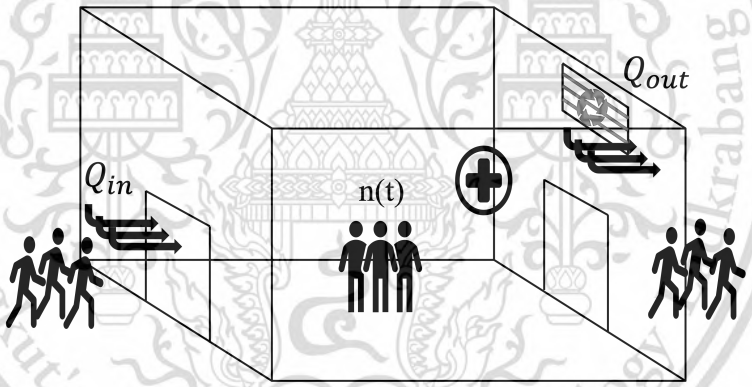

Figure 2.1: The domain of outpatient department rooms with an open ventilation system.

The model of carbon dioxide Concentration measurement in a room with an outlet ventilation system

We consider airborne infections generated by inhabitants [5], and the value of Q is assumed by Q_{out}, then this value is named the outlet ventilation rate. In a simple scenario, the number of people is varied and depends on the time are assumed by $n(t)$, and $n(t)$ is a continuous function. the fundamental equation for exhaled air accumulation rate in the room with environmental CO_2 in Eq.(2.1) can be written as:

$$V\frac{dC}{dt} = n(t)pC_a - Q_{out}C, \tag{2.3}$$

for all $0 \leq t \leq T$.

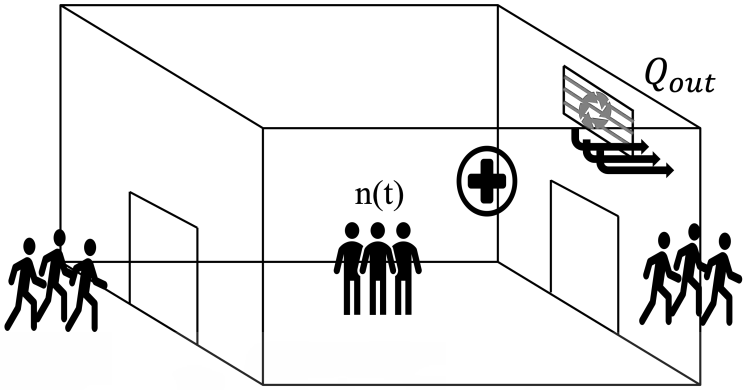

Figure 2.2: The domain of outpatient department rooms with an outlet ventilation system.

The two-dimensional equation of the accumulation rate exhaled air concentration in a room with an outlet ventilation rate

We consider airborne infections generated by inhabitants, and the value of Q is assumed by Q_{out}, then this value is named the outlet ventilation rate. In a simple scenario, the number of people in each position are varied and assumed by $n(x, y, t)$. The two-dimensional equation of the accumulation rate exhaled air concentration in a room with outlet ventilation rate becomes :

$$V\frac{\partial C}{\partial t} = n(x, y, t)pC_a + k(\frac{\partial^2 C}{\partial x^2} + \frac{\partial^2 C}{\partial y^2}) - Q_{out}C, \tag{2.4}$$

for all $(x, y, t) \in \Omega \times \tau$ such that $\Omega = \{(x, y); 0 \leq x \leq L, 0 \leq y \leq W\}$, and $\tau = \{t; 0 \leq t \leq T\}$, where k is the diffusion coefficient of CO_2.

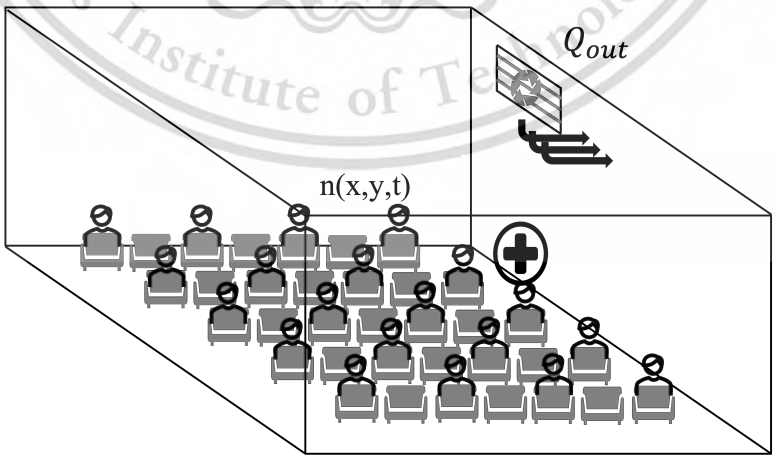

Figure 2.3: The two-dimensional domain of outpatient department rooms with an outlet ventilation rate.

2.2 The volume fraction of exhaled air under unsteady-state

In the rate of exhaled air concentration equation Eqs.(2.2)-(2.3), we can determine the volume fraction of exhaled air in a room with an outlet ventilation system at unsteady state conditions [5]. Consider the volume fraction of exhaled air, we get

$$f(t) = \frac{C(t)}{C_a}. \tag{2.5}$$

In Eq.(2.4), we can determine the volume fraction of exhaled air in a room with an outlet ventilation system at unsteady state conditions.

$$f(x, y, t) = \frac{C(x, y, t)}{C_a}. \tag{2.6}$$

2.3 The airborne infectious particles concentration

In [3], [18], they proposed when a susceptible individual inhales the infectious particles, a limited amount of contaminated particles may reach the location of the respiratory ailment. This is because infectious particles have varied sizes and deposition percentages in different parts of the respiratory system. Determining the risk of airborne infections The accumulation proportion of airborne infectious particles in the airways must also be considered.

Given $\beta - \mu$ is the number of infectious particles in the air that survive and reach an infected target in a susceptible individual (particles/s) as illustrated in Figure 2.6,

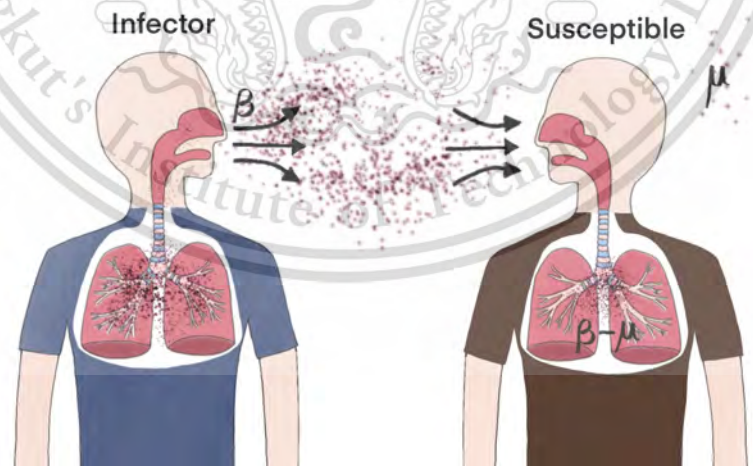

Figure 2.4: Movement of airborne infectious particles.

where β be the rate of airborne infectious particles released by an infected person and μ be the rate of mortality of infectious particles in the air that cannot reach the alveolar layer.

The infection-causing concentration of airborne infectious particles, $N(t)$, is expressed as [5]:

$$N(t) = \frac{If(t)(\beta - \mu)}{n(t)p}, \tag{2.7}$$

where I is the number of people infected in the room. Substituting Eq.(2.5) into Eq.(2.7), we obtain the concentration of infectious airborne particles under unstable conditions,

$$N(t) = \frac{IC(t)(\beta - \mu)}{n(t)pC_a}. \tag{2.8}$$

In the two-dimensional equation of exhaled air concentration accumulation rate in a room with an outlet ventilation rate is employed in this research. $f(x, y, t)$ can be calculated for all $(x, y, t) \in \Omega \times \tau$. So, the airborne infectious particles concentration that causes airborne infection unsteady-state conditions, $N(x, y, t)$ is expressed as

$$N(x, y, t) = \frac{IC(x, y, t)(\beta - \mu)}{pC_a}. \tag{2.9}$$

2.4 The number of airborne infectious particles

Because not all infected particles may reach and deposit in the alveoli, let θ be the fraction of airborne infected particles that are embedded and accumulate at the target location. We obtain $\lambda(t)$ to be an infectious airborne particle that causes infection when breathed by a susceptible individual, which is expressed as [5],

$$\lambda(t) = pt\theta N(t), \tag{2.10}$$

where t is the time spent in the room up to the point of infection and $0 < \theta < 1$.

In the two-dimensional equation of exhaled air concentration accumulation rate in a room with an outlet ventilation rate, we can assume the number of airborne infectious particles,

$$\lambda(x, y, t) = pt\theta N(x, y, t), \tag{2.11}$$

2.5 The probability of airborne infectors

In [19],[5] and [16], they proposed that TB transmission is governed by a Poisson distribution, the probability of airborne infectors is expressed as:

$$P(t) = 1 - e^{-\lambda(t)}, \tag{2.12}$$

where P is the probability of an airborne infection of a person within the room.

In the two-dimensional equation of exhaled air concentration accumulation rate in a room with an outlet ventilation rate, we can assume the probability of airborne infectors,

$$P(x, y, t) = 1 - e^{-\lambda(x,y,t)}, \tag{2.13}$$

2.6 Physical parameters setting techniques

The physical parameters are listed below [5].

Table 2.1: Physical parameter

Parameter	Symbol	Values	Unites
The concentration of air exhaled indoors	$C(t)$	-	ppm
The concentration of air exhaled indoors in each position	$C(x,y,t)$	-	ppm
The environmental carbon dioxide concentration	C_E	0.004	ppm
The breathing rate of each person in the room	p	0.12	L/s
The carbon dioxide fraction contained in breathed air	C_a	0.04	L/s
The number of people varies on the time	$n(t)$	assumed	-
the number of people in each position	$n(x,y,t)$	assumed	-
The inlet ventilation rate	Q_{in}	assumed	m^3/min
The outlet ventilation rate	Q_{out}	assumed	m^3/min
The size of the room	V	assumed	m^3

2.7 Numerical techniques

The first part of this chapter is concerned with approximating the solution $y(t)$ to a problem of the form

$$\frac{dy}{dt} = f(t,y), \tag{2.14}$$

for $a \leq t \leq b$, subject to an initial condition $y(a) = \alpha$.

The object of approximation method is to obtain approximations to the well-posed initial-value problem

$$\frac{dy}{dt} = f(t,y), \quad a \leq t \leq b, \quad y(a) = \alpha. \tag{2.15}$$

A continuous approximation to the solution $y(t)$ will not be obtained; instead, approximations to y will be generated at various values, called mush points, in the interval $[0,T]$.

Once the approximate solution is obtained at the points, the approximate solution at other points in the interval can be found by interpolation. We first make the stipulation that the mesh points are distributed equally over the interval $[0,T]$. This condition is ensured by choosing a positive integer N and selecting the mesh points

$$t_i = a + ih, \tag{2.16}$$

for each $i = 0, 1, 2, ..., N$. The common distance between the points $h = (T - 0)/N = t_{i+1} - t_i$ is called the step size. From now on, it is convenient to replace $y(t_i) = y_i$ with $C(t_i) = C_i$.

2.7.1 The classical fourth-order Runge-Kutta method

The classical fourth-order Runge-Kutta method is expressed as [4],

$$C \cong C_i, \tag{2.17}$$

$$C_{i+1} = C_i + \frac{1}{6}(k_1 + 2k_2 + 2k_3 + k_4)h, \tag{2.18}$$

$$k_1 = f(t_i, C_i), \tag{2.19}$$

$$k_2 = f(t_i + \frac{1}{2}h, C_i + \frac{1}{2}k_1 h), \tag{2.20}$$

$$k_3 = f(t_i + \frac{1}{2}h, C_i + \frac{1}{2}k_2 h), \tag{2.21}$$

$$k_4 = f(t_i + h, C_i + k_3 h), \tag{2.22}$$

for each $i = 0, 1, ..., N - 1$. This method has local truncation error $O(h^4)$, provide the solution $C(t)$ has five continuous derivatives. We introduce the notation k_1, k_2, k_3, k_4 into the method is to eliminate the need for successive nesting in the second variable of $f(t, y)$.

2.7.2 Computational comparisons

The main computational effort in applying the Runge-Kutta method is the evaluation of f. In this second-order method, the local truncation error is $O(h^2)$, and the cost is two function evaluations per step. The Runge-Kutta method of order four requires 4 evaluations per step, and the local truncation error is $O(h^4)$. In [4], they have established the relationship between the number of evaluations per step and the order of the local truncation error shown in Table. This table indicates why the methods of order less than five with smaller step size used in preference to the higher-order methods using a larger step size.

One measure of comparing the lower-order Runge-Kutta methods is descriced as follow: The Runge-Kutta method of order four requires four evaluations per step, where as Euler's method requires only one evaluation. Hence if the Runge-Kutta method of order four is to be superior it should give more accurate answer than Euler's method with one-fourth the step size. Similarly, if the Runge-Kutta method of order four is to be superior to the second-order Runge-Kutta methods, which require two evaluations per step, it should give more accuracy with step size h than a second-order method with step size $h/2$.

Table 2.2: The order of the local truncation error [4]

Evaluations per step	2	3	4	$5 \leq n \leq 7$	$8 \leq n \leq 9$	$10 \leq n$
Best possible local truncation error	$O(h^2)$	$O(h^3)$	$O(h^4)$	$O(h^{n-1})$	$O(h^{n-2})$	$O(h^{n-3})$

2.7.3 The adaptive Runge-Kutta method

This technique uses a Runge-Kutta method with local truncation error of order five. The Adaptive Runge-Kutta method is expressed as, [4],

$$\tilde{C}_{i+1} = C_i + \frac{16}{135}k_1 + \frac{6656}{12825}k_3 + \frac{28561}{56430}k_4 - \frac{9}{50}k_5 + \frac{2}{55}k_6, \tag{2.23}$$

to estimate the local error in a Runge-Kutta method of order four given by

$$C_{i+1} = C_i + \frac{25}{216}k_1 + \frac{1408}{2565}k_3 + \frac{2197}{4140}k_4 - \frac{1}{5}k_5, \tag{2.24}$$

where the coefficient equations are

$$C \cong C_i, \tag{2.25}$$

$$k_1 = hf(t_i, C_i), \tag{2.26}$$

$$k_2 = hf(t_i + \frac{h}{4}, C_i + \frac{1}{4}k_1), \tag{2.27}$$

$$k_3 = hf(t_i + \frac{3h}{8}, C_i + \frac{3}{32}k_1 + \frac{9}{32}k_2), \tag{2.28}$$

$$k_4 = hf(t_i + \frac{12h}{13}, C_i + \frac{1932}{2197}k_1 - \frac{7200}{2197}k_2 + \frac{7296}{2197}k_3), \tag{2.29}$$

$$k_5 = hf(t_i + h, C_i + \frac{439}{216}k_1 - 8k_2 + \frac{3680}{513}k_3 - \frac{845}{4104}k_4), \tag{2.30}$$

$$k_6 = hf(t_i + \frac{h}{2}, C_i - \frac{8}{27}k_1 + 2k_2 - \frac{3544}{2565}k_3 + \frac{1859}{4104}k_4 - \frac{11}{40}k_5). \tag{2.31}$$

An advantage to this method is that only six evaluations of f are required per step. Arbitrary Runge-Kutta methods of orders four and five used together see Table 2.2 require at least four evaluations of f for the fourth-order method and an additional six for the fifth-order method, for a total of at least ten function evaluations. So the Adaptive Runge Kutta method has at least a 40% decrease in the number of function evaluations over the use of a pair of arbitrary fourth- and fifth-order methods.

In error-control theory, an initial value of h is utilized at the ith step to identify the first values of C_{i+1} and $\tilde{C}_{i+1}$, which leads to the determination of q for that step, and the computations are then repeated. Without error control, this technique necessitates twice as many function evaluations every step. In practice, the value of q to be used is chosen somewhat differently in order to make the increased function-evaluation cost worthwhile. The value of q determined at the ith step is used for two purposes. When $q < 1$: reject the initial choice of h at the ith step and restart the computations with qh; when $q \geq 1$: accept the computed value at the step with

step size h but modify the step size to qh for the $(i+1)$st step. q is typically selected carefully due to the penalty in terms of function evaluations that must be paid if the steps are repeated. In reality, a popular choice for the adaptive Runge-Kutta method with $n = 4$ is [4],

$$q = \left(\frac{\varepsilon h}{2 \mid \tilde{C}_{i+1} - C_{i+1} \mid}\right)^{1/4} = 0.84\left(\frac{\varepsilon h}{\mid \tilde{C}_{i+1} - C_{i+1} \mid}\right)^{1/4}. \tag{2.32}$$

To eliminate substantial changes in step size, Eq.2.32 is added to the Algorithm for the adaptive Runge-Kutta method. This is done to avoid wasting time with tiny step sizes in regions with abnormalities in the derivatives of y, as well as to avoid using excessive step sizes, which can result in bypassing crucial regions between steps. The step-size increase technique might be removed entirely from the algorithm, and the step-size decrease procedure is utilized only when necessary to control the error.

2.8 Interpolation

Interpolation is the process of determining a function that passes through a given point. This enables us to determine the value of the chosen point function. Utilizing function interpolation between the points 2 or more possible points. In this research, the number of people who stay in the room varies over time. The Lagrange interpolating polynomial and the cubic splines interpolation are used to represent the number of individuals in the room.

2.8.1 Lagrange interpolating polynomial

Suppose we formulate a linear interpolating polynomial as the weighted average of the two values that we are connecting by a straight line [6]:

$$f(x) = L_1 f(x_1) + L_2 f(x_2), \tag{2.33}$$

where the L_1 and L_2 are the weighting coefficients. It is logical that the first weighting coefficient is the straight line that is equal to 1 at x_1 and 0 at x_2:

$$L_1 = \frac{x - x_2}{x_1 - x_2}. \tag{2.34}$$

Similarly, the second coefficient is the straight line that is equal to 1 at x_2 and 0 at x_1:

$$L_2 = \frac{x - x_1}{x_2 - x_1}. \tag{2.35}$$

Substituting these coefficients into Eq. (2.33),

$$f_1(x) = \frac{x - x_2}{x_1 - x_2} f(x_1) + \frac{x - x_1}{x_2 - x_1} f(x_2), \tag{2.36}$$

where the nomernclature $f_1(x)$ designates that this is a first-order polynomial. Eq. (2.36) is referred to as the linear lagrange interpolating polynomial. Such a second-order Lagrange interpolating polynomial can be written as [6],

$$f_2(x) = \frac{(x-x_2)(x-x_3)}{(x_1-x_2)(x_1-x_3)} f(x_1) + \frac{(x-x_1)(x-x_3)}{(x_2-x_1)(x_2-x_3)} f(x_2) + \frac{(x-x_1)(x-x_2)}{(x_3-x_1)(x_3-x_2)} f(x_3). \tag{2.37}$$

Notice how the first term is equal to $f(x_1)$ at x_1 and is equal to zero at x_2 and x_3. The other terms work in a similar fashion. Both the first-order and second-order versions as well as higher-order Lagrange polynomials can be represented concisely as,

$$f_{n-1}(x) = \sum_{i=1}^{n} L_i(x) f(x_i). \tag{2.38}$$

2.8.2 Cubic splines interpolation

The most common piecewise-polynomial approximation uses cubic polynomials between each successive pair of nodes and is called cubic spine interpolation. A general cubic polynomial involves four constants, so there is sufficient flexibility in the cubic spline procedure to ensure that the interpolant is not only continuously differentiable on the interval, but also has a continuous second derivative. The construction of the cubic spline does not, however, assume that the derivatives of the interpolant agree with those of the function it is approximating, even at the nodes [4]. (See Fig.2.5.)

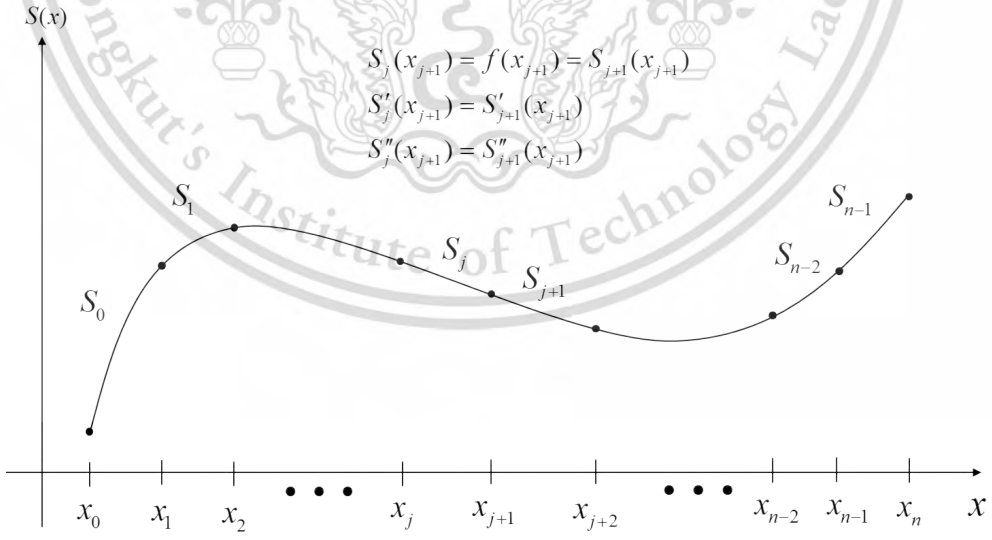

Figure 2.5: Cubic spline interpolant [4]

Definition 2.1. Given a function f defined on $[a,b]$ and a set of nodes $a = x_0 < x_1 < \cdots < x_n = b$, a cubic spine interpolant S for f is a function that satisfies the following conditions [4],

(a) $S(x)$ is a cubic polynomial, denoted $S_j(x)$, on the subinterval $[x_j, x_{j+1}]$ for each $j = 0,\ 1,\ \ldots,\ n-1$.

(b) $S_j(x_j) = f(x_j)$ and $S_j(x_{j+1}) = f(x_{j+1})$ for each $j = 0,\ 1,\ \ldots,\ n-1$.

(c) $S_{j+1}(x_{j+1}) = S_j(x_{j+1})$ for each $j = 0,\ 1,\ \ldots,\ n-2$. (Implied by (b).)

(d) $S'_{j+1}(x_{j+1}) = S'_j(x_{j+1})$ for each $j = 0,\ 1,\ \ldots,\ n-2$.

(e) $S''_{j+1}(x_{j+1}) = S''_j(x_{j+1})$ for each $j = 0,\ 1,\ \ldots,\ n-2$.

(f) One of the following sets of boundary conditions is satisfied:

(i) $S''(x_0) = S''(x_n) = 0$ (natural (or free) boundary).

(ii) $S'(x_0) = f'(x_0)$ and $S'(x_n) = f'(x_n)$ (clamped boundary.)

Although cubic splines are defined with other boundary conditions, the conditions given if (f) are sufficient for our purposes. When the free boundary conditions occur, the spine is called a natural spline, and its graph approximates the shape that a long flexible rod would assume if forced to go through the data points $\{(x_0, f(x_0)), (x_1, f(x_1)), \ldots, (x_n, f(x_n))\}$.

In general, clamped boundary conditions lead to more accurate approximations because they include more information about the function. However, for this type of boundary condition to hold, it is necessary to have either the values of the derivative at the endpoints or an accurate approximation to those values.

2.8.3 Construction of a cubic spline

As the preceding example demonstrates, a spline defined on an interval that is divided into n subintervals will require determining $4n$ constants. To construct the cubic spline interpolant for a given function f, the conditions in the definition are applied to the cubic polynomials [4],

$$S_j(x) = a_j + b_j(x - x_j) + c_j(x - x_j)^2 + d_j(x - x_j)^3, \tag{2.39}$$

for each $j = 0, 1, \ldots, n-1$. Since $S_j(x_j) = a_j = f(x_j)$, condition (c) can be applied to obtain,

$$a_{j+1} = S_{j+1}(x_{j+1}) = a_j + b_j(x_{j+1} - x_j) + c_j(x_{j+1} - x_j)^2 + d_j(x_{j+1} - x_j), \tag{2.40}$$

for $j = 0, 1, \ldots, n-2$.

Thus terms $x_{j+1} - x_j$ are used repeatedly in this development, so it is convenient to introduce the simpler notation

$$h_j = x_{j+1} + x_j$$

for each $j = 0, 1, \ldots, n-1$. If we also define $a_n = f(x_n)$, then the equation

$$a_{j+1} = a_j + b_j h_j + c_j h_j^2 + d_j h_j^3 \tag{2.41}$$

holds for each $j = 0, 1, \ldots, n-1$. In a similar manner, define $b_n = S'(x_n)$ and observe that

$$S'_j(x) = b_j + 2c_j(x - x_j) + 3d_j(x - x_j)^2$$

Implines $S'_j(x) = b_j$, for each $j = 0, 1, \ldots, n-1$. Applying condition (d) gives

$$b_{j+1} = b_j + 2c_j h_j + 3d_j h_j^2, \tag{2.42}$$

for each $j = 0, 1, \ldots, n-1$. Another relationship between the coefficients of S_j is obtained by defining $c_n = S''(x_n)/2$ and applying condition Then, for each $j = 0, 1, \ldots, n-1$,

$$c_{j+1} = c_j + 3d_j h_j. \tag{2.43}$$

Solving for d_j in Eq.2.43 and substituting this value into Eqs.2.41 and 2.42 gives, for each $j = 0, 1, \ldots, n-1$, the new equations

$$a_{j+1} = a_j + b_j h_j + \frac{{h_j}^2}{3}(2c_j + c_{j+1}), \tag{2.44}$$

and

$$b_{j+1} = b_j + h_j(c_j + c_{j+1}). \tag{2.45}$$

The final relationship involving the coefficients is obtained by solving the appropriate equation in the form of Eq.2.44, first for b_j,

$$b_{j+1} = \frac{1}{h_j}(a_{j+1} - a_j) - \frac{h_j}{3}(2c_j + c_{j+1}). \tag{2.46}$$

and then, with a reduction of the index, for b_{j-1}. This gives

$$b_{j-1} = \frac{1}{h_{j-1}}(a_j - a_{j-1}) - \frac{h_{j-1}}{3}(2c_{j-1} + c_j).$$

Substituting these values into the equation derived from Eq.2.45, with the index reduced by one, gives the linear system of equations,

$$h_{j-1}c_{j-1} + 2(h_{j-1} + h_j)c_j + h_j c_{j+1} = \frac{3}{h_j}(a_{j+1} - a_j) - \frac{3}{h_{j-1}}(a_j - a_{j-1}), \tag{2.47}$$

for each $j = 0, 1, \ldots, n-1$. This system involves only the $\{c_j\}_{j=0}^{n}$ as unknowns. The values of $\{h_j\}_{j=0}^{n-1}$ and $\{a_j\}_{j=0}^{n}$ are given, respectively, by the spacing of the nodes $\{x_j\}_{j=0}^{n}$ and the values of f at the nodes. So once the values of $\{c_j\}_{j=0}^{n}$ are determined, it is a simple matter to find the reminder of the constant $\{b_j\}_{j=0}^{n-1}$ from Eq.2.46 and $\{d_j\}_{j=0}^{n-1}$ from Eq.2.43, Then we can construct the cubic polynomials $\{S_j(x)\}_{j=0}^{n-1}$

Theorem 2.2. If f is defined at $a = x_0 < x_1 < \cdots < x_n = b$, then f has a unique natural soline interpolant S on the nodes $x_0, x_1, \ldots, x_n$; that is, a spline interpolant that satisfies the natural boundary conditions $S''(a) = 0$ and $S''(b) = 0$, [4].

Example 1 : We gave some Taylor polynomials to approximate the exponential $f(x) = e^x$. Use the data points $(0,1)$, $(1,e)$, $(2,e^2)$, and $(3,e^3)$ to form a natural spline $S(x)$ that approximates $f(x) = e^x$. We have $n = 3, h_0 = h_1 = h_2 = 1, a_0 = 1, a_1 = e, a_2 = e^2$, and $a_3 = e^3$. So the matrix A and the vectors v and given in Theorem 2.2 have the forms

$$A = \begin{bmatrix} 1 & 0 & 0 & 0 \\ 1 & 4 & 1 & 0 \\ 0 & 1 & 4 & 1 \\ 0 & 0 & 0 & 1 \end{bmatrix}, \; v = \begin{bmatrix} 0 \\ 3\left(e^2 - 2e + 1\right) \\ 3\left(e^3 - 2e^2 + e\right) \\ 0 \end{bmatrix}, \text{ and } x_c = \begin{bmatrix} c_0 \\ c_1 \\ c_2 \\ c_3 \end{bmatrix}.$$

The vector-matrix equation $Ax_c = v$ is equivalent to the system of equations

$$\begin{aligned} c_0 &= 0 \\ c_0 + 4c_1 + c_2 &= 3\left(e^2 - 2e + 1\right), \\ c_1 + 4c_2 + c_3 &= 3\left(e^3 - 2e^2 + e\right), \\ c_0 &= 0. \end{aligned}$$

This system has the solution $c_0 = c_3 = 0$, and to 5 decimal places, $c_1 = \frac{1}{5}\left(-e^3 + 6e^2 - 9e + 4\right) \approx 0.75685$, and $c_2 = \frac{1}{5}\left(4e^3 - 9e^2 + 6e - 1\right) \approx 5.83007$. Solving for the remaining constants gives

$$\begin{aligned} b_0 &= \frac{1}{h_0}(a_1 - a_0) - \frac{h_0}{3}(c_1 + 2c_0) \\ &= (e-1) - \frac{1}{15}\left(-e^3 + 6e^2 - 9e + 4\right) \approx 1.46600, \\ b_1 &= \frac{1}{h_1}(a_2 - a_1) - \frac{h_1}{3}(c_2 + 2c_1) \\ &= \left(e^2 - e\right) - \frac{1}{15}\left(2e^3 + 3e^2 - 12e + 7\right) \approx 2.22285, \\ b_2 &= \frac{1}{h_2}(a_3 - a_2) - \frac{h_2}{3}(c_3 + 2c_2) \\ &= \left(e^3 - e^2\right) - \frac{1}{15}\left(8e^3 - 18e^2 + 12e - 2\right) \approx 8.80977, \\ d_0 &= \frac{1}{3h_0}(c_1 - c_0) = \frac{1}{15}\left(-e^3 + 6e^2 - 9e + 4\right) \approx 0.25228, \\ d_1 &= \frac{1}{3h_1}(c_2 - c_1) = \frac{1}{15}\left(e^3 - 3e^2 + 3e - 1\right) \approx 1.69107, \\ d_2 &= \frac{1}{3h_2}(c_3 - c_2) = \frac{1}{15}\left(-4e^3 + 9e^2 - 6e + 1\right) \approx -1.94336. \end{aligned}$$

The natural cubic spine is described piecewise by

$$S(x) = \begin{cases} 1 + 1.46600x + 0.25228x^3, & for\, x \in [0,1] \\ 2.71828 + 2.22285\,(x-1) + 0.75685(x-1)^2 + 1.69107(x-1)^3\,, & for\, x \in [1,2] \\ 7.38906 + 8.80977\,(x-2) + 5.83007(x-2)^2 - 1.94336(x-2)^3, & for\, x \in [2,3] \end{cases}$$

The spline and its agreement with $f(x) = e^x$

2.9 The forward time central space finite difference scheme

We now discretize the domain by dividing the interval $[0, L]$ into M subintervals such that $M\Delta x = L$, the interval $[0, W]$ into N subintervals such that $N\Delta y = W$, and the time interval $[0, T]$ into R subintervals such that $R\Delta t = T$. The grid points (x_i, y_j, t_n) are defined by $x_i = i\Delta x$ for all $i = 0, 1, 2, \ldots, M$, $y_j = j\Delta y$ for all $j = 0, 1, 2, \ldots, N$ and $t_n = n\Delta t$ for all $n = 0, 1, 2, \ldots, R$, in which M, N and R are positive integers. We can then approximate $C(x_i, y_j, t_n)$ by $C^n_{i,j}$, value of the difference approximation of $C(x, y, t)$ at point $x = i\Delta x$ $y = j\Delta y$ and $t = n\Delta t$, where $0 \leq i \leq M$ $0 \leq j \leq N$.and $0 \leq n \leq R$. We will employ the forward time central space finite difference scheme (FTCS) into Eq.(2.4).

$$C(x_i, y_j, t_n) \cong C^n_{i,j}, \tag{2.48}$$

$$\left.\frac{\partial C}{\partial t}\right|_{(x_i, y_j, t_n)} \cong \frac{C^{n+1}_{i,j} - C^n_{i,j}}{\Delta t}, \tag{2.49}$$

$$\left.\frac{\partial^2 C}{\partial x^2}\right|_{(x_i, y_j, t_n)} \cong \frac{C^n_{i+1,j} + C^n_{i-1,j} - 2C^n_{i,j}}{(\Delta x)^2}, \tag{2.50}$$

$$\left.\frac{\partial^2 C}{\partial y^2}\right|_{(x_i, y_j, t_n)} \cong \frac{C^n_{i,j+1} + C^n_{i,j-1} - 2C^n_{i,j}}{(\Delta y)^2}. \tag{2.51}$$

A two dimensional mathematical model of airborne infection in an outpatient room with an outlet ventilation system is proposed. Substituting Eqs.(2.48)-(2.51) into Eq.(2.4), we get the finite difference equation,

$$V\left(\frac{C^{n+1}_{i,j} - C^n_{i,j}}{\Delta t}\right) = n(x_i, y_j, t_n)pC_a - Q_{out}C^n_{i,j}$$

$$+k\left(\frac{C^n_{i+1,j} + C^n_{i-1,j} - 2C^n_{i,j}}{(\Delta x)^2} + \frac{C^n_{i,j+1} + C^n_{i,j-1} - 2C^n_{i,j}}{(\Delta y)^2}\right). \tag{2.52}$$

for all $i = 0, 1, 2, 3, \ldots, M$, $j = 0, 1, 2, \ldots, N$ and $n = 0, 1, 2, \ldots, R-1$. Then the explicit finite difference equation becomes

$$C^{n+1}_{i,j} = A^n_{i,j} + \lambda_1\left(C^n_{i+1,j} + C^n_{i-1,j}\right) + \beta_1\left(C^n_{i,j+1} + C^n_{i,j-1}\right) + \left(1 - 2\lambda_1 - 2\beta_1 - \frac{\Delta t Q_{out}}{V}\right)C^n_{i,j}, \tag{2.53}$$

where $A^n_{i,j} = \frac{n(x_i, y_j, t_n)p\Delta t C_a}{V}$, $\lambda_1 = \frac{k\Delta t}{V(\Delta x)^2}$, and $\beta_1 = \frac{k\Delta t}{V(\Delta y)^2}$.

The forward time central space scheme is conditionally stable subject to constraints in Eq.2.53. The stability requirements for the scheme are [10][2],

$$\lambda_1 = \frac{k\Delta t}{V(\Delta x)^2} < \frac{1}{2}, \tag{2.54}$$

$$\beta_1 = \frac{k\Delta t}{V(\Delta y)^2} < \frac{1}{2}. \tag{2.55}$$

It can be obtained that the strict stability requirements are the main disadvantage of this scheme.

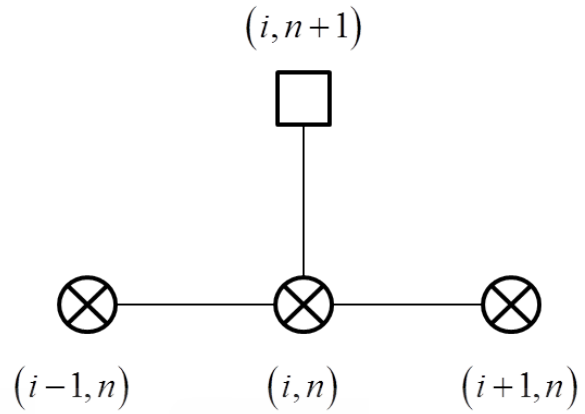

Figure 2.6: Stencil diagram of forward time central space finite difference scheme.

2.10 The initial condition and boundary conditions

2.10.1 The initial condition

The initial condition is assumed by,

$$C(x,y,0) = g(x,y,0), \tag{2.56}$$

for all $0 \leq x \leq L$ and $0 \leq y \leq W$, where $g(x,y,0)$ is the latent airborne infection concentration.

2.10.2 The boundary conditions

The boundary conditions is assumed by,

$$\frac{\partial C(0,y,t)}{\partial x} = k_1, \tag{2.57}$$

$$\frac{\partial C(L,y,t)}{\partial x} = k_2, \tag{2.58}$$

$$\frac{\partial C(x,0,t)}{\partial y} = k_3, \tag{2.59}$$

$$\frac{\partial C(x,W,t)}{\partial y} = k_4, \tag{2.60}$$

for all $0 \leq x \leq L$, $0 \leq y \leq W$ and $0 \leq t \leq T$, where k_1, k_2, k_3 and k_4 are given rate of change of airborne infection concentration. The boundary conditions are shown in Fig.2.7.

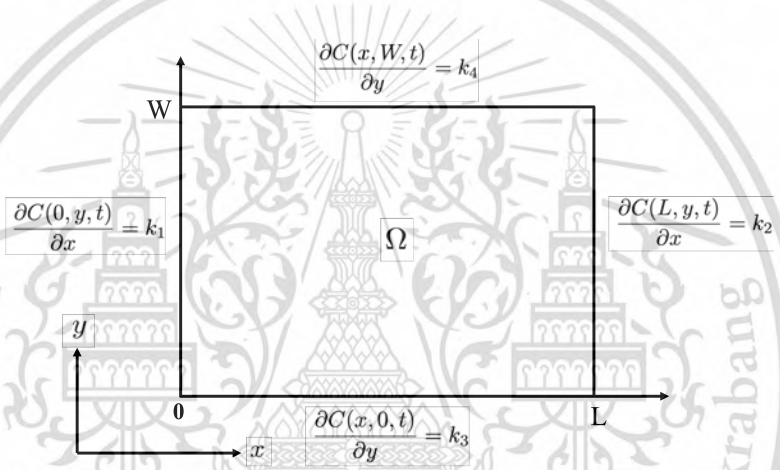

Figure 2.7: The boundary condition.

Chapter 3

A zero-dimensional mathematical model of risk assessment on airborne infection

In this chapter, the numerical model of carbon dioxide concentration measurement in a space with an opened ventilation system is proposed. The model sets the concentration of carbon dioxide at any point when the number of people and the rate of ven- tilation varies. The classical fourth-order Runge-Kutta method is employed to approximate the model solution. There are many cases of scenarios for improving air quality in the proposed simulations. In the air quality management process, the proposed model provides a balance between the number of persons allowed to stay in the room and the capacity of the air ventilation system.

It is indeed difficult to measure and manage carbon dioxide in a hospital with a ventilation system when the number of patients in each room changes over time. This chapter provided a risk model of airborne transmission and vaccination effectiveness in an outpatient room with a ventilation system. When the number of people and the rate of ventilation change, the model modifies the carbon dioxide concentration. To approximate the model solution, the forth-order Runge-Kutta technique is used. In the presented simulations, there are several scenarios for improving air quality. The proposed approach balances the number of people allowed to stay in the room with the capacity of the air ventilation system in the air quality management process. As can seen, the risk of infection is dependent on the number of people present, the rate of ventilation, and the efficacy of each type of vaccination. If there is public vaccination database system, this chapter may be used to help control the risk of airborne infection to the desired level.

Airborne transmission may happen across long ranges and time periods. Increased infection rates or clusters of airborne infections are linked to a lack of ventilation or low ventilation rates. While normal people remain in the same room as infectors, this research will utilize a mathematical model for estimating the concentration of exhaled air in a space with an outlet ventilation system, as well as the risk of infection. As a result, the exhaled air concentration and infection risk are affected by the actual concentration level, the number of users, and the rate of ventilation. The adaptive Runge-Kutta technique and the standard fourth-order Runge-Kutta technique are used to estimate the model solution. Because the number of individuals who stay in the space varies over time, the Lagrange interpolating polynomial and cubic splines interpolation are employed to represent the number of individuals in the space. A good agreement solution is obtained using the adaptive Runge- Kutta

method with cubic spline interpolation. The proposed strategy represents the balance in the air quality management process between the number of individuals allowed to stay in the space and the performance of the air ventilation system. For the optimal outcomes, the proposed technique was capable of converting field data from a the number of individuals using cubic splines and adaptive RK methods.

3.1 A numerical model of carbon dioxide concentration measurement in a room with an opened ventilation system

3.1.1 Traditional the classical fourth-order Runge-Kutta method applied to a numerical model of carbon dioxide concentration measurement

In section, a numerical model of carbon dioxide concentration measurement in a room with an opened ventilation system is proposed. Substituting Eqs.(2.17)-(2.22) into Eq.(2.2), we get the classical fourth-order RK method,

$$C \cong C_i, \tag{3.1}$$

$$C_{i+1} = C_i + \frac{1}{6}(k_1 + 2k_2 + 2k_3 + k_4)h, \tag{3.2}$$

$$k_1 = f(t_i, C_i), \tag{3.3}$$

$$k_2 = f(t_i + \frac{1}{2}h, C_i + \frac{1}{2}k_1 h), \tag{3.4}$$

$$k_3 = f(t_i + \frac{1}{2}h, C_i + \frac{1}{2}k_2 h), \tag{3.5}$$

$$k_4 = f(t_i + h, C_i + k_3 h), \tag{3.6}$$

$$\frac{dC}{dt} = f(t_i, C_i), \tag{3.7}$$

$$f(t_i, C_i) = \frac{1}{V}(n(t)pC_a + Q_{in}C_E - Q_{out}C_i). \tag{3.8}$$

Assuming that the class room of volume $V = 75\ (m^3)$, each person's breathing rate in the room assumed by $p = 0.12\ (L/s)$ and the carbon dioxide fraction included in inbreathed air $C_a = 0.04$. The step size of the classical fourth-order Runge-Kutta method is $\triangle t = 0.1$ and $T = 180$.

Simulation 3.1 : an ideal carbon dioxide concentration measurement.

Table 3.1 lists the model's physical parameters. $C_0 = 0.0025$ is the ambient carbon dioxide concentration (ppm). The analytical solution for this case can be obtained by [5] such as,

$$C(t) = C_E + \frac{npC_a}{Q}[1 - e^{-Qt/V}]. \tag{3.9}$$

Table 3.2 presents the approximated solution's maximum errors. As seen in Fig.3.1, the approximated solutions are compared to the analytical solution.

Table 3.1: Physical parameters.

$n(t)$	C_E	Q
50	0.004	8

Table 3.2: The maximum l_2 norm error of the RK4 solution with the analytical solution.

$\triangle t$	Maximum error
0.100	0.1660×10^{-10}
0.050	0.0146×10^{-10}
0.025	0.0013×10^{-10}

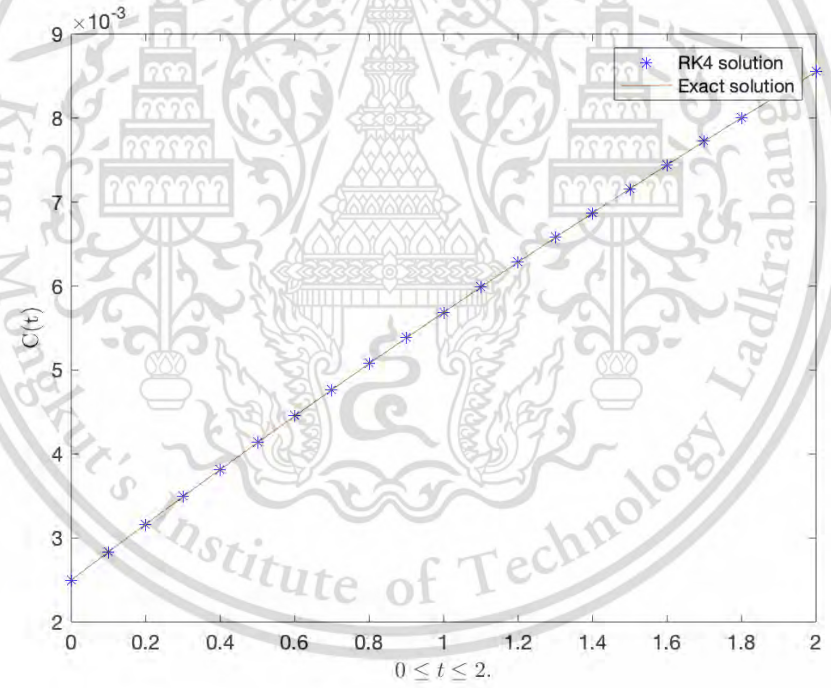

Figure 3.1: The comparison of the RK4 solution and the analytical solution in a room with a ventilation system $\triangle t = 0.1$ $T = 180$.

The RK4 solution and the analytical solution is used Eq.(2.1), The comparison of approximation techniques is illustrated in Fig.3.1. The RK4 method gives accurately approximated carbon dioxide concentration as show in Table 3.2.

Simulation 3.2 : a small number of people in the room carbon dioxide concentration measurement.

Table 3.3 lists the physical parameters. C_0 = 0.01, 0.005, and 0.0025 are the initial carbon dioxide concentrations. We achieve the approximated solutions illustrated in Fig.3.2 by using the RK4 method Eqs.(3.1)-(3.8).

Table 3.3: Physical parameters.

$n(t)$	C_E	Q_{in}	Q_{out}
5	0.004	8	4

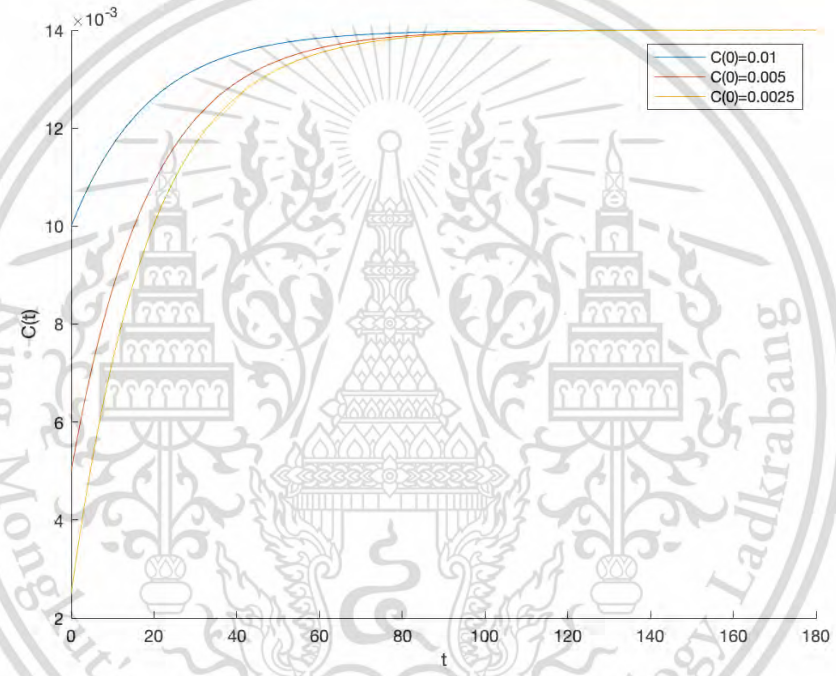

Figure 3.2: The approximated carbon dioxide concentration in a room with a ventilation system $\triangle t = 0.1$ $T = 180$.

We can see that the carbon dioxide concentration along with the starting and the middle of the simulation depends on the potential concentration level. The carbon dioxide concentration for each case becomes close to 0.014 around 1.5 hours, the approximate RK4 solutions when $C(0)$ is divided by a half for each case and assume the number of people $n(t) = 5$ as show in Fig.3.2.

Simulation 3.3 : a large number of people in the room carbon dioxide concentration measurement.

Table 3.4 lists the physical parameters. C_0 = 0.01, 0.005, and 0.0025 are the initial carbon dioxide concentrations. We achieve the approximated solutions illustrated in Fig.3.3 by using the RK4 method Eqs.(3.1)-(3.8).

Table 3.4: Physical parameters.

$n(t)$	C_E	Q_{in}	Q_{out}
50	0.004	8	4

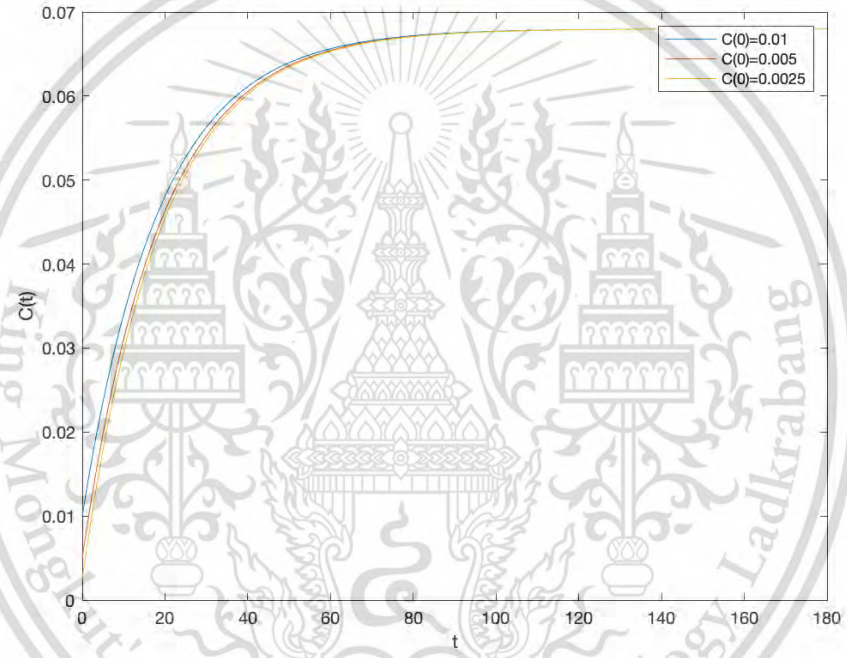

Figure 3.3: The approximated carbon dioxide concentration in a room with a ventilation system $\triangle t = 0.1$ $T = 180$.

We can see that the carbon dioxide concentration along with the starting and the middle of the simulation depends on the potential concentration level and the number of people. When the number of people increases the carbon dioxide concentration is increases. The carbon dioxide concentration for each case becomes close to 0.065 around 1.5 hours, the approximate RK4 solutions when $C(0)$ is divided by a half for each case and assume the number of people $n(t) = 50$ as show in Fig.3.3.

Simulation 3.4 : a different number of people in the room carbon dioxide concentration measurement.

Table 3.5 lists the physical parameters. $n(t) = 5, 25$ and 50 are a number of people. We achieve the approximated solutions illustrated in Figs.3.4-3.6 by using the RK4 method Eqs.(3.1)-(3.8).

Table 3.5: Physical parameters.

C_0	C_E	Q_{in}	Q_{out}
0.01	0.004	4	8

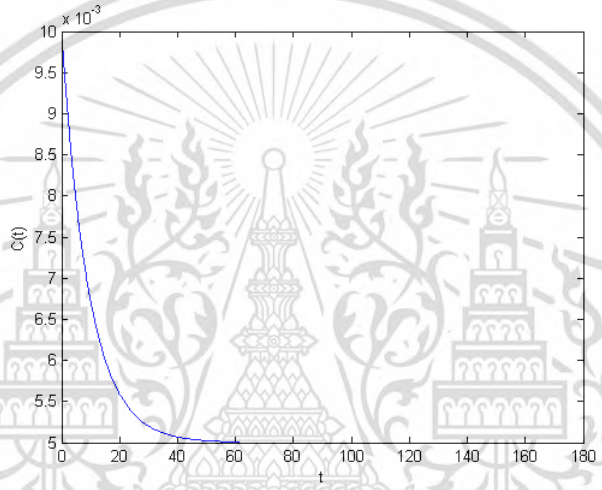

Figure 3.4: The approximated carbon dioxide concentration in a room with a ventilation system $\triangle t = 0.1$ $T = 180$.

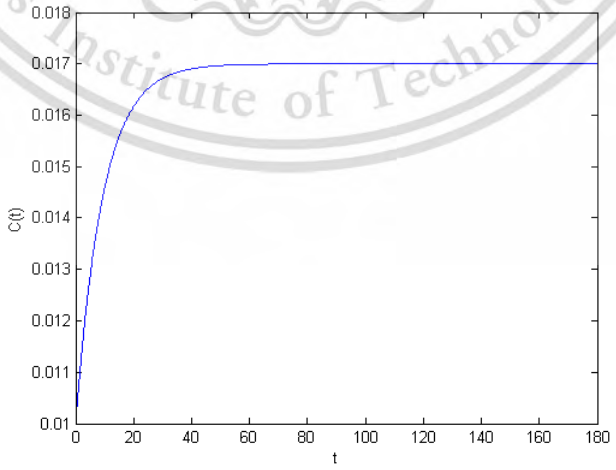

Figure 3.5: The approximated carbon dioxide concentration in a room with a ventilation system $\triangle t = 0.1$ $T = 180$.

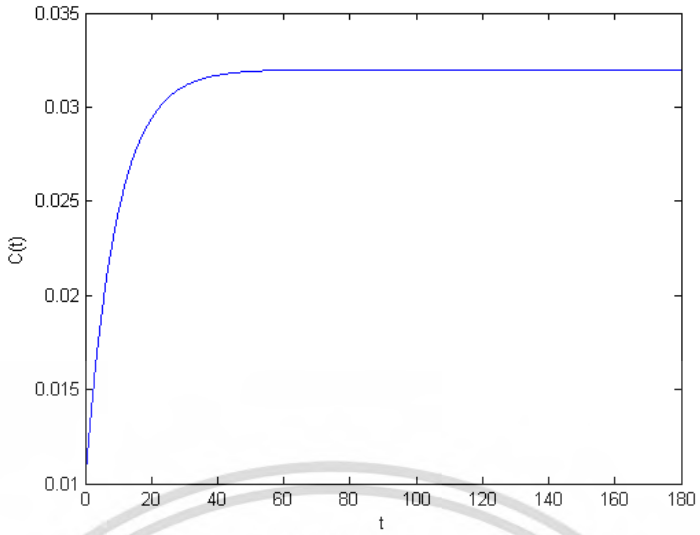

Figure 3.6: The approximated carbon dioxide concentration in a room with a ventilation system $\triangle t = 0.1$ $T = 180$.

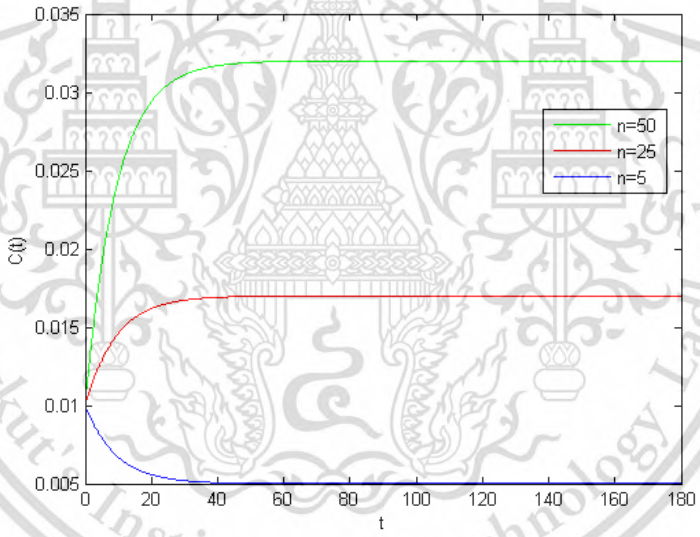

Figure 3.7: The comparison of RK4 solutions.

When the inlet ventilation rate less than the outlet ventilation rate, the carbon dioxide concentration is reduced at $n(t) = 5$, in case $n(t) = 25$ and 50, the carbon dioxide concentration is increases. The carbon dioxide concentration for case 1 becomes close to 0.005 around 1 hours, The carbon dioxide concentration for case 2 becomes close to 0.017 around 1 hours, and The carbon dioxide concentration for case 3 becomes close to 0.033 around 1 hours. The approximate RK4 solutions when assume $n(t) = 5, 25$ and 50 in 3 case and the inlet ventilation rate less than the outlet ventilation as show in Figs.3.4-3.6 and the comparison of 3 cases are illustrated in Fig.3.7.

Simulation 3.5 : varying number of people in the room carbon dioxide concentration measurement.

Table 3.6 lists the physical parameters. A number of people are unstable as show in table 3.7. We achieve the approximated solutions illustrated in Fig.3.8 by using the RK4 method Eqs.(3.1)-(3.8).

Table 3.6: Physical parameters.

C_0	C_E	Q_{in}	Q_{out}
0.0025	0.004	8	4

Table 3.7: A number of people $n(t)$.

t	0	20	40	60	80	100	120	140	160	180
$n(t)$	5	10	15	30	45	50	45	30	20	10

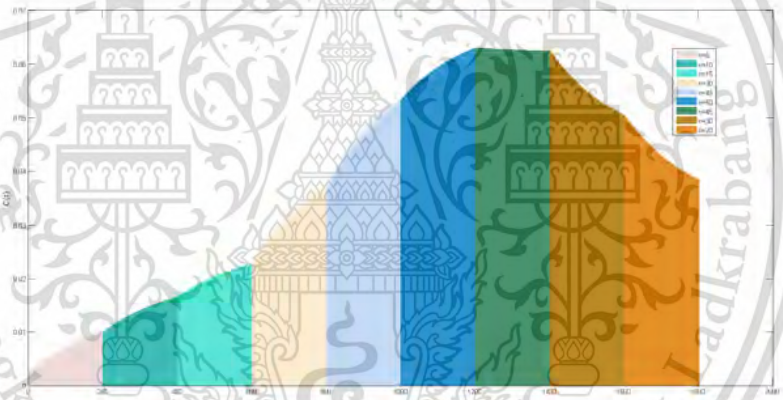

Figure 3.8: The approximated carbon dioxide concentration in a room with a ventilation system when the number of people are unstable $\triangle t = 0.1$ $T = 180$.

When the number of people is varied, the carbon dioxide concentration of interval $0-2$ hours are increases, we can see that the maximum carbon dioxide concentration is 0.062, and the carbon dioxide concentration interval $2-3$ hours is reduced, the carbon dioxide concentration in last time is 0.04. The approximate RK4 solutions when $n(t)$ is varied as shown in Fig.3.8 and the parameter of $n(t)$ as show in Table 3.7.

Simulation 3.6 : changing rate of ventilation in a room carbon dioxide concentration measurement.

Table 3.8 lists the physical parameters. The rate of ventilations are unstable as show in table 3.9. We achieve the approximated solutions illustrated in Fig.3.9 by using the RK4 method Eqs.(3.1)-(3.8).

Table 3.8: Physical parameters.

C_0	C_E	$n(t)$
0.0025	0.004	50

Table 3.9: The rate of ventilations.

t	0-60	61-140	141-180
$Q_{in}(t)$	8	4	8
$Q_{out}(t)$	4	8	4

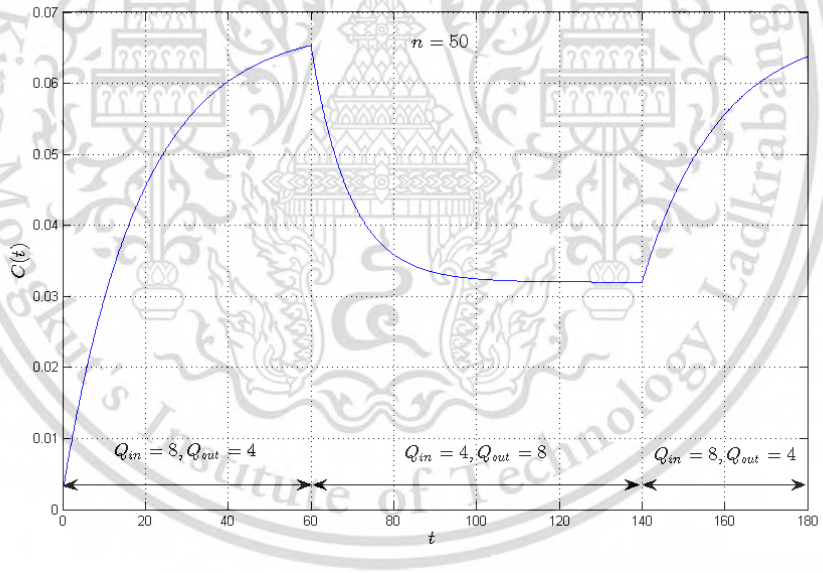

Figure 3.9: The approximated carbon dioxide concentration in a room with a ventilation system when $n(t)$ is unstable.

We can see that the carbon dioxide concentration is increases interval $0-1$ hours and $2.3-3$ hours, when the inlet ventilation rate more than the outlet ventilation rate, but the carbon dioxide concentration reduces interval $1-2.3$ hours when the inlet ventilation rate less than the outlet ventilation rate. The approximate RK4 solutions when the rate of ventilations are unstable as shown in Fig.3.9 and the parameter of the rate of ventilation as shown in Table 3.9.

Simulation 3.7 : the varying number of people when the outlet ventilation rate greater than inlet ventilation rate in the room carbon dioxide concentration measurement

Table 3.10 lists the physical parameters. A number of people are unstable as show in table 3.11. We achieve the approximated solutions illustrated in Fig.3.10 by using the RK4 method Eqs.(3.1)-(3.8).

Table 3.10: Physical parameters.

C_0	C_E	Q_{in}	Q_{out}
0.0025	0.004	4	8

Table 3.11: A number of people $n(t)$.

t	0	20	40	60	80	100	120	140	160	180
$n(t)$	5	10	15	30	45	50	45	30	20	10

Figure 3.10: The approximated carbon dioxide concentration in a room with a ventilation system when $n(t)$ is unstable.

When the number of people is varied with the inlet ventilation rate less than the outlet ventilation, the carbon dioxide concentration around interval $0-2$ hours are increases, we can see that the maximum carbon dioxide concentration is 0.032, and the carbon dioxide concentration around interval $2-3$ hours reduces, the carbon dioxide concentration in last time is 0.015. the approximate RK4 solutions when $n(t)$ is varied and the inlet ventilation rate less than the outlet ventilations show in Fig 3.10 and the parameter of $n(t)$ as show in Table 3.11.

Simulation 3.8 : changing rate of ventilation which depends on the number of people in the room carbon dioxide concentration measurement.

Table 3.12 lists the physical parameters. A number of people and the rate of ventilations are unstable as show in table 3.13-3.14. We achieve the approximated solutions illustrated in Fig.3.11 by using the RK4 method Eqs.(3.1)-(3.8).

Table 3.12: Physical parameters.

C_0	C_E
0.0025	0.004

Table 3.13: A number of people $n(t)$.

t	0	20	40	60	80	100	120	140	160	180
$n(t)$	5	10	15	30	45	50	45	30	20	10

Table 3.14: The rate of ventilations.

t	0-60	61-140	141-180
$Q_{in}(t)$	8	4	8
$Q_{out}(t)$	4	8	4

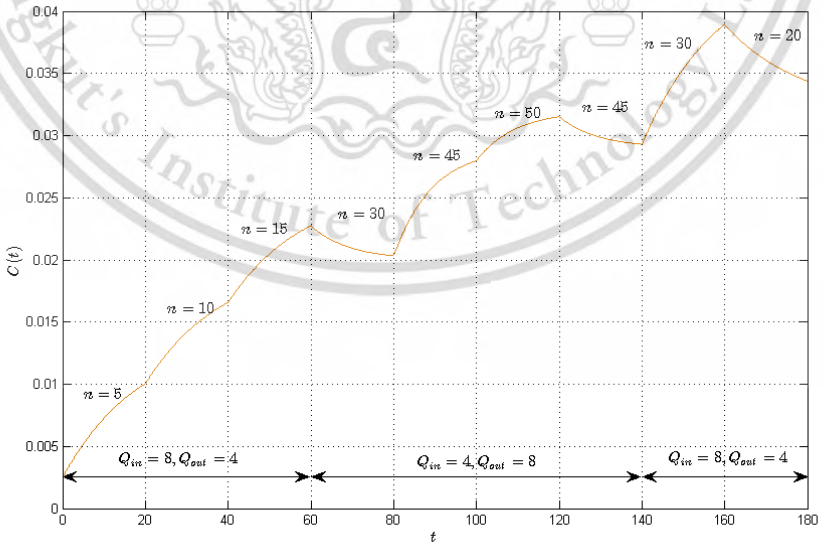

Figure 3.11: The approximated carbon dioxide concentration in a room with a ventilation system when $n(t)$, Q_{in} and Q_{out} are unstable.

The rate of ventilation and the number of people are varied. If the inlet ventilation rate is higher than the outlet ventilation rate, the carbon dioxide concentration will rise. However if the number of people is reduced, the concentration of carbon dioxide is also reduced. In the other hand, if the inlet ventilation rate is smaller than the outlet ventilation rate, the carbon dioxide concentration would decrease. On the other hand, if the inlet ventilation rate is less than the outlet ventilation rate, then the carbon dioxide concentration becomes reducing. However, if the number of people is increased, then the carbon dioxide concentration is also increasing. The approximated RK4 solutions of the simulation are shown in Fig 3.11 when their parameters are given in Tables 3.12-3.14 respectively.

Simulation 3.9 : number of people is represented as a function in the room carbon dioxide concentration measurement.

Table 3.15 lists the physical parameters. A number of people assumed by $n(t) = 20 + 5\sin(\pi t)$. We achieve the approximated solutions illustrated in Fig 3.13 by using the RK4 method Eqs.(3.1)-(3.8).

Table 3.15: Physical parameters.

C_0	C_E	Q_{in}	Q_{out}
0.0025	0.004	8	4

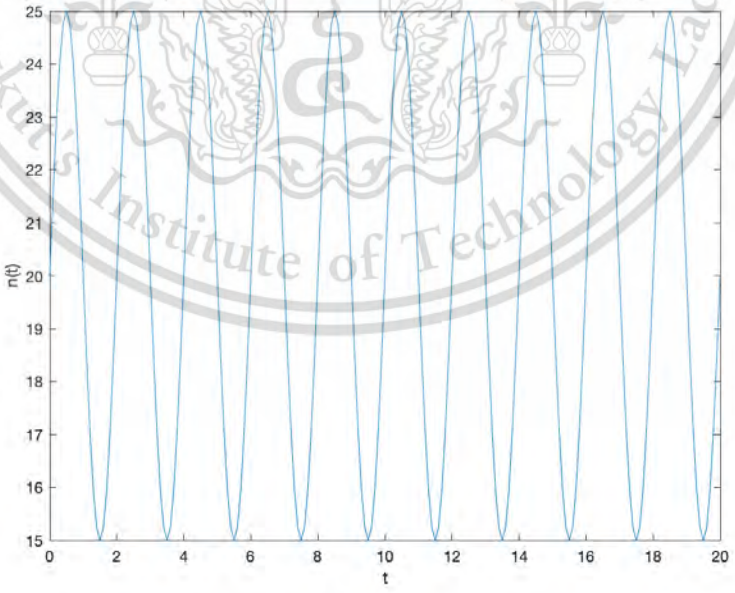

Figure 3.12: A number of people in a room $0 \leq n(t) \leq 20$.

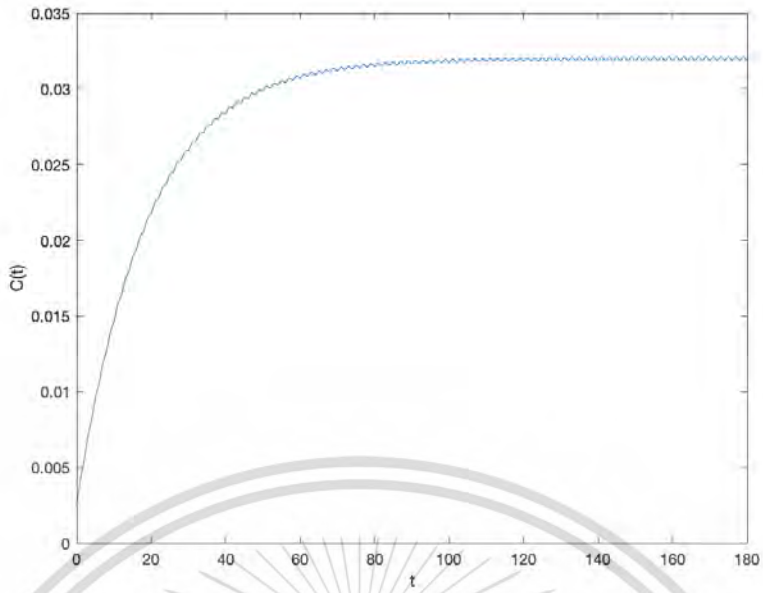

Figure 3.13: The approximated carbon dioxide concentration in a room with a ventilation system when $n(t) = 20 + 5\sin(\pi t)$.

Assume the number of people $n(t) = 20 + 5\sin(\pi t)$, we can see that the carbon dioxide concentration depends on the number of people. The approximate RK4 solutions when $n(t) = 20 + 5\sin(\pi t)$ as show in Fig 3.13 and the number of people in the room as show in Fig 3.12.

3.2 A mathematical model of risk assessment on airborne infection in a room with an outlet ventilation system

3.2.1 Traditional the classical fourth-order Runge-Kutta method applied to a mathematical model of risk assessment on airborne infection in a room with an outlet ventilation system

In section, a mathematical model of risk assessment on airborne infection in a room with an outlet ventilation system is proposed. Substituting Eqs.(2.17)-(2.22) into Eq.(2.3), we get the classical fourth-order RK method,

$$C \cong C_i, \tag{3.10}$$

$$C_{i+1} = C_i + \frac{1}{6}(k_1 + 2k_2 + 2k_3 + k_4)h, \tag{3.11}$$

$$k_1 = f(t_i, C_i), \tag{3.12}$$

$$k_2 = f(t_i + \frac{1}{2}h, C_i + \frac{1}{2}k_1 h), \tag{3.13}$$

$$k_3 = f(t_i + \frac{1}{2}h, C_i + \frac{1}{2}k_2 h), \tag{3.14}$$

$$k_4 = f(t_i + h, C_i + k_3 h), \tag{3.15}$$

$$\frac{dC}{dt} = f(t_i, C_i), \tag{3.16}$$

$$f(t_i, C_i) = \frac{1}{V}(n(t)pC_a - Q_{out}C_i). \tag{3.17}$$

Assuming that the respiration rate assumed by $p = 0.12\ (L/s)$ and a fraction of the Covid-19 concentration contained inbreathed air $C_a = 0.04$. By employing the classical fourth-order Runge-Kutta method Eqs.3.10-3.17. The step size of the classical fourth-order Runge-Kutta method is $\triangle t = 0.05$ and $T = 180$.

Simulation 3.10 : the concentration measurement of exhaled air with difference number of people in a room.

The physical parameters are assumed in Table 3.16. The number of people in the room is assumed in three cases by $n(t) = 5, 25$, and 50.

Table 3.16: Physical parameters.

C_0	V	Q_{out}
0.0025	75	4

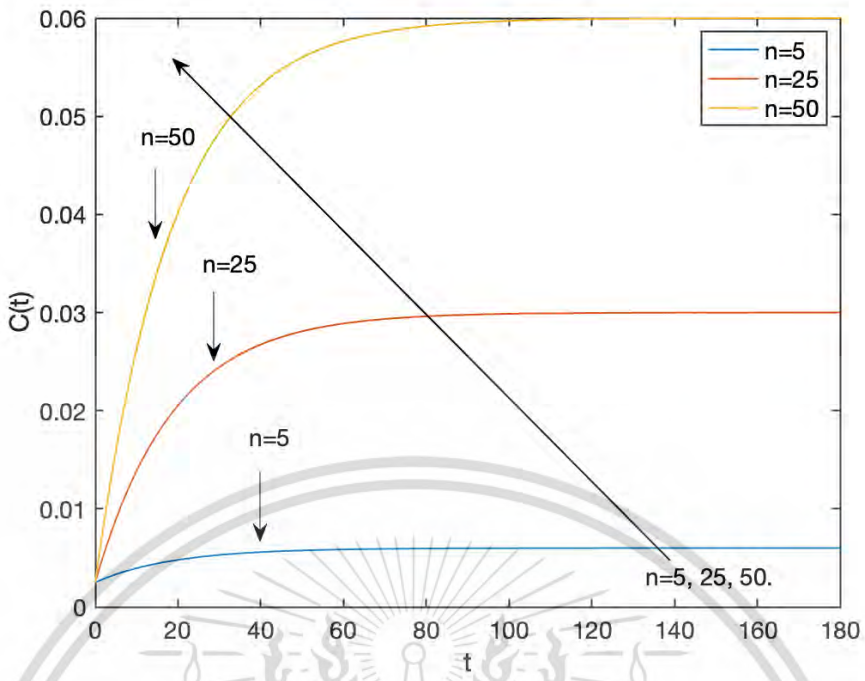

Figure 3.14: The approximated air exhaled indoors concentration in a room with difference number of people in a room $\triangle t = 0.05$ $T = 180$.

The exhaled air concentration the simulation depends on the number of persons in a room. If the number of persons in the room increases, the exhaled air concentration will increases. Figure 3.14 illustrates the approximate RK4 solutions when the number of persons is different.

Simulation 3.11 : the concentration measurement of exhaled air with difference primitive levels.

The physical parameters are assumed in Table 3.17. The initial condition is assumed in three cases by $C_0 = 0.01, 0.005$ and 0.0025.

Table 3.17: Physical parameters.

$n(t)$	V	Q_{out}
50	75	4

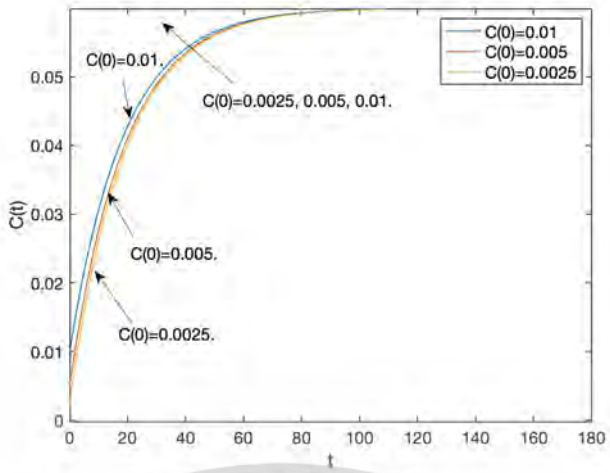

Figure 3.15: The approximated air exhaled indoors concentration in a room with difference primitive levels $\triangle t = 0.05$ $T = 180$.

The exhaled air concentration along with the starting and the middle of the simulation depends on the potential concentration level. The exhaled air concentration for each case becomes close to 0.060 around 1.5 hours.Figure 3.15 illustrates the approximate RK4 solutions when $C(0)$ is divided by half for each case.

Simulation 3.12 : the concentration measurement of exhaled air when difference outlet ventilation levels.

The physical parameters are assumed in Table 3.18. The outlet ventilation is assumed in three cases by $Q_{out} = 1, 4,$ and 8.

Table 3.18: Physical parameters.

$n(t)$	V	C_0
50	75	0.0025

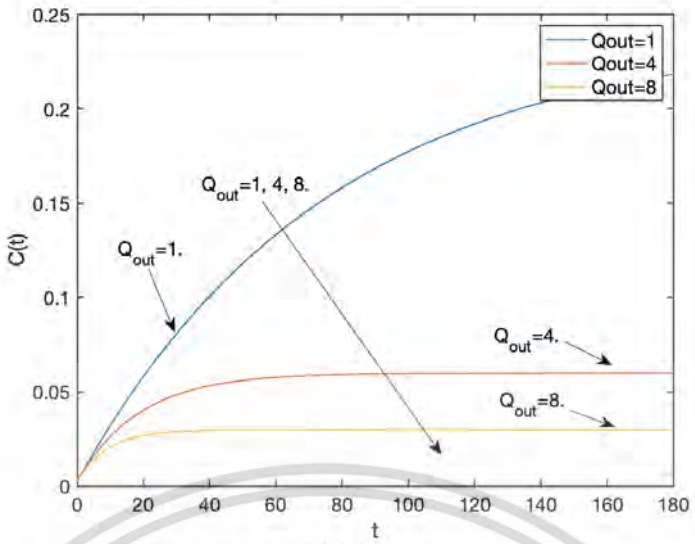

Figure 3.16: The approximated air exhaled indoors concentration in a room when difference outlet ventilation levels $\triangle t = 0.05$ $T = 180$.

The exhaled air concentration the simulation depends on the outlet ventilation level. If the outlet ventilation level is increased, the exhaled air concentration is reduced. Figure 3.16 illustrates the approximate RK4 solutions when the outlet ventilation level is different.

Simulation 3.13 : the concentration measurement of exhaled air with difference room sizes.

The physical parameters are assumed in Table 3.19. The class room of volume is assumed in three cases by $V = 50, 75$, and 100.

Table 3.19: Physical parameters.

$n(t)$	Q_{out}	C_0
50	4	0.0025

The exhaled air concentration along with the starting and the middle of the simulation depends on the room sizes. If the room sizes are increased, the exhaled air concentration is reduced. Figure 3.17 illustrates the approximate RK4 solutions when the different room sizes.

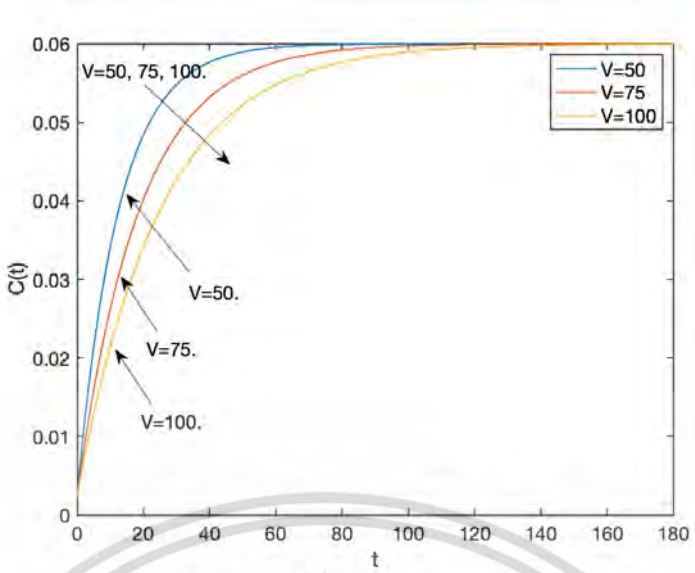

Figure 3.17: The approximated air exhaled indoors concentration in a room with difference room sizes $\triangle t = 0.05$ $T = 180$.

Simulation 3.14 : the concentration measurement of exhaled air with varied numbers of people.

The physical parameters are assumed in Table 3.20. As assumed in Table 3.21, the number of people changes over time.

Table 3.20: Physical parameters.

V	Q_{out}	C_0
50	8	0.0025

Table 3.21: A number of people $n(t)$.

t	0	20	40	60	80	100	120	140	160	180
$n(t)$	5	10	15	30	45	50	45	30	20	10

The exhaled air concentration of the simulation depends on the various number of persons in time. The exhaled air concentration of interval $0-2$ hours is increased and the exhaled air concentration interval $2-3$ hours are reduced. Figure 3.18 illustrates the approximate RK4 solutions when $n(t)$ is varied in time.

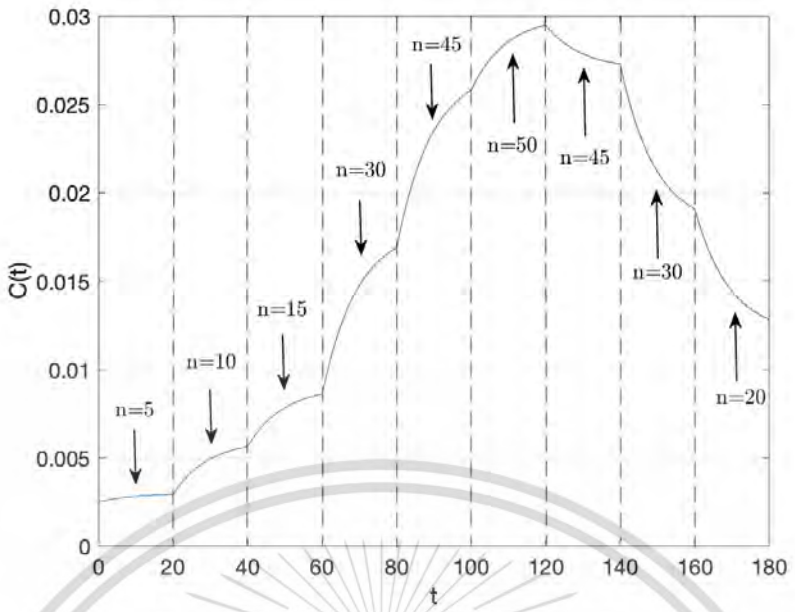

Figure 3.18: The approximated air exhaled indoors concentration in a room with varied numbers of people $\triangle t = 0.05$ $T = 180$.

Simulation 3.15 : the concentration measurement of exhaled air when the outlet ventilation levels depend on the stayed number of people.

The initial condition is assumed by $C_0 = 0.0025$. As asumed in Tables 3.22-3.23, the number of people and the rate of ventilation change over time.

Table 3.22: A number of people $n(t)$.

t	0	20	40	60	80	100	120	140	160	180
$n(t)$	5	10	15	30	45	50	45	30	20	10

Table 3.23: The rate of ventilations.

t	0-60	61-140	141-180
$Q_{out}(t)$	4	8	4

The exhaled air concentration when the number of persons is varied with the out ventilation level depends on the staying number of persons in the room. If we change the outlet ventilation level varies on the number of persons, the exhaled air concentration values will change. Figure 3.19 illustrates the approximate RK4 solutions when $n(t)$ is varied with the out ventilation level.

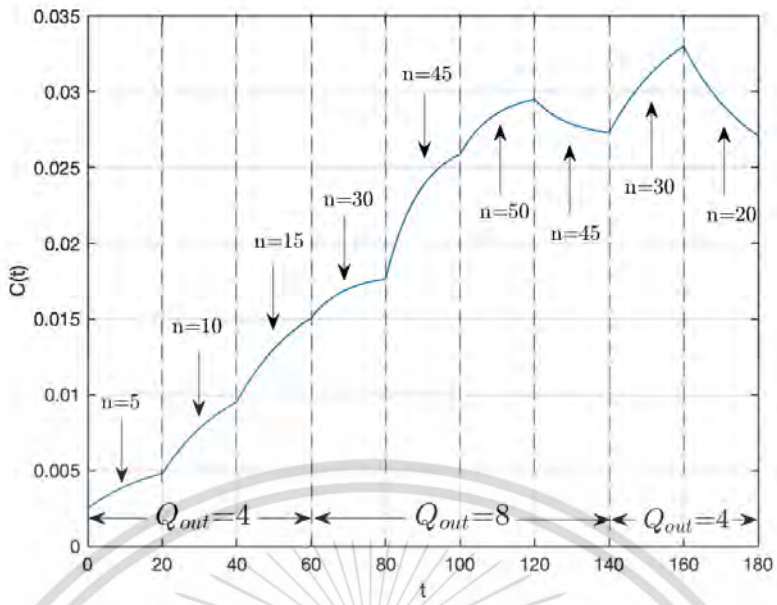

Figure 3.19: The approximated air exhaled indoors concentration in a room when the outlet ventilation levels depend on the stayed number of people $\triangle t = 0.05$ $T = 180$.

Simulation 3.16 : the risk of normal peoples who staying in a room with infectors.

The physical parameters are assumed in Table 3.24. The number of infected people in the room is assumed in three cases by $I = 1, 2$, and 4.

Table 3.24: Physical parameters.

$n(t)$	Q_{out}	C_0	V	β	μ
50	4	0.0025	50	30	20

The risk of infectors depends on the number of infectors in the room. If we change the number of infectors in the room, the risk of infection will change. We can see that the more time spent in the room, the greater the risk of infection. Figure 3.20 illustrates the risk of normal people staying in a room with infectors.

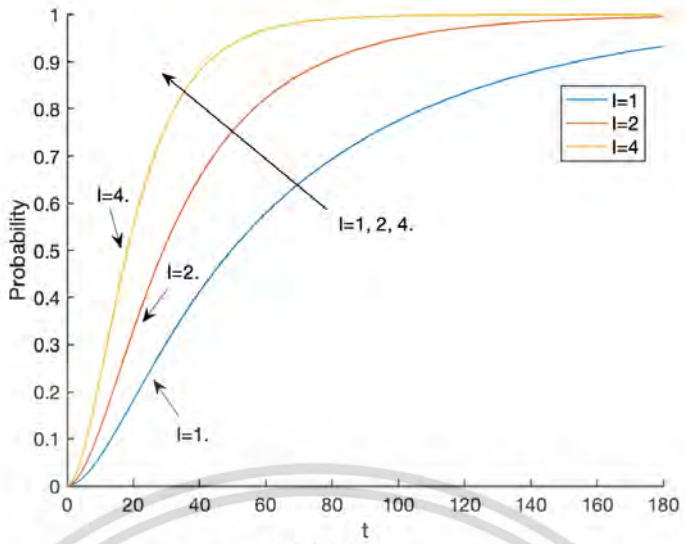

Figure 3.20: The risk of normal peoples who staying in a room with infectors $\triangle t = 0.05$ $T = 180$.

Simulation 3.17 : the risk of vaccinated peoples who constantly staying in a room with an infectors.

The physical parameters are assumed in Table 3.25. The survival rate of airborne infectious particles is assumed in three cases by $\beta - \mu = 20, 10,$ and 2.

Table 3.25: Physical parameters.

$n(t)$	Q_{out}	C_0	V	I
50	4	0.0025	50	1

The risk of infectors depends on the number of vaccinated persons constantly staying in a room. In case $\beta - \mu = 2$, the risk of infection is very low, when compared to cases $\beta - \mu = 20$ and $\beta - \mu = 10$. When a person gets an effective vaccine, the risk of infection is low. Figure 3.21 illustrates the risk of vaccinated people who constantly stay in a room with infectors.

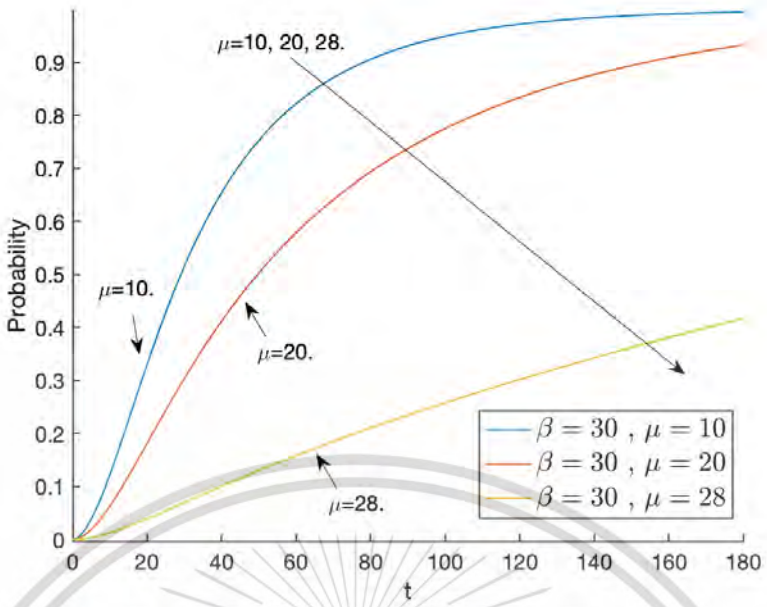

Figure 3.21: The risk of vaccinated peoples who constantly staying in a room with an infectors $\triangle t = 0.05$ $T = 180$.

Simulation 3.18 : the risk of vaccinated peoples who varied staying in a room with infectors.

The physical parameters are assumed in Table 3.26. As assumed in Table 3.27, the number of people changes over time.

Table 3.26: Physical parameters.

Q_{out}	C_0	V	β	μ	I
4	0.0025	50	30	20	1

Table 3.27: A number of people $n(t)$.

t	0	20	40	60	80	100	120	140	160	180
$n(t)$	5	10	15	30	45	50	45	30	20	10

The risk of vaccinated people remaining in a room containing infectors is related to the number of persons staying. If we change the number of vaccinated persons in the room, the risk of infection will change. At intervals of 2.4 – 3.0 hours, the number of vaccinated persons is reduced, and the risk of infection is reduced. Figure 3.22 illustrates the risk of vaccinated persons who vary their time in a room containing infectors.

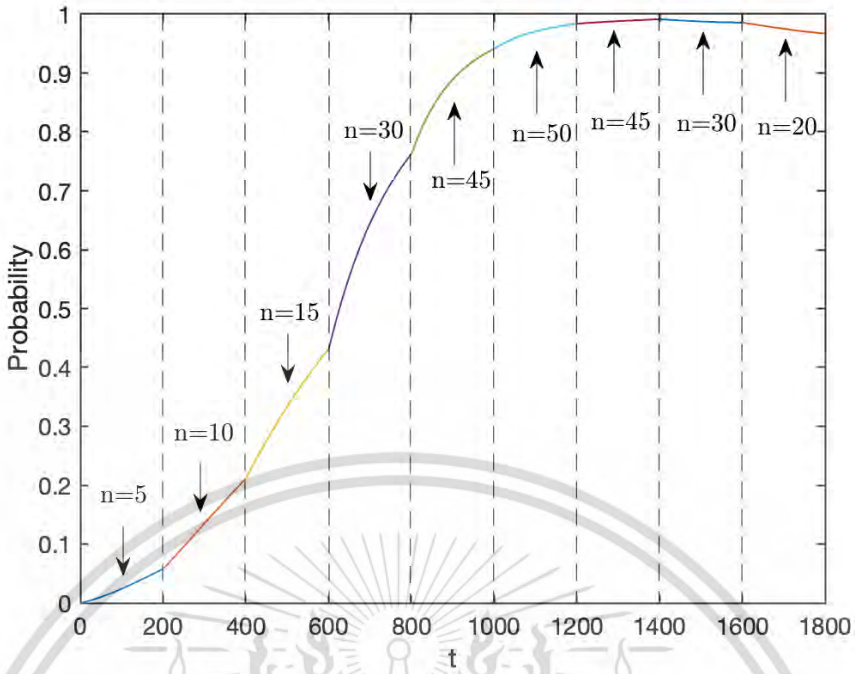

Figure 3.22: The risk of vaccinated peoples who varied staying in a room with infectors $\triangle t = 0.05$ $T = 180$.

3.3 A risk assessment model for airborne infection in a ventilated room using the adaptive Runge-Kutta method with Cubic Spline interpolation

3.3.1 Traditional adaptive Runge-Kutta method applied to a mathematical model of risk assessment on airborne infection in a room with an outlet ventilation system

In section, a risk Assessment model for airborne infection in a ventilated room using the adaptive RK method with cubic spline interpolation is proposed. Substituting Eqs.(2.23)-(2.31) into Eq.(2.3), we get the adaptive fourth-order RK method,

$$\tilde{C}_{i+1} = C_i + \frac{16}{135}k_1 + \frac{6656}{12825}k_3 + \frac{28561}{56430}k_4 - \frac{9}{50}k_5 + \frac{2}{55}k_6, \tag{3.18}$$

to estimate the local error in a Runge-Kutta method of order four given by

$$C_{i+1} = C_i + \frac{25}{216}k_1 + \frac{1408}{2565}k_3 + \frac{2197}{4140}k_4 - \frac{1}{5}k_5, \tag{3.19}$$

where the coefficient equations are

$$C \cong C_i, \tag{3.20}$$

$$k_1 = hf(t_i, C_i), \tag{3.21}$$

$$k_2 = hf(t_i + \frac{h}{4}, C_i + \frac{1}{4}k_1), \tag{3.22}$$

$$k_3 = hf(t_i + \frac{3h}{8}, C_i + \frac{3}{32}k_1 + \frac{9}{32}k_2), \tag{3.23}$$

$$k_4 = hf(t_i + \frac{12h}{13}, C_i + \frac{1932}{2197}k_1 - \frac{7200}{2197}k_2 + \frac{7296}{2197}k_3), \tag{3.24}$$

$$k_5 = hf(t_i + h, C_i + \frac{439}{216}k_1 - 8k_2 + \frac{3680}{513}k_3 - \frac{845}{4104}k_4), \tag{3.25}$$

$$k_6 = hf(t_i + \frac{h}{2}, C_i - \frac{8}{27}k_1 + 2k_2 - \frac{3544}{2565}k_3 + \frac{1859}{4104}k_4 - \frac{11}{40}k_5), \tag{3.26}$$

$$\frac{dC}{dt} = f(t_i, C_i), \tag{3.27}$$

$$f(t_i, C_i) = \frac{1}{V}(n(t)pC_a + Q_{in}C_E - Q_{out}C_i), \tag{3.28}$$

$$f(t_i, C_i) = \frac{1}{V}(n(t)pC_a - Q_{out}C_i). \tag{3.29}$$

Assuming that the respiration rate assumed by $p = 0.12\ (L/s)$ and a fraction of the Covid-19 concentration contained inbreathed air $C_a = 0.04$. By employing the classical fourth-order Runge-Kutta method Eqs.3.10-3.17 and the adaptive fourth-order Runge-Kutta method Eqs.3.18-3.29. The number of people in the room is represented using the Lagrange interpolating polynomial and the cubic splines interpolation since the number of people who stay in the room varies over time. The step size of the classical fourth-order Runge-Kutta method and and the adaptive fourth-order Runge-Kutta method are $\triangle t = 0.025$ and $T = 180$.

Simulation 3.19 : an ideal carbon dioxide concentration measurement.

$C_0 = 0.01$ is the ambient carbon dioxide concentration (ppm). The number of people is 50, and ventilation fan level is $8(L/s)$. The analytical solution for this case can be obtained by [5] such as,

$$C(t) = C_E + \frac{npC_a}{Q}[1 - e^{-Qt/V}]. \tag{3.30}$$

Table 3.28 presents the maximum error of the fourth-order Runge-Kutta solution and the adaptive fourth-order Runge-Kutta solution with the analytical solution. As seen in Figure 3.23, the adaptive fourth-order Runge-Kutta solution and the fourth-order Runge-Kutta solution are compared to the analytical solution.

Compares the analytical solution with the classical fourth-order Runge-Kutta method and the Adaptive Runge-Kutta method. In Table 3.28, the maximum error of the classical fourth-order Runge-Kutta method is more than the Adaptive Runge-Kutta method. Figure 3.23 shows the comparison of both approximation techniques.

Table 3.28: The maximum error of the RK4 solution and the ADRK4 solution with the analytical solution.

$\triangle t$	Maximum error RK4	Maximum error ADRK4
0.100	9.6097×10^{-13}	1.1102×10^{-15}
0.050	5.9789×10^{-14}	1.3184×10^{-16}
0.025	3.7192×10^{-15}	1.3878×10^{-16}

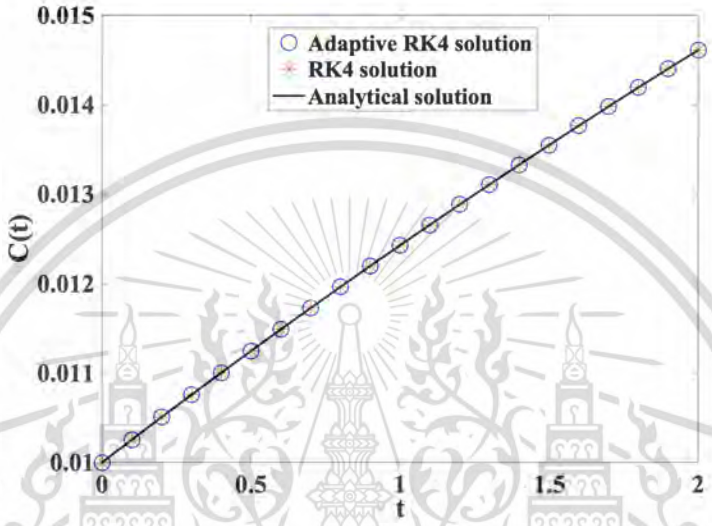

Figure 3.23: The approximated air exhaled indoor concentration in a room $T = 180$.

Simulation 3.20 : the concentration measurement of exhaled air with $n(t)$ is function.

The physical parameters are assumed in Table 3.29. A number of people are assumed by $n(t) = 45 + 5\sin(\pi t)$ is illustrated in Figure 3.24. Figure 3.25 shows the approximated solution.

Table 3.29: Physical parameters.

V	Q_{out}	C_0
75	4	0.01

In reality, people were constantly entering and leaving our room, implying that $n(t)$ is a function. Figure 3.24 shows the number of individuals in the room is between 40 and 50. The approximated air exhaled indoor concentration in a room with $n(t)$ is function as illustrated in Figure 3.25.

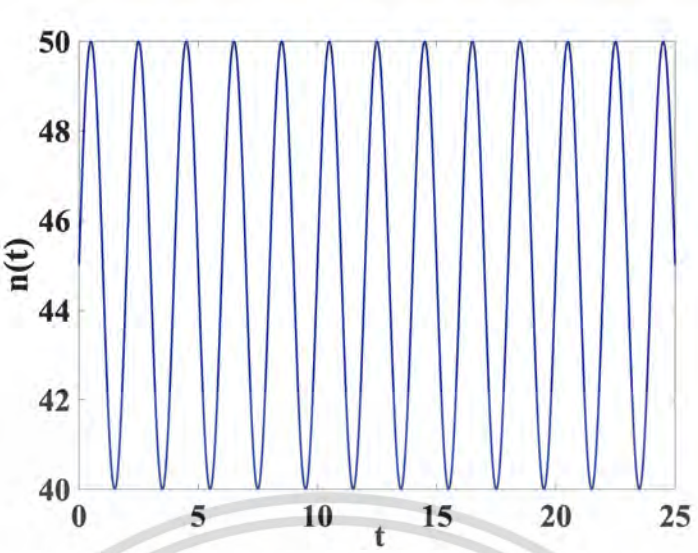

Figure 3.24: A number of people in a room $0 \leq t \leq 25$.

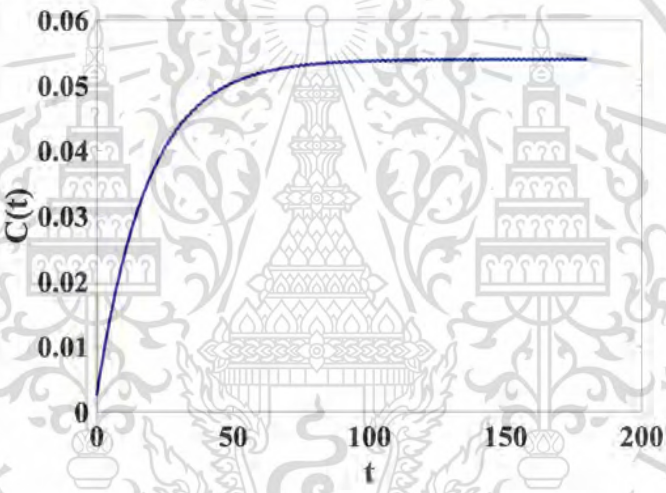

Figure 3.25: The approximated air exhaled indoor concentration in a room with $n(t)$ is function $\triangle t = 0.025$ $T = 180$.

Simulation 3.21 : the concentration measurement of exhaled air with cubic splines interpolation of function $n(t)$.

The physical parameters are assumed in Table 3.30. A number of people are assumed by $n(t) = 45 + 5\sin(\pi t)$. As seen in Figure 3.26, the cubic spline interpolation is compared to the function of $n(t)$. Figure 3.27 shows the approximated solution.

Table 3.30: Physical parameters.

V	Q_{out}	C_0
75	4	0.01

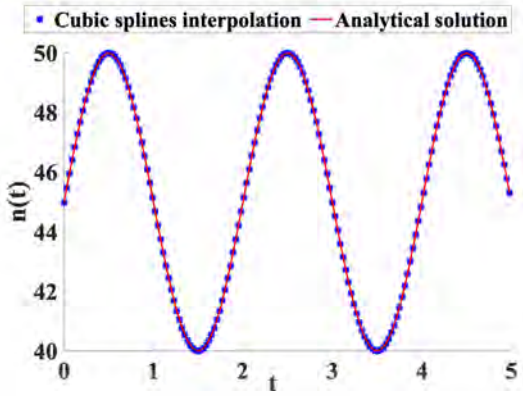

Figure 3.26: The cubic splines interpolation is compared to the function of $n(t)$

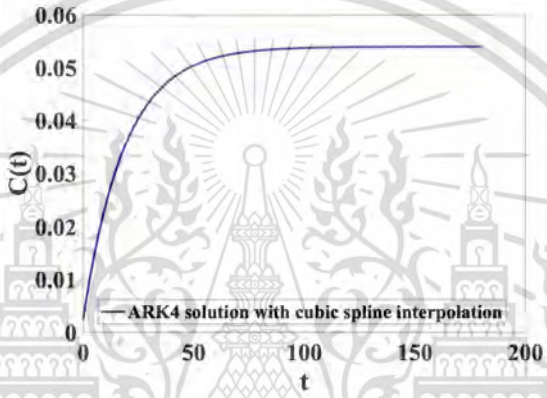

Figure 3.27: The approximated air exhaled indoor concentration in a room with cubic splines interpolation of function $n(t)$ $\triangle t = 0.025$ $T = 180$.

The cubic spline interpolation is used to interpolate the function $n(t)$. Figure 3.26 shows the comparison of the cubic spline interpolation and the exact solution. Figure 3.27 shows the approximated air exhaled indoor concentration in a room with cubic spline interpolation of the function $n(t)$.

Simulation 3.22 : the concentration measurement of exhaled air with lagrange interpolation of function $n(t)$.

The physical parameters are assumed in Table 3.31. A number of people are assumed by $n(t) = 45 + 5\sin(\pi t)$. As seen in Figure 3.28, the lagrange interpolation is compared to the function of $n(t)$. Figure 3.29 shows the approximated solution.

Table 3.31: Physical parameters.

V	Q_{out}	C_0
75	4	0.01

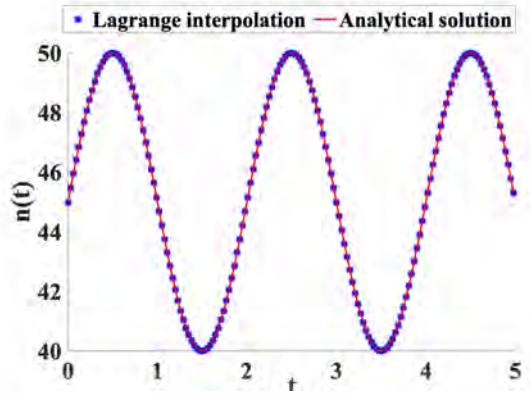

Figure 3.28: The lagrange interpolation is compared to the function of $n(t)$

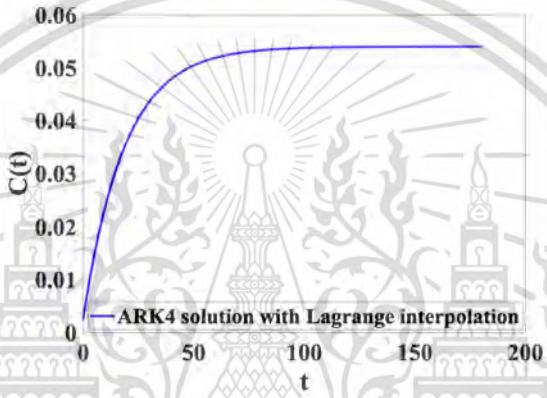

Figure 3.29: The approximated air exhaled indoor concentration in a room with lagrange interpolation of function $n(t)$ $\triangle t = 0.025$ $T = 180$.

Table 3.32: The root mean square error of the cubic splines interpolation and the lagrange interpolation are compared to the function of $n(t)$

RMSE of the lagrange polynomial	RMSE of the cubic splines
3.8748×10^{-5}	1.0157×10^{-7}

The Lagrange interpolation is used to interpolate the function $n(t)$. Figure 3.28 shows the comparison of the Lagrange interpolation and the exact solution. Figure 3.29 shows the approximated air exhaled indoor concentration in a room with the Lagrange interpolation of the function $n(t)$. Table 3.32 shows the root mean square error of both interpolation techniques.

Simulation 3.23 : the risk of normal peoples who staying in a room with infectors.

The initial condition is assumed by $C_0 = 0.01$. The size of the room is 75 (m^3) and ventilation fan levels are assumed in three cases by $0.18, 0.36$, and 0.54 (m^3/min).

As assumed in Table 3.33, the number of people changes over time.

Table 3.33: A number of people $n(t)$.

t	0	20	40	60	80	100	120	140	160	180
$n(t)$	5	10	15	30	45	50	45	30	20	10

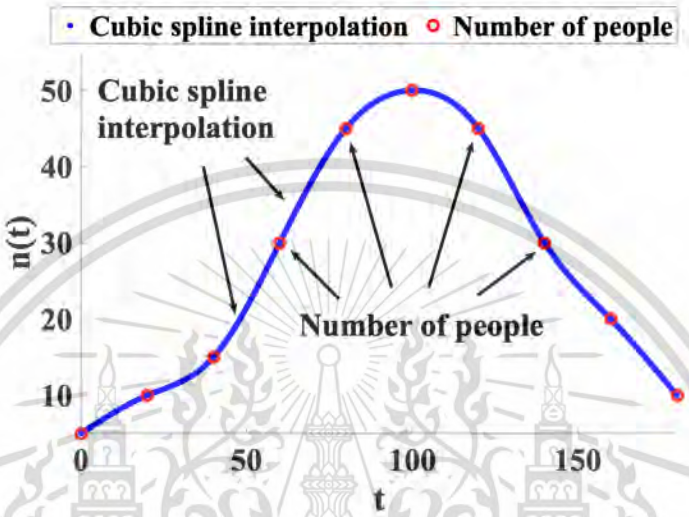

Figure 3.30: The cubic spline interpolation is compared to the number of people

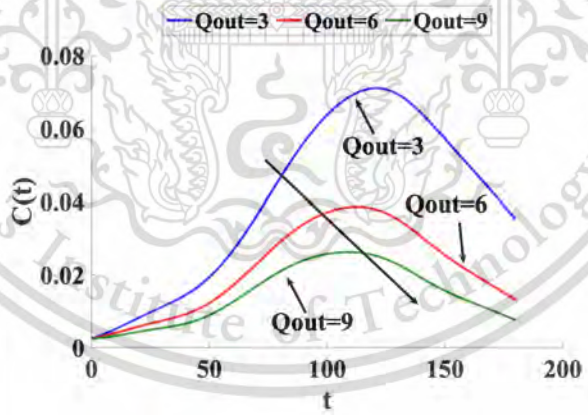

Figure 3.31: The approximated air exhaled indoor concentration in a room with cubic spline interpolation $\triangle t = 0.025$ $T = 180$.

Table 3.34: The approximated air exhaled indoor concentration in a room

t	C		
	$Q_{out} = 3$	$Q_{out} = 6$	$Q_{out} = 9$
20	0.0082	0.0058	0.0044
40	0.0145	0.0092	0.0067
60	0.0267	0.0171	0.0126
80	0.0464	0.0290	0.0209
100	0.0637	0.0371	0.0258
120	0.0711	0.0380	0.0254
140	0.0642	0.0305	0.0192
160	0.0500	0.0211	0.0128
180	0.0352	0.0131	0.0076

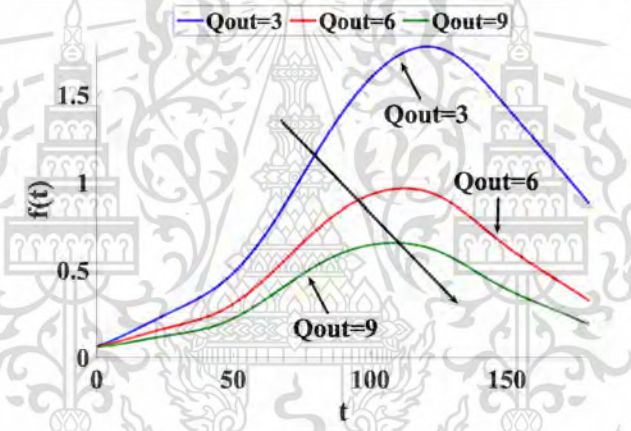

Figure 3.32: The percentage of exhaled air

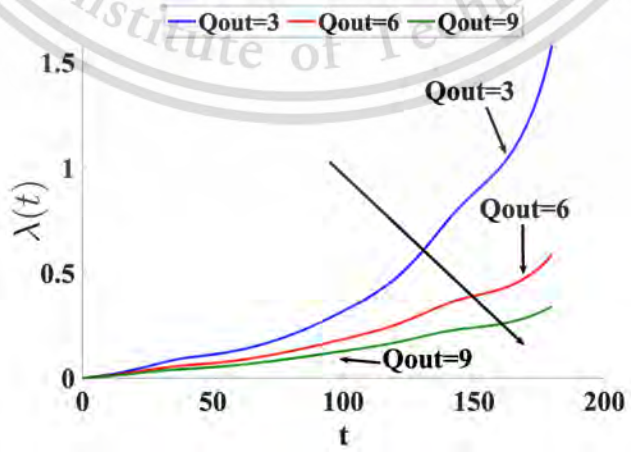

Figure 3.33: The number of airborne infection particles

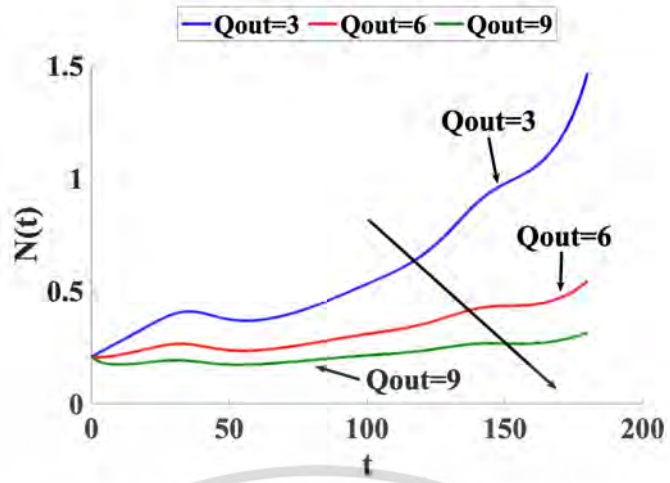

Figure 3.34: The airborne infection particles concentration

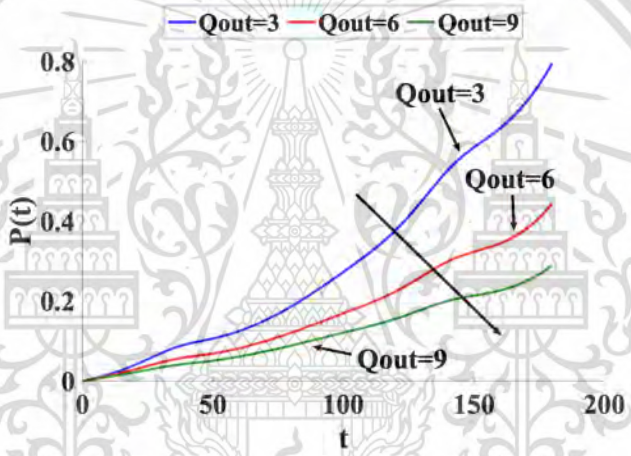

Figure 3.35: The probability of airborne infector

The number of people as illustrated in Table 3.33 and interpolated by the cubic spline interpolation. Fig.3.30 shows the comparison of the cubic spline interpolation and the number of people. Figure 3.31 shows the approximated air exhaled indoor concentration has reduced when outlet ventilation has increased. Figures 3.32-3.35 shows the percentage of exhaled air, the number of airborne infection particles, the airborne infection particles concentration, and the probability of airborne infector.

Chapter 4

A two dimensional mathematical model of airborne infection in an outpatient room with an outlet ventilation system

While normal people remain in the same outpatient room as infectors, this chapter will utilize a two-dimensional mathematical model for estimating the concentration of exhaled air in a space with an outlet ventilation system and the risk of infection. As a result, the exhaled air concentration and infection risk are affected by the initial concentration level, the distance of the seating position, and the rate of ventilation. The forward time center space technique is used to estimate the model solution. A good agreement solution is obtained using the forward time center space. The model can also be used as part of an internet of things (IoT) system to explore inventive ways to infection- free zone management. The proposed strategy represents the balance in the air quality management process between the distance of the seating position and the performance of the air ventilation system for optimal outcomes. We illustrate that the suggested technique works in real-world circumstances.

4.1 The setting of the initial condition

The quantity of exhaled air of one person is 1004.22 ppm, [5]. The quantity of latent exhaled air is 0.00008 ppm, [5]. The available people who are seated in a room Eq.2.56 are assumed by a function,

$$g(x,y,t) = \begin{cases} 0.01, & \text{if} \quad (x,y,t) \in A; \\ 0.00008, & \text{if} \quad (x,y,t) \notin A; \end{cases}$$

where A is a set of seated positions. A is defined by $A = \{(x_i, y_j, t) : x_i$ and y_j are coordinates of seat positions in a room over time $t > 0$, $i = 1, 2, \ \dots \ , K$, $j = 1, 2, \ \dots \ , S$, for all $t > 0$,$\}$ where K is a row number and S is column number i.e. $K \times S$ is a number of seat in the room.

Over time, the exhaled air around the available people seated in a room increases. So, the average exhaled air within 0.5 meters of people who move around the point (x_i, y_j) is defined by a particular example of a two-dimensional Gaussian function,

$$C(x,y,0) = g(x,y,0) \times exp\Big(- \Big(\frac{(x-x_i)}{2\sigma_x^2} + \frac{(y-y_j)}{2\sigma_y^2} \Big) \Big), \tag{4.1}$$

where σ_x and σ_y are the flatten coefficients, and x and y is within 0.5 meters of people who move around the point x_i and y_j.

4.1.1 Boundary conditions approximation

According to the boundary conditions Eqs.(2.57)-(2.60). we can divide Eq.(2.53) into eight cases. The boundary condition is illustrated in Figure 2.7.

Case 1: the bottom left corner boundary condition

If $i = 0$ and $j = 0$, substituting the approximate unknown value of the boundary, we can let $C^n_{i-1,j} = C^n_{i+1,j} - 2\Delta x k_1$ and $C^n_{i,j-1} = C^n_{i,j+1} - 2\Delta y k_3$ and by rearranging, we obtain

$$C^{n+1}_{i,j} = A^n_{i,j} + 2\lambda\left(C^n_{i+1,j} - \Delta x k_1\right) + 2\beta\left(C^n_{i,j+1} - \Delta y k_3\right) + \left(1 - 2\lambda - 2\beta - \frac{\Delta t Q_{out}}{V}\right) C^n_{i,j}, \tag{4.2}$$

Case 2: the bottom boundary condition

If $1 \le i \le M-1$ and $j = 0$, we can let $C^n_{i,j-1} = C^n_{i,j+1} - 2\Delta y k_3$ and by rearranging, we obtain

$$C^{n+1}_{i,j} = A^n_{i,j} + \lambda\left(C^n_{i+1,j} + C^n_{i-1,j}\right) + 2\beta\left(C^n_{i,j+1} - \Delta y k_3\right) + \left(1 - 2\lambda - 2\beta - \frac{\Delta t Q_{out}}{V}\right) C^n_{i,j}, \tag{4.3}$$

Case 3: the bottom right corner boundary condition

If $i = M$ and $j = 0$, we can let $C^n_{i+1,j} = C^n_{i-1,j} + 2\Delta x k_2$ and $C^n_{i,j-1} = C^n_{i,j+1} - 2\Delta y k_3$ and by rearranging, we obtain

$$C^{n+1}_{i,j} = A^n_{i,j} + 2\lambda\left(C^n_{i-1,j} + \Delta x k_2\right) + 2\beta\left(C^n_{i,j+1} - \Delta y k_3\right) + \left(1 - 2\lambda - 2\beta - \frac{\Delta t Q_{out}}{V}\right) C^n_{i,j}, \tag{4.4}$$

Case 4: the left boundary condition

If $1 \le j \le N-1$ and $i = 0$, we can let $C^n_{i-1,j} = C^n_{i+1,j} - 2\Delta y k_1$ and by rearranging, we obtain

$$C^{n+1}_{i,j} = A^n_{i,j} + 2\lambda\left(C^n_{i+1,j} - \Delta y k_1\right) + \beta\left(C^n_{i,j+1} + C^n_{i,j-1}\right) + \left(1 - 2\lambda - 2\beta - \frac{\Delta t Q_{out}}{V}\right) C^n_{i,j}, \tag{4.5}$$

Case 5: the upper left corner boundary condition

If $j = N$ and $i = 0$, we can let $C^n_{i-1,j} = C^n_{i+1,j} - 2\Delta x k_1$ and $C^n_{i,j+1} = C^n_{i,j-1} + 2\Delta y k_4$ and by rearranging, we obtain

$$C^{n+1}_{i,j} = A^n_{i,j} + 2\lambda\left(C^n_{i+1,j} - \Delta x k_1\right) + 2\beta\left(C^n_{i,j-1} - \Delta y k_4\right) + \left(1 - 2\lambda - 2\beta - \frac{\Delta t Q_{out}}{V}\right) C^n_{i,j}, \tag{4.6}$$

Case 6: the upper boundary condition

If $1 \leq i \leq M-1$ and $j = N$, we can let $C^n_{i,j+1} = C^n_{i,j-1} + 2\Delta y k_4$ and by rearranging, we obtain

$$C^{n+1}_{i,j} = A^n_{i,j} + \lambda\left(C^n_{i+1,j} + C^n_{i+1,j}\right) + \beta\left(C^n_{i,j-1} + \Delta y k_4\right) + \left(1 - 2\lambda - 2\beta - \frac{\Delta t Q_{out}}{V}\right) C^n_{i,j}, \tag{4.7}$$

Case 7: the upper right corner boundary condition

If $i = M$ and $j = N$, we can let $C^n_{i+1,j} = C^n_{i+1,j} + 2\Delta x k_2$ and $C^n_{i,j+1} = C^n_{i,j-1} + 2\Delta y k_4$ and by rearranging, we obtain

$$C^{n+1}_{i,j} = A^n_{i,j} + 2\lambda\left(C^n_{i-1,j} + \Delta x k_2\right) + 2\beta\left(C^n_{i,j-1} + \Delta y k_4\right) + \left(1 - 2\lambda - 2\beta - \frac{\Delta t Q_{out}}{V}\right) C^n_{i,j}, \tag{4.8}$$

Case 8: the right boundary condition

If $1 \leq j \leq N-1$ and $i = M$, we can let $C^n_{i+1,j} = C^n_{i-1,j} + 2\Delta x k_2$ and by rearranging, we obtain

$$C^{n+1}_{i,j} = A^n_{i,j} + 2\lambda\left(C^n_{i+1,j} + \Delta x k_2\right) + \beta\left(C^n_{i,j+1} + C^n_{i,j-1}\right) + \left(1 - 2\lambda - 2\beta - \frac{\Delta t Q_{out}}{V}\right) C^n_{i,j}, \tag{4.9}$$

In this chapter, assuming that the latent CO2 concentration in each seat position is equal. Assuming that the respiration rate is $p = 0.12\ (L/s)$, and a fraction of the CO_2 concentration contained in inbreathed air $C_a = 0.04$. By employing the forward time central space method Eqs.2.33-2.37 and the step size of the forward time central space method is $\triangle x = 0.1$, $\triangle y = 0.1$, and $T = 180$.

Simulation 4.1 : the concentration measurement of exhaled air and the probability of airborne infection when normal people sit in every seat.

The parameters and point of the seat are assumed in Tables 4.1-Table 4.2. The boundary conditions and the initial condition are assumed by Eqs.2.56-2.60. Figures 4.1-4.3 present the number of people in the room and the initial condition of the latent CO_2 concentration respectively. The approximated solutions are illustrated in Figures 4.4-4.7. Figures 4.8-4.9 show the line plot of the approximated air exhaled indoor concentration in a room and the line plot of the probability of airborne infection in a room.

Table 4.1: parameter

V	Q_{out}	I	θ	σ_x	σ_y	$\beta - \mu$
72	2	1	0.05	0.5	0.5	2
k_1	k_2	k_3	k_4	K	S	k
0	0	0	0	6	5	0.106×10^{-4}

Table 4.2: Point of the seat

x_i/y_i	1	2	3	4	5
1	(1,1)	(1,2)	(1,3)	(1,4)	(1,5)
2	(2,1)	(2,2)	(2,3)	(2,4)	(2,5)
3	(3,1)	(3,2)	(3,3)	(3,4)	(3,5)
4	(4,1)	(4,2)	(4,3)	(4,4)	(4,5)

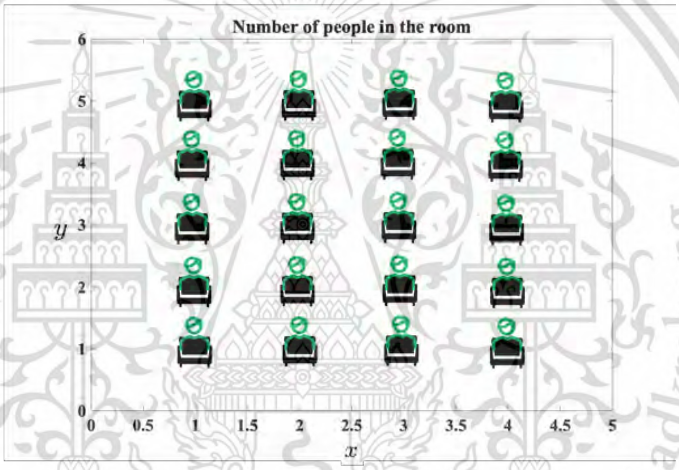

Figure 4.1: The number of people in the room.

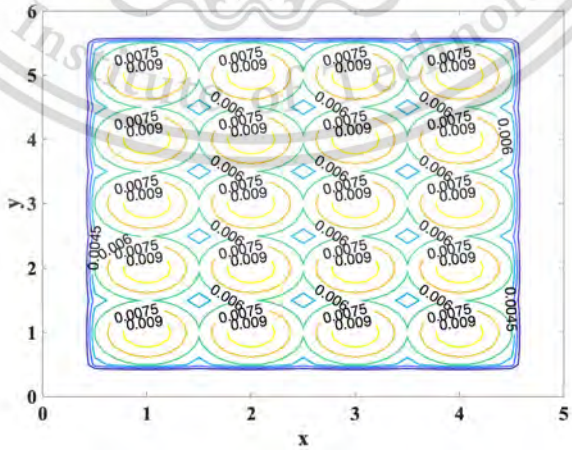

Figure 4.2: The contour plot of the latent CO_2 concentration.

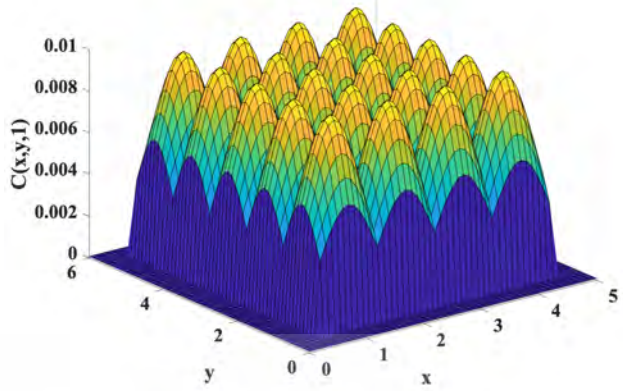

Figure 4.3: The surface plot of the latent CO_2 concentration.

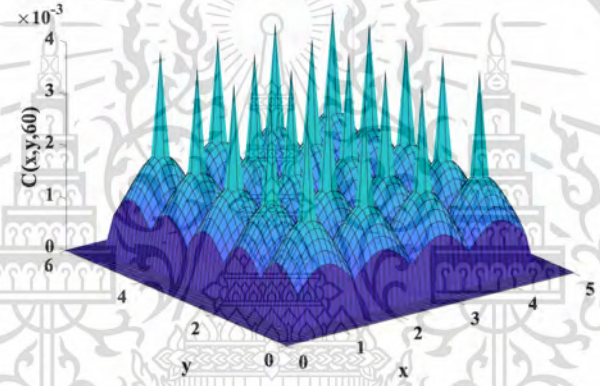

Figure 4.4: The surface plot of the approximated air exhaled indoor concentration around the people who stays in the room at $t = 60$.

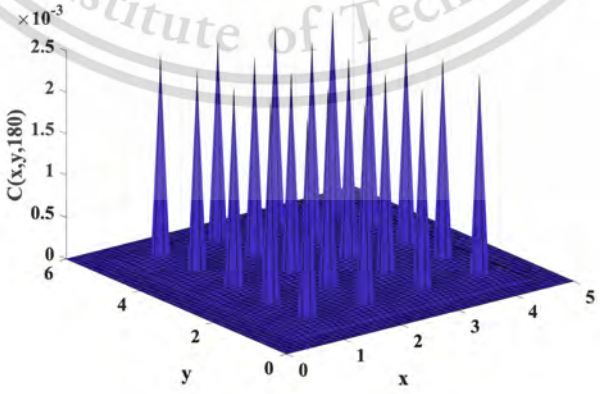

Figure 4.5: The surface plot of the approximated air exhaled indoor concentration around the people who stays in the room at $t = 180$.

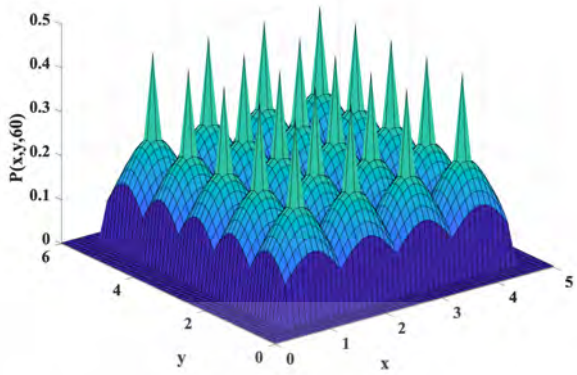

Figure 4.6: The surface plot of the probability of airborne infection around the people who stays in the room at $t = 60$.

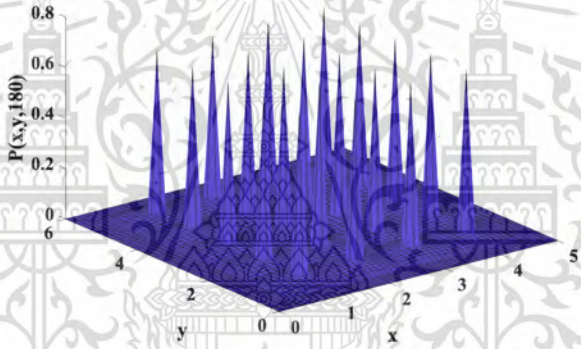

Figure 4.7: The surface plot of the probability of airborne infection around the people who stays in the room at $t = 180$.

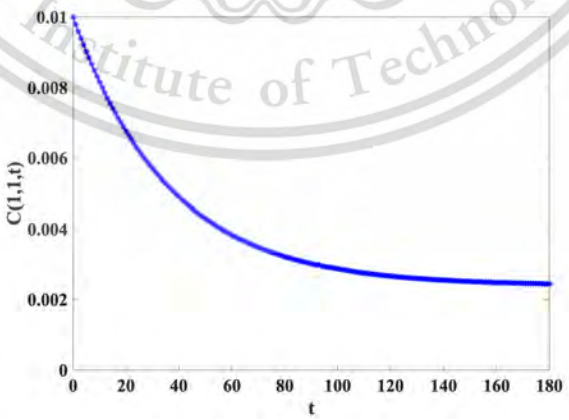

Figure 4.8: The line plot of the approximated air exhaled indoor concentration in a room at $x = 1, y = 1$.

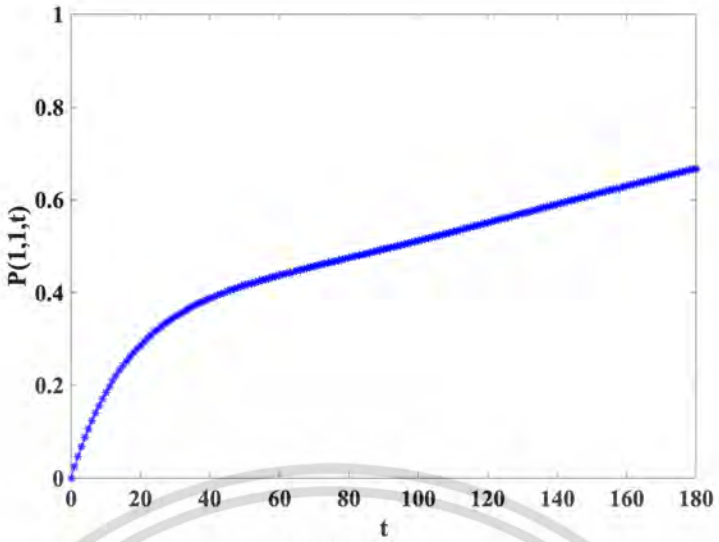

Figure 4.9: The line plot of the probability of airborne infection in a room at $x = 1, y = 1$.

The concentration measurement of exhaled air and the risk of airborne infection when normal people sit in every seat. Figs.4.4-4.5 shows the approximation of the concentration of exhaled air around the people who stays in the room. We can see that the point where the person sits has a carbon dioxide concentration distributed around it. Figs.4.6-4.7 shows the probability of airborne infection. We can see that the risk of airborne infection is spread across the person's sitting position. Fig.4.8 shows the line plot of the approximated air exhaled indoor concentration in a room at x = 1 and y = 1. We can see that when time increases, the concentration of exhaled air is reduced. Fig.4.9 shows the line plot of the probability of airborne infection in a room at x = 1 and y = 1. We can see that when time increases, the probability of airborne infection increases.

Simulation 4.2 : the concentration measurement of exhaled air and the probability of airborne infection when normal people are not seated in the room for all seats.

The parameters and point of the seat are assumed in Tables 4.3-4.4. The boundary conditions and the initial condition are assumed by Eqs.2.56-2.60. Figures 4.10-4.12 present the number of people in the room and the initial condition of the latent CO_2 concentration respectively. The approximated solutions are illustrated in Figures 4.13-4.16. Figures 4.17-4.18 show the line plot of the approximated air exhaled indoor concentration in a room and the line plot of the probability of airborne infection in a room.

Table 4.3: parameter

V	Q_{out}	I	θ	σ_x	σ_y	$\beta - \mu$
72	2	1	0.05	0.5	0.5	2
k_1	k_2	k_3	k_4	K	S	k
0	0	0	0	6	5	0.106×10^{-4}

Table 4.4: Point of the seat

x_i/y_i	1	2	3	4	5
1	(1,1)	–	–	–	(1,5)
2	–	–	(2,3)	–	–
3	–	(3,2)	–	(3,4)	–
4	–	–	(4,3)	–	(4,5)

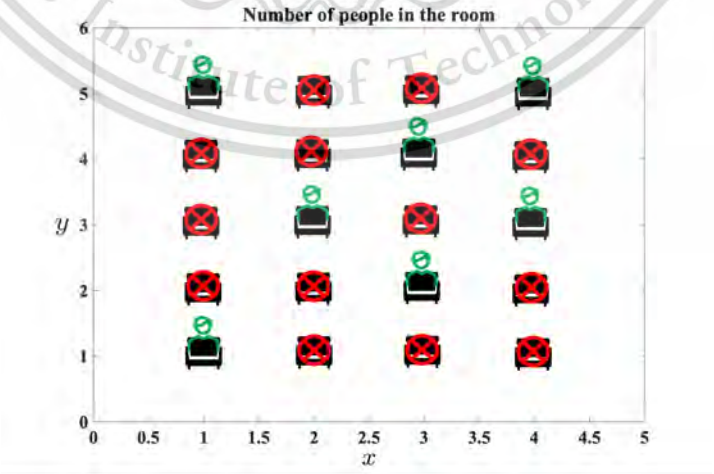

Figure 4.10: The number of people in the room.

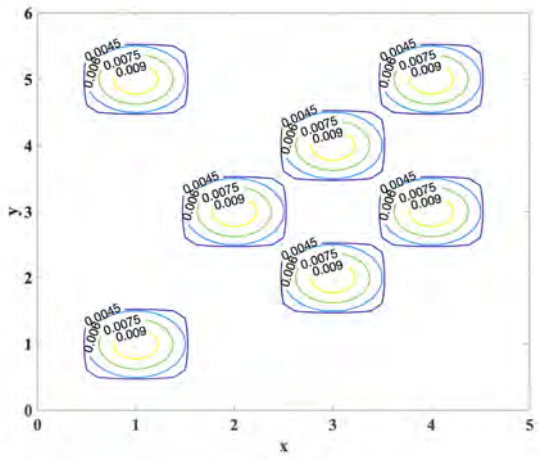

Figure 4.11: The contour plot of the latent CO_2 concentration.

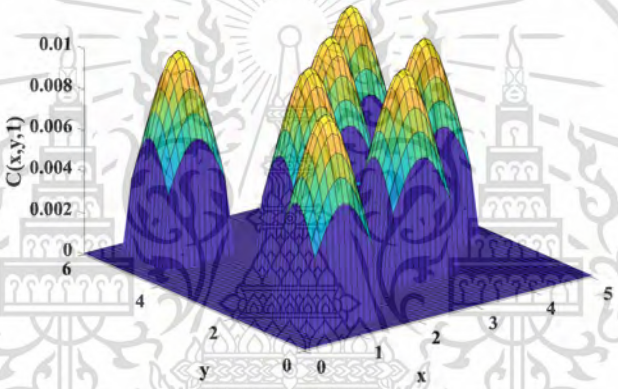

Figure 4.12: The surface plot of the latent CO_2 concentration.

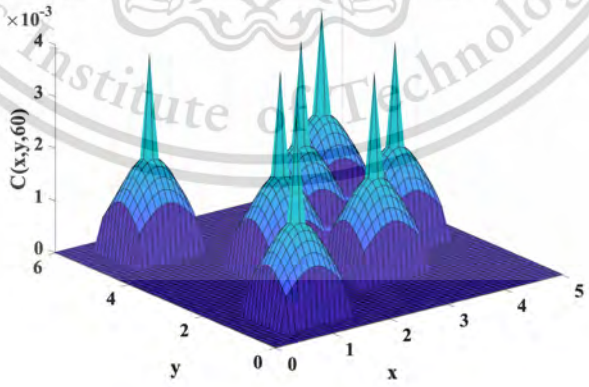

Figure 4.13: The surface plot of the approximated air exhaled indoor concentration in a room around the people who stays in the room at t=60.

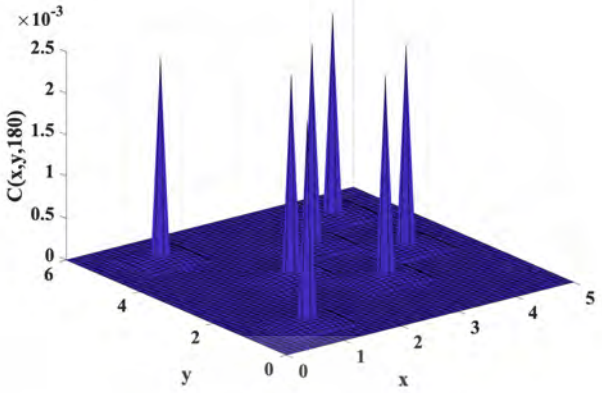

Figure 4.14: The surface plot of the approximated air exhaled indoor concentration in a room around the people who stays in the room at t=180.

Figure 4.15: The surface plot of the probability of airborne infection around the people who stays in the room at t=60.

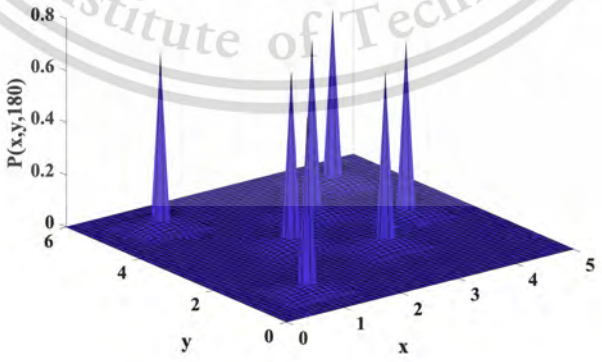

Figure 4.16: The surface plot of the probability of airborne infection around the people who stays in the room at t=180.

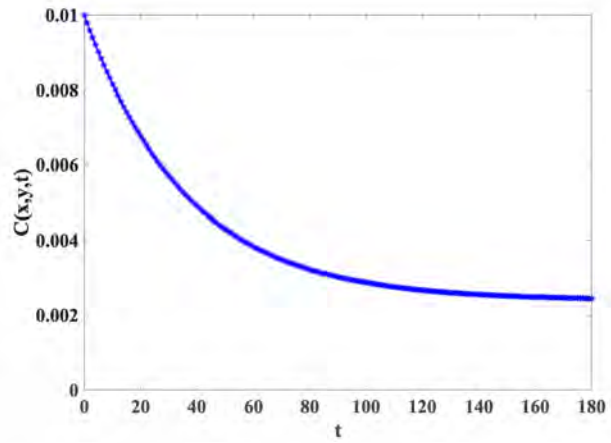

Figure 4.17: The line plot of the approximated air exhaled indoor concentration in a room at $x = 1, y = 1$.

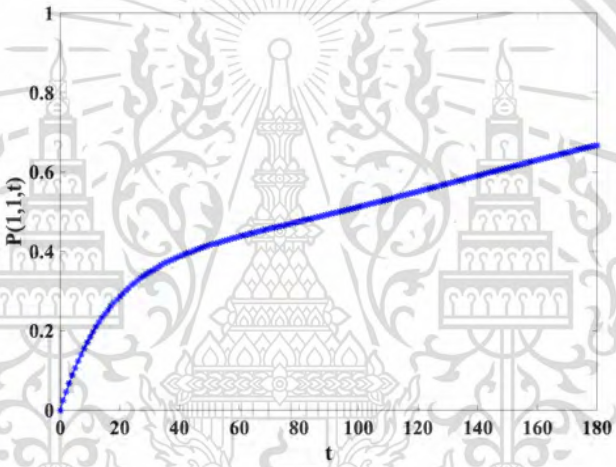

Figure 4.18: The line plot of he probability of airborne infection in a room at x=1, y=1.

The concentration measurement of exhaled air and the risk of airborne infection are proposed when normal people are not seated in the room for all seats. Figs.4.13-4.14 shows the approximation of the concentration of exhaled air when normal people are not seated in the room for all seats. We can see that the point where the person sits has a carbon dioxide concentration distributed around it. Figs.4.15-4.16 shows the probability of airborne infection. We can see that the risk of airborne infection is spread across the person's sitting position. Fig.4.17 shows the line plot of the approximated air exhaled indoor concentration in a room at x = 1 and y = 1. We can see that when time increases, the concentration of exhaled air is reduced. Fig.4.18 shows the line plot of the probability of airborne infection in a room at $x = 1$ and $y = 1$. We can see that when time increases, the probability of airborne infection increases.

Simulation 4.3 : the concentration measurement of exhaled air and the probability of airborne infection when different outlet ventilation levels.

The parameters and point of the seat are assumed in Tables 4.9-4.8. The boundary conditions and the initial condition are assumed by Eqs.2.56-2.60. Figures 4.19-4.21 present the number of people in the room and the initial condition of the latent CO_2 concentration respectively. The approximated solutions are illustrated in Figures 4.22-4.27. Figures 4.28-4.29 show the line plot of the comparison approximated air exhaled indoor concentration and the line plot of the probability of airborne infection in a room.

Table 4.5: parameter

V	Q_{out}	I	θ	σ_x	σ_y	$\beta - \mu$
72	2, 4, 6	1	0.05	0.5	0.5	2
k_1	k_2	k_3	k_4	K	S	k
0	0	0	0	6	5	0.106×10^{-4}

Table 4.6: Point of the seat

x_i/y_i	1	2	3	4	5
1	(1,1)	(1,2)	(1,3)	(1,4)	(1,5)
2	(2,1)	(2,2)	(2,3)	(2,4)	(2,5)
3	(3,1)	(3,2)	(3,3)	(3,4)	(3,5)
4	(4,1)	(4,2)	(4,3)	(4,4)	(4,5)

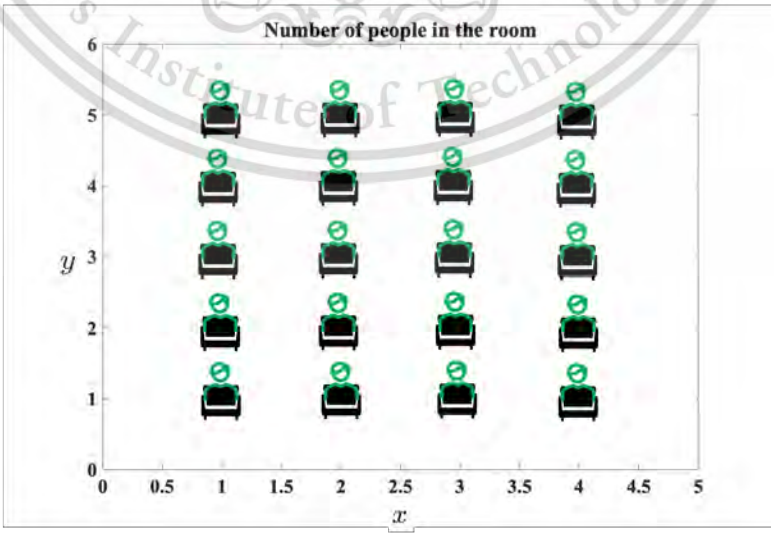

Figure 4.19: The number of people in the room.

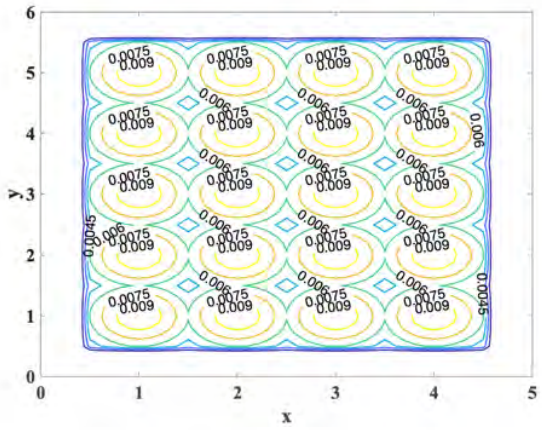

Figure 4.20: The contour plot of the latent CO_2 concentration.

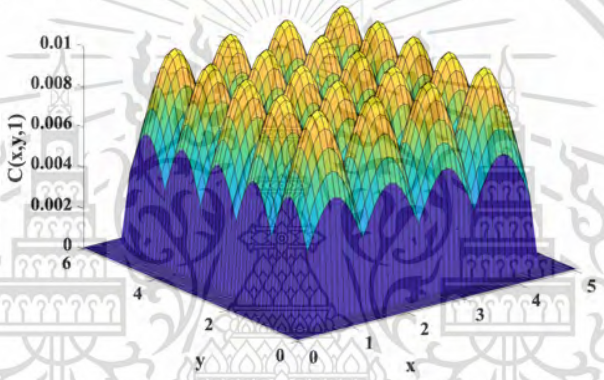

Figure 4.21: The surface plot of the latent CO_2 concentration.

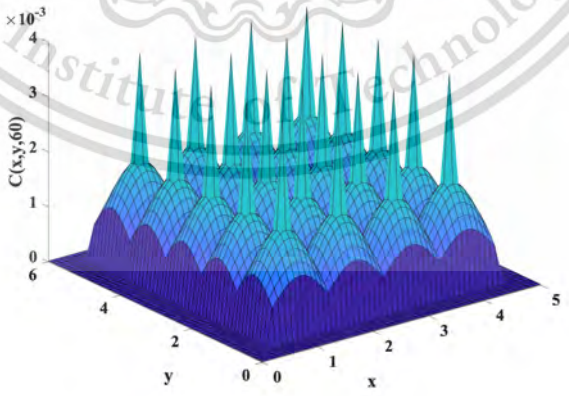

Figure 4.22: The surface plot of the approximated air exhaled indoor concentration in a room around the people who stays in the room at $t = 60$ with the outlet ventilation rate $Q_{out} = 2$.

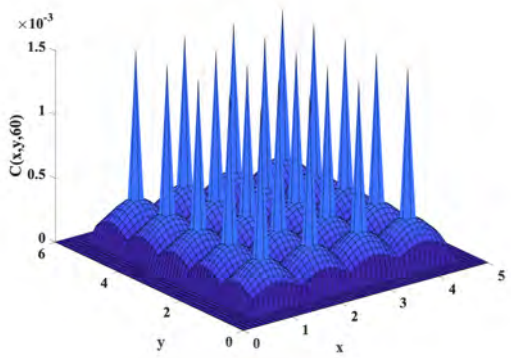

Figure 4.23: The surface plot of the approximated air exhaled indoor concentration in a room around the people who stays in the room at $t = 60$ with the outlet ventilation rate $Q_{out} = 4$.

Figure 4.24: The surface plot of the approximated air exhaled indoor concentration in a room around the people who stays in the room at $t = 60$ with the outlet ventilation rate $Q_{out} = 6$.

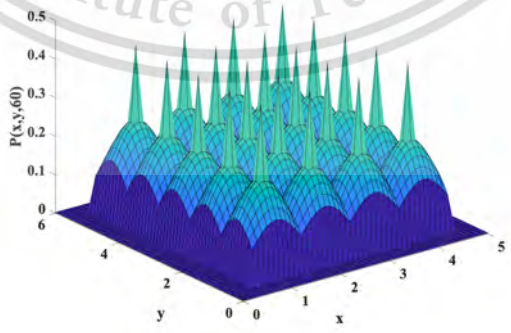

Figure 4.25: The surface plot of the probability of airborne infection around the people who stays in the room at t=60 with the outlet ventilation rate $Q_{out} = 2$.

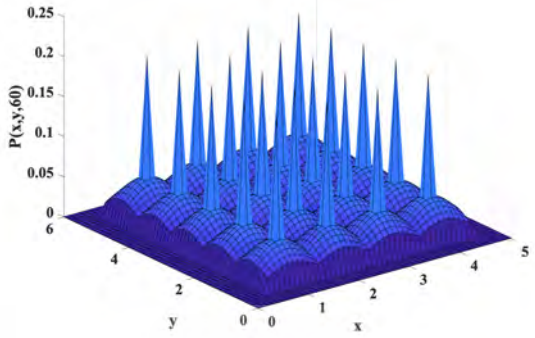

Figure 4.26: The surface plot of the probability of airborne infection around the people who stays in the room at t=60 with the outlet ventilation rate $Q_{out} = 4$.

Figure 4.27: The surface plot of the probability of airborne infection around the people who stays in the room at t=60 with the outlet ventilation rate $Q_{out} = 6$.

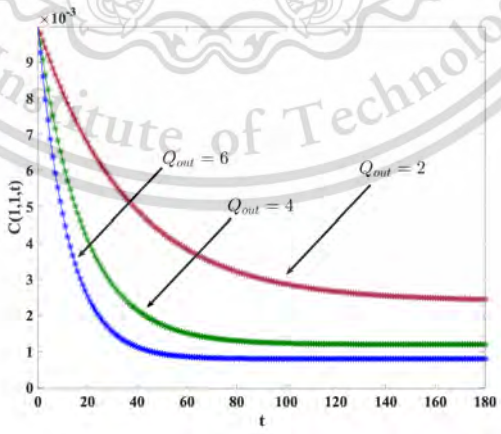

Figure 4.28: The line plot of the comparison approximated air exhaled indoor concentration in a room at x=1, y=1 when the difference outlet ventilation rate.

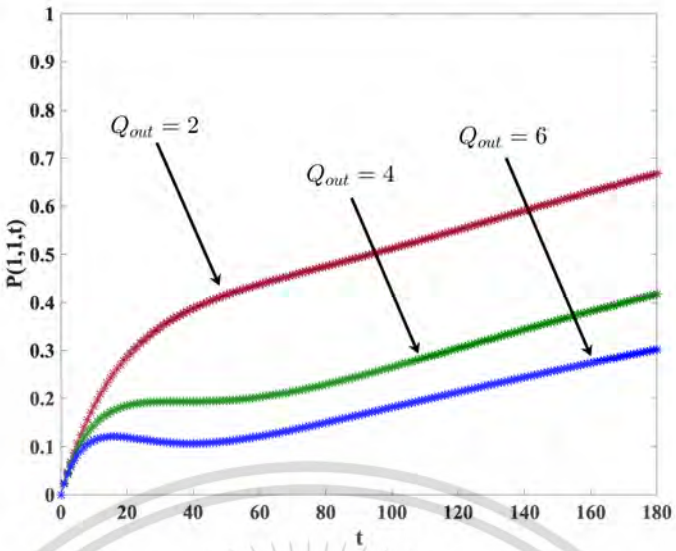

Figure 4.29: The line plot of the comparison probability air exhaled indoor concentration in a room at x=1, y=1 when the difference outlet ventilation rate.

The concentration measurement of exhaled air and the risk of airborne infection are proposed when different outlet ventilation levels. Figs.4.22-4.24 show the approximation of the concentration of exhaled air when outlet ventilation levels are $2, 4$ and 6 respectively. We can see that when the outlet ventilation level increases, the concentration of exhaled air around the people who stays in the room is reduced. Figs.4.25-4.27 show the probability of airborne infection when outlet ventilation levels are $2, 4$ and 6 respectively. We can see that when the outlet ventilation level increases, the probability of airborne infection around the people who stays in the room is reduced. Fig.4.28 shows the line plot of the comparison the concentration of exhaled air in a room at $x = 1$ and $y = 1$. We can see that when the outlet ventilation level increase, the concentration of exhaled air is reduced. Fig.4.29 shows the line plot of the comparison probability air exhaled indoor concentration in a room at $x = 1$ and $y = 1$. We can see that when the outlet ventilation level increase, the probability of airborne infection is reduced.

Simulation 4.4: the concentration measurement of exhaled air and the probability of airborne infection when normal people sit beside each other.

Table 4.7: parameter

V	Q_{out}	I	θ	σ_x	σ_y	$\beta - \mu$
72	2	1	0.05	0.5	0.5	2
k_1	k_2	k_3	k_4	K	S	k
0	0	0	0	6	5	0.106×10^{-4}

Table 4.8: Point of the seat

x_i/y_i	1	2	3	4	5
1	(1,1)	(1,2)	(1,3)	(1,4)	(1,5)
1.5	(1.5,1)	-	-	-	-
2	(2,1)	(2,2)	(2,3)	(2,4)	(2,5)
3	(3,1)	(3,2)	(3,3)	(3,4)	(3,5)
4	(4,1)	(4,2)	(4,3)	(4,4)	(4,5)

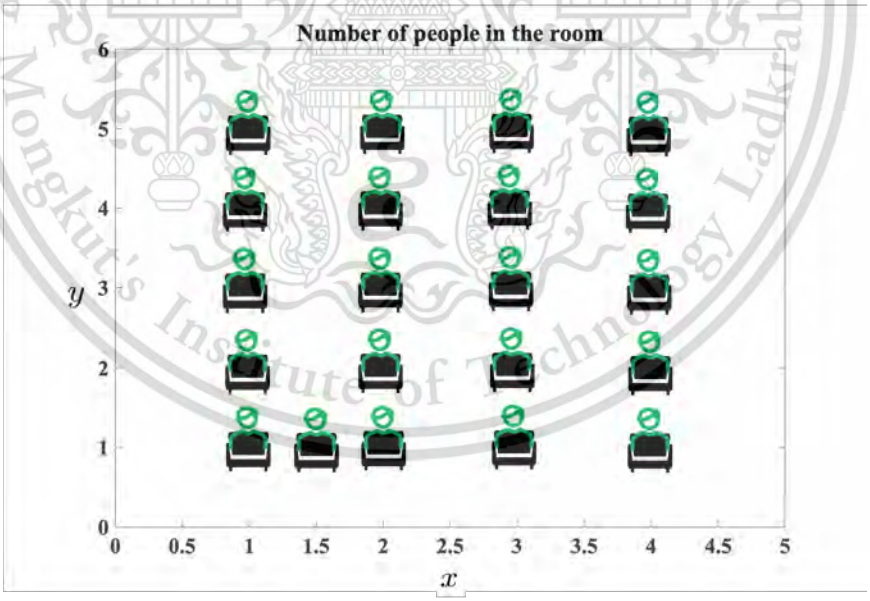

Figure 4.30: The number of people in the room.

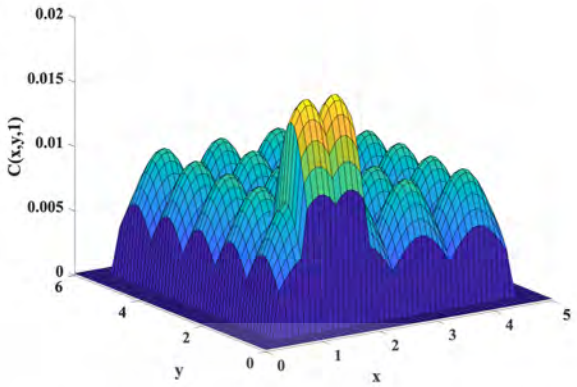

Figure 4.31: The surface plot of the latent CO_2 concentration.

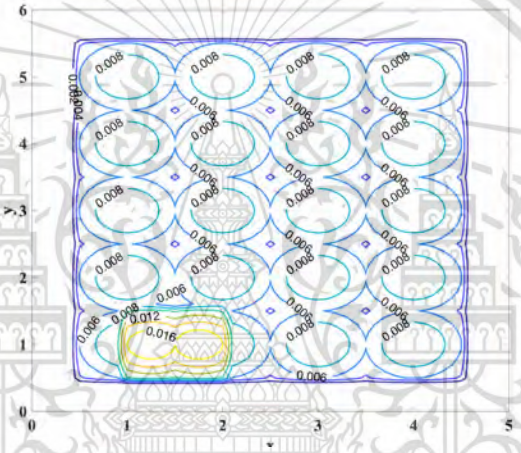

Figure 4.32: The contour plot of the latent CO_2 concentration.

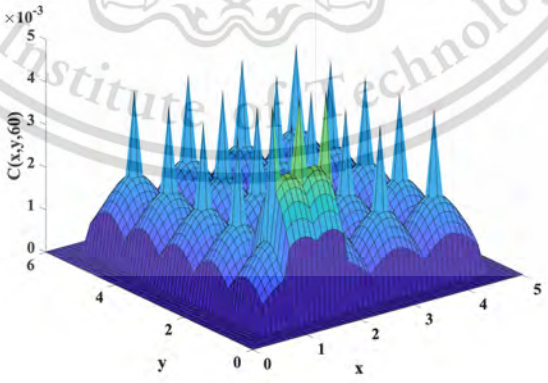

Figure 4.33: The surface plot of the approximated air exhaled indoor concentration around the people who stays in the room at $t = 60$.

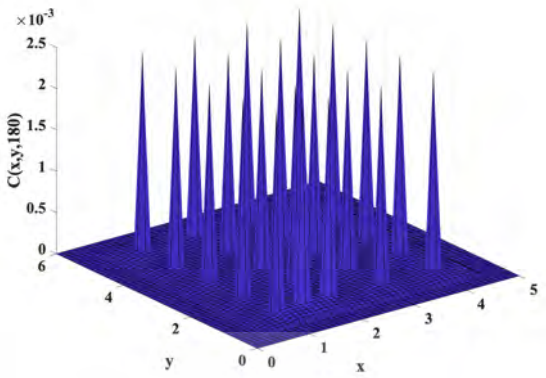

Figure 4.34: The surface plot of the approximated air exhaled indoor concentration around the people who stays in the room at $t = 180$.

Figure 4.35: The surface plot of the probability of airborne infection around the people who stays in the room at $t = 60$.

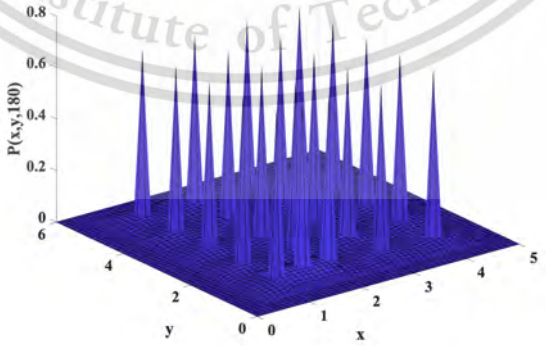

Figure 4.36: The surface plot of the probability of airborne infection around the people who stays in the room at $t = 180$.

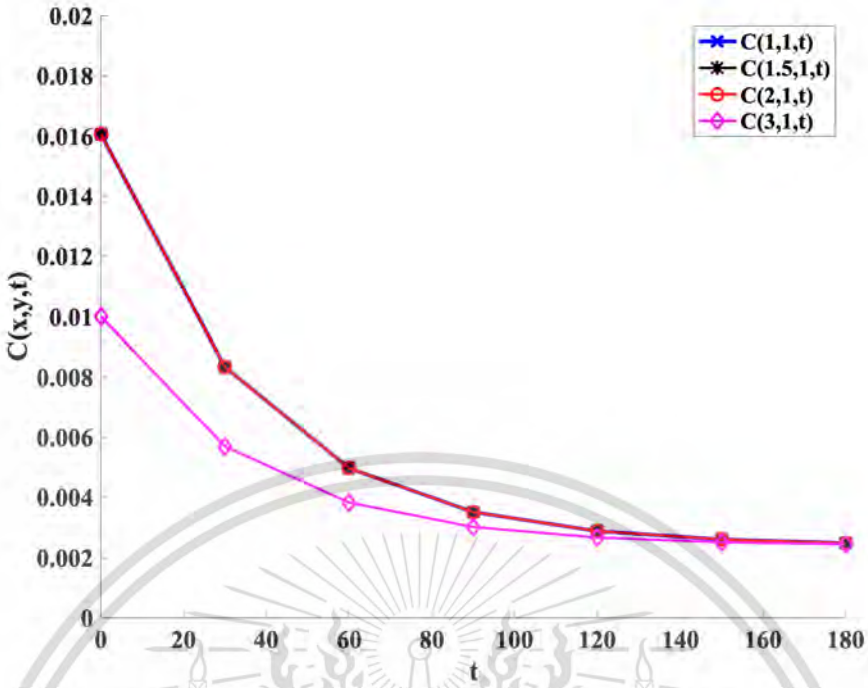

Figure 4.37: The comparison of the approximated air exhaled indoor concentration in a room every half hour.

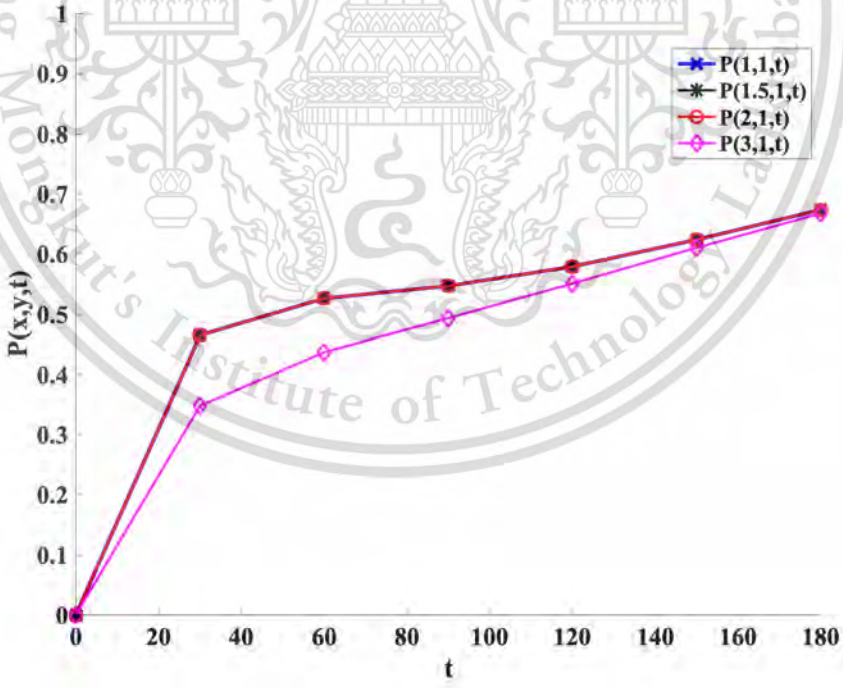

Figure 4.38: The comparison of the probability of airborne infection in a room every half hour.

Table 4.9: The approximated air exhaled indoor concentration in a room

$t_i/C(x_i, y_i)$	$C(1,1)$	$C(1.5,1)$	$C(2,1)$
0	0.0160653065971263	0.0160653065971263	0.0160653065971263
30	0.00833606473256277	0.00833745788249497	0.00833606473256277
60	0.00497693974686963	0.00497814974491216	0.00497693974686963
90	0.00351706624078756	0.00351785443425952	0.00351706624078756
120	0.00288260647088840	0.00288306285295417	0.00288260647088840
150	0.00260687092812793	0.00260711866786667	0.00260687092812793
180	0.00248703660904305	0.00248716571138082	0.00248703660904305

The concentration measurement of exhaled air and the probability of airborne infection, when normal people sit beside each other, are proposed. Figs.4.33-4.34 show the approximation of the concentration of exhaled air when normal people sit beside each other. We can see that when normal people sit beside each other, the concentration of exhaled air around it is increased. Figs.4.35-4.36 show the approximation of the probability of airborne infection when normal people sit beside each other. We can see that when normal people sit beside each other, the probability of airborne infection around it is increased. Fig.4.37 shows the line plot of the comparison of the concentration of exhaled air in a room every half hour. We can see that the approximation of the concentration of exhaled air around normal persons sitting next to one other is greater than sitting 1 meter apart. Fig.4.38 shows the line plot of the comparison of the concentration of exhaled air in a room every half hour. We can see that the probability of airborne infection around normal persons sitting next to one other is greater than sitting 1 meter apart.

Chapter 5

Discussion and conclusion

5.1 Discussion

5.1.1 Discussion of a numerical model of carbon dioxide concentration measurement in a room with an opened ventilation system

In simulation 3.1, the RK4 solution and the analytical solution is used Eq.(2.1), The comparison of approximation techniques shows that the accuracy of the RK4 method. The RK4 method gives accurately approximated carbon dioxide concentration.

In simulation 3.2, we can see that the carbon dioxide concentration along with the starting and the middle of the simulation depends on the potential concentration level. The carbon dioxide concentration for each case becomes close to 0.014 around 1.5 hours, the approximate RK4 solutions when $C(0)$ is divided by a half for each case and assume the number of people $n(t) = 5$.

In simulation 3.3, we can see that the carbon dioxide concentration along with the starting and the middle of the simulation depends on the potential concentration level and the number of people. When the number of people increases the carbon dioxide concentration is increases. The carbon dioxide concentration for each case becomes close to 0.065 around 1.5 hours, the approximate RK4 solutions when $C(0)$ is divided by a half for each case and assume the number of people $n(t) = 50$.

In simulation 3.4, when the inlet ventilation rate less than the outlet ventilation rate, the carbon dioxide concentration is reduced at $n(t) = 5$, in case $n(t) = 25$ and 50, the carbon dioxide concentration is increases. The carbon dioxide concentration for case 1 becomes close to 0.005 around 1 hours, The carbon dioxide concentration for case 2 becomes close to 0.017 around 1 hours, and The carbon dioxide concentration for case 3 becomes close to 0.033 around 1 hours.

In simulation 3.5, when the number of people is varied, the carbon dioxide concentration of interval $0 - 2$ hours are increases, we can see that the maximum carbon dioxide concentration is 0.062, and the carbon dioxide concentration interval $2 - 3$ hours is reduced, the carbon dioxide concentration in last time is 0.04.

In simulation 3.6, we can see that the carbon dioxide concentration is increases interval $0 - 1$ hours and $2.3 - 3$ hours, when the inlet ventilation rate more than the outlet ventilation rate, but the carbon dioxide concentration reduces interval $1 - 2.3$ hours when the inlet ventilation rate less than the outlet ventilation rate.

In simulation 3.7, when the number of people is varied with the inlet ventilation rate less than the outlet ventilation, the carbon dioxide concentration around interval $0-2$ hours are increases, we can see that the maximum carbon dioxide concentration is 0.032, and the carbon dioxide concentration around interval $2-3$ hours reduces, the carbon dioxide concentration in last time is 0.015.

In simulation 3.8, the rate of ventilation and the number of people are varied. If the inlet ventilation rate is higher than the outlet ventilation rate, the carbon dioxide concentration will rise. However if the number of people is reduced, the concentration of carbon dioxide is also reduced. In the other hand, if the inlet ventilation rate is smaller than the outlet ventilation rate, the carbon dioxide concentration would decrease. On the other hand, if the inlet ventilation rate is less than the outlet ventilation rate, then the carbon dioxide concentration becomes reducing. However, if the number of people is increased, then the carbon dioxide concentration is also increasing.

In simulation 3.9, assume the number of people $n(t) = 20 + 5\sin(\pi t)$, we can see that the carbon dioxide concentration depends on the number of people.

5.1.2 discussion of a mathematical model of risk assessment on airborne Infection in a room with an outlet ventilation system

In simulation 10, the exhaled air concentration the simulation depends on the number of persons in a room. If the number of persons in the room increases, the exhaled air concentration will increases.

In simulation 3.11, the exhaled air concentration along with the starting and the middle of the simulation depends on the potential concentration level. The exhaled air concentration for each case becomes close to 0.060 around 1.5 hours.

In simulation 3.12, the exhaled air concentration the simulation depends on the outlet ventilation level. If the outlet ventilation level is increased, the exhaled air concentration is reduced.

In simulation 3.13, the exhaled air concentration along with the starting and the middle of the simulation depends on the room sizes. If the room sizes are increased, the exhaled air concentration is reduced.

In simulation 3.14, the exhaled air concentration of the simulation depends on the various number of persons in time. The exhaled air concentration of interval $0-2$ hours is increased and the exhaled air concentration interval $2-3$ hours are reduced.

In simulation 3.15, the exhaled air concentration when the number of persons is varied with the out ventilation level depends on the staying number of persons in the room. If we change the outlet ventilation level varies on the number of persons,

the exhaled air concentration values will change.

In simulation 3.16, the risk of infectors depends on the number of infectors in the room. If we change the number of infectors in the room, the risk of infection will change. We can see that the more time spent in the room, the greater the risk of infection.

In simulation 3.17, the risk of infectors depends on the number of vaccinated persons constantly staying in a room. In case $\beta - \mu = 2$, the risk of infection is very low, when compared to cases $\beta - \mu = 20$ and $\beta - \mu = 10$. When a person gets an effective vaccine, the risk of infection is low.

In simulation 3.18, the risk of vaccinated people remaining in a room containing infectors is related to the number of persons staying. If we change the number of vaccinated persons in the room, the risk of infection will change. At intervals of 2.4 – 3.0 hours, the number of vaccinated persons is reduced, and the risk of infection is reduced.

5.1.3 Discussion of a risk assessment model for airborne infection in a ventilated room using the adaptive Runge-Kutta method with Cubic Spline interpolation

Simulation 3.19 compares the analytical solution with the classical fourth-order Runge-Kutta method and the Adaptive Runge-Kutta method. The maximum error of the classical fourth-order Runge-Kutta method is more than the Adaptive Runge-Kutta method.

Simulation 3.20, in reality, people were constantly entering and leaving our room, implying that $n(t)$ is a function. The approximated air exhaled indoor concentration in a room with $n(t)$ is function, we can see that the approximated air exhaled indoor concentration in a room depends on the function of the number of people.

Simulation 3.21, the cubic spline interpolation is used to interpolate the function $n(t)$. The comparison of the cubic spline interpolation and the exact solution shows the cubic spline interpolation is accurate. The approximated air exhaled indoor concentration in a room with cubic spline interpolation of the function $n(t)$, we can see that the approximated air exhaled indoor concentration in a room depends on the function of the number of people interpolated by the cubic spline.

Simulation 3.22, the Lagrange interpolation is used to interpolate the function $n(t)$. The comparison of the Lagrange interpolation and the exact solution shows the Lagrange interpolation is accurate. The approximated air exhaled indoor concentration in a room with the Lagrange interpolation of the function $n(t)$, we can see that the approximated air exhaled indoor concentration in a room depends on the function of the number of people interpolated by the Lagrange interpolation. The root mean

square error of both interpolation techniques shows that the cubic spline interpolation is accurate more than the Lagrange interpolation.

Simulation 3.23, the comparison of the cubic spline interpolation and the number of people show that the cubic spline interpolation is accurate. The adaptive Runge-Kutta method with cubic spline interpolation is used to approximate air exhaled indoor concentration. The approximated air exhaled indoor concentration has reduced when outlet ventilation has increased.

5.1.4 Discussion of a two dimensional mathematical model of airborne infection in an outpatient room with an outlet ventilation system

In simulation 4.1, the concentration measurement of exhaled air and the risk of airborne infection when normal people sit in every seat. The approximation of the concentration of exhaled air around the people who stays in the room, we can see that the point where the person sits has a carbon dioxide concentration distributed around it. The probability of airborne infection, we can see that the risk of airborne infection is spread across the person's sitting position. The line plot of the approximated air exhaled indoor concentration in a room at x = 1 and y = 1. We can see that when time increases, the concentration of exhaled air is reduced. The line plot of the probability of airborne infection in a room at x = 1 and y = 1. We can see that when time increases, the probability of airborne infection increases.

In simulation 4.2, the concentration measurement of exhaled air and the risk of airborne infection are proposed when normal people are not seated in the room for all seats. The approximation of the concentration of exhaled air when normal people are not seated in the room for all seats, we can see that the point where the person sits has a carbon dioxide concentration distributed around it. The probability of airborne infection, we can see that the risk of airborne infection is spread across the person's sitting position. The line plot of the approximated air exhaled indoor concentration in a room at x = 1 and y = 1. We can see that when time increases, the concentration of exhaled air is reduced. The line plot of the probability of airborne infection in a room at $x = 1$ and $y = 1$. We can see that when time increases, the probability of airborne infection increases.

In simulation 4.3, the concentration measurement of exhaled air and the risk of airborne infection are proposed when different outlet ventilation levels. The approximation of the concentration of exhaled air when outlet ventilation levels are $2, 4$ and 6 respectively, we can see that when the outlet ventilation level increases, the concentration of exhaled air around the people who stays in the room is reduced. The probability of airborne infection when outlet ventilation levels are $2, 4$ and 6 respec-

tively. We can see that when the outlet ventilation level increases the probability of airborne infection around the people who stays in the room is reduced. The line plot of the comparison the concentration of exhaled air in a room at $x = 1$ and $y = 1$. We can see that when the outlet ventilation level increase, the concentration of exhaled air is reduced. The line plot of the comparison probability air exhaled indoor concentration in a room at $x = 1$ and $y = 1$. wW can see that when the outlet ventilation level increase, the probability of airborne infection is reduced.

In simulation 4.4, the concentration measurement of exhaled air and the probability of airborne infection, when normal people sit beside each other, are proposed. The approximation of the concentration of exhaled air when normal people sit beside each other. We can see that when normal people sit beside each other, the concentration of exhaled air around it is increased. The approximation of the probability of airborne infection when normal people sit beside each other. We can see that when normal people sit beside each other, the probability of airborne infection around it is increased. The line plot of the comparison of the concentration of exhaled air in a room every half hour. We can see that the approximation of the concentration of exhaled air around normal persons sitting next to one other is greater than sitting 1 meter apart. The line plot of the comparison of the probability of airborne infection in a room every half hour. We can see that the the probability of airborne infection around normal persons sitting next to one other is greater than sitting 1 meter apart.

5.2 Conclusion

5.2.1 Conclusion of a numerical model of carbon dioxide concentration measurement in a room with an opened ventilation system

A computational model is used in this article to estimate the carbon dioxide concentration in a room with an open ventilation system. Because the number of persons in the room varies, a realistic carbon dioxide concentration measurement model is proposed. We can see that the concentration of carbon dioxide depends on the actual concentration level, the number of persons, and the rate of ventilation. We demonstrate that the proposed technique is applicable to real-world problems using the standard fourth order RK method. In an ideal scenario, the approximated solutions are compared to the analytical solution. It was determined that the numerical model produces good agreement findings. The proposed model in the air quality management process achieves a balance between the number of people allowed to remain in the room and the potential of the air ventilation system.

5.2.2 Conclusion of a mathematical model of risk assessment on airborne infection in a room with an outlet ventilation system

This section can use mathematical analysis to simulate the exhaled air concentration in a space with an outlet ventilation system and the risk of infection while normal people and vaccinated people remain in the same room as infectors. As a result, the exhaled air concentration and infection risk are affected by the actual concentration level, the number of users, and the rate of ventilation. Using the classical fourth-order RK method, we show that the proposed method applies to real-world situations. In the air quality management process, the proposed model achieves a balance between the number of people permitted to stay in the room and the potential of the air ventilation system.

5.2.3 Conclusion of a risk assessment model for airborne infection in a ventilated room using the adaptive Runge-Kutta method with Cubic Spline interpolation

This study will use a mathematical model to predict the concentration of exhaled air in a space with an outlet ventilation system and the risk of infections when healthy people remain in the same room as infected people. As a result, the actual concentration level, the number of users, and the ventilation rate all impact the exhaled air concentration and infection risk. The adaptive Runge-Kutta approach and the classic fourth-order Runge-Kutta method are all used to estimate the model solution. The number of people in the room is represented using the Lagrange interpolating polynomial and the cubic splines interpolation since the number of individuals who stay in the room varies over time. The adaptive Runge-Kutta technique with cubic splines interpolation turns out to be a good agreement solution. The proposed strategy represents the balance in the air quality management process between the number of individuals allowed to stay in the space and the performance of the air ventilation system. For the optimal outcomes, the proposed technique was capable of converting field data from a number of people using cubic splines and adaptive RK methods. The model can also be utilized as a part of an internet of things (IoT) system to develop new approaches to controlling infection-free zones. Due to the proposed numerical enhancement of the adaptive Runge-Kutta technique with cubic spline interpolation, we show that the suggested strategy is effective in real-world scenarios.

5.2.4 Conclusion of a two dimensional mathematical model of airborne infection in an outpatient room with an outlet ventilation system

A two-dimensional mathematical model for predicting the concentration of exhaled air in a room with an outlet ventilation system is introduced. The risk of infection when healthy people remain in the same room as infected people is considered. To predict the exhaled air concentration, we set a 1-meter distance between persons in the room to assess the reduction of the infection risk associated with social distancing measures. A two-dimensional Gaussian function is used to determine the initial conditions. So that the initial carbon dioxide value corresponds to the individual seated in each location within the enclosed area. As a result, the initial concentration level, the distance between persons in the room, the number of users, and the ventilation rate all impact the exhaled air concentration and infection risk. The forward time center space is used to estimate the model solution. The proposed strategy represents a balance in the air quality management process between the distance of individuals allowed to stay in the room and the performance of the air ventilation system. Due to the proposed numerical enhancement of the finite difference technique, we show that the suggested strategy is effective in real-world scenarios.

5.3 Summarize

In this research, we introduce mathematical analysis to simulate the exhaled air concentration in an outpatient room and the risk of infection while normal people and vaccinated people remain in the same room as infectors. In section 1, we proposed a numerical model of carbon dioxide concentration measurement in a room with an opened ventilation system. A numerical model of carbon dioxide concentration measurement is approximated using the classical fourth-order Runge-Kutta method(RK4). In section 2, we proposed a mathematical model of risk assessment for airborne infection in a room with an outlet ventilation system. A mathematical model of risk assessment for airborne infection in a room with an outlet ventilation system is approximated using the classical fourth-order Runge-Kutta method(RK4). In section 3, we proposed a risk assessment model for airborne infection in a ventilated room using the adaptive Runge-Kutta method with cubic spline interpolation. A mathematical model of risk assessment for airborne infection in a room with an outlet ventilation system is approximated using the adaptive Runge-Kutta method(ADRK4). The number of people in the room is represented using the Lagrange interpolating polynomial and the cubic splines interpolation since the number of individuals who stay there varies over time. The adaptive Runge-Kutta technique with cubic splines interpolation turns out to be

a good agreement solution, the proposed technique was capable of converting field data from a number of people using cubic splines and adaptive RK methods.

From the result of the simulation of 3 sections, we can see that the model can be utilized as a part of an Internet of Things (IoT) system to develop new approaches to controlling infection-free zones. In the air quality management process, the proposed model achieves a balance between the number of people permitted to stay in the room and the potential of the air ventilation system. The proposed numerical enhancement of the adaptive Runge-Kutta technique with cubic spline interpolation, we show that the suggested strategy is effective in real-world scenarios.

In the last section, we proposed a two-dimensional mathematical model for predicting the concentration of exhaled air in a room with an outlet ventilation system. A mathematical model of the two-dimensional mathematical model is approximated using the forward time center space(FTCS). To predict the exhaled air concentration, we set a 1-meter distance between persons in the room to assess the reduction of the infection risk associated with social distancing measures. We introduce the initial condition-setting approach, and boundary condition techniques to adjust the case of the study. The proposed strategy represents a balance in the air quality management process between the distance of individuals allowed to stay in the room and the performance of the air ventilation system and we show that the suggested strategy is effective in real-world scenarios.

5.4 Further work

1) We will simulate a three-dimension mathematical model for predicting the concentration of exhaled air in a room
2) We will change the function of the initial conditions.

References

[1] Outpatient and emergency nursing section maharaj nakorn chiang mai hospital. 2022.

[2] William F Ames. *Numerical methods for partial differential equations*. Academic press, 2014.

[3] C. B. Beggs, C.J. Noakes, P. A. Sleigh, L. A. Fletcher, and K. Siddiqi. the transmission of tuberculosis in confined spaces: an analytical review of alternative epidemiological models. *Int. J. Tuberc. Lung Dis*, 7(11):1015–1026, 2003.

[4] RL. Burden and JD. Faires. *Numerical Analysis*. Richard Strtton, nine edition.

[5] M.I. Chacha, M. Nicola, and W. Robin. Modelling the risk of airborne infectious disease using exhaled air. *Journal of Theoretical Biology*, (372):100–106, 2015.

[6] S. C. Chapra. *Applied Numerical Methods with MATLAB for Engineers and Scientists*. McGraw Hill, third edition.

[7] Mahmoud F El-Sharkawy and Mohamed EH Noweir. Indoor air quality levels in a university hospital in the eastern province of saudi arabia. *Journal of family community medicine*, 21(1):39, 2014.

[8] S. J. Emmerich and A. K. Persily. State-of-the-art review of carbon dioxide bemand controlled ventilation technology an application. *NISTIR 6729*, 2001.

[9] H. Furuya. Risk of transmission of airborne infection during train commute based on mathematical model. *Environmental health and preventive medicine*, 12(2):78–83, 2007.

[10] Li G and Jackson CR. Simple, accurate, and efficient revisions to maccormack and saulyev schemes: high peclet numbers. *Applied mathematics and computation*, 186(1):610–622, 2007.

[11] C. M. Liao, C. F. Chang, and H. M. Liang. A probabilistic transmission dynamic model to assess indoor airborne infection risks. *Risk Analysis: An International Journal*, 25(5):1097–1107, 2005.

[12] M. Lygizos, S. V. Shenoi, B. P. Brooks, A. Bhushan, J. C. Brust, D. Zeltenman, and G. H. Friedland. Natural ventilation reduces high tb transmission risk in traditional homes in rural kwazulu-natal. *South Africa. BMC Infect. Dis.*, 13(1):300, 2013.

[13] A. K. Persily. Evaluating building iaq and ventilation with indoor carbon dioxide. *Transactions-American society of heating refrigerating and air conditioning engineers*, (103):193–204, 1997.

[14] H. Qian, Y. Li, W. H. Seto, P. Ching, W. H.Ching, and H. Q. Sun. Natural ventilation for reducing airborne infection in hospitals. *Building and Environment*, 45(3):559–565, 2010.

[15] E. T. Richardson, C. D. Morrow, D. B. Kalil, and L. G. Bekker. Shared air: a renewed focus on ventilation for the prevention of tuberculosis transmission. *PloS One 9*, (5):e96334, 2014.

[16] S. N. Rudnick and D. K. Milton. Rick of indoor airborne infection transmission estimated from carbon dioxide concentration. *Indoor Air*, 13(3):237–245, 2003.

[17] J. Shen, M. Kong, B. Dong, M. J. Birnkrant, and J. Zhang. A systematic approach to estimating the effectiveness of multi-scale iaq strategies for reducing the risk of airborne infection of sars-cov-2. *Building and environment*, 200:107926, 2021.

[18] G. N. Sze To and C. Y. H. Chao. Review and comparison between the wells-riley and dose-response approaches to risk assessment of infections respiratory diseases. *Indoor Air*, 20(1):2–16, 2010.

[19] W. F. Well. *Airborne Contagion and Air Hygiene. An Ecological Study of Droplet infections*. 1995.

[20] Jiali Yao, Jiachen Zhong, and Ning Yang. Indoor air quality test and air distribution cfd simulation in hospital consulting room. *International Journal of Low-Carbon Technologies*, 17:33–37, 2022.

Appendix

Appendix A

Environment and Ecology Research 9(3): 107-113, 2021
DOI: 10.13189/eer.2021.090302

http://www.hrpub.org

A Numerical Model of Carbon Dioxide Concentration Measurement in a Room with an Opened Ventilation System

Wasu Timpitak[1,2], **Nopparat Pochai**[1,2,*]

[1]Department of Mathematics, King Mongkut's Institute of Technology Ladkrabang, Bangkok 10520, Thailand

[2]Centre of Excellence in Mathematics, CHE, Si Ayutthaya Road, Bangkok 10400, Thailand

Received March 5, 2021; Revised June 5, 2021; Accepted June 20, 2021

Cite This Paper in the following Citation Styles

(a): [1] Wasu Timpitak, Nopparat Pochai, "A Numerical Model of Carbon Dioxide Concentration Measurement in a Room with an Opened Ventilation System," Environment and Ecology Research, Vol.9, No.3, pp. 107-113, 2021. DOI: 10.13189/eer.2021.090302

(b): Wasu Timpitak, Nopparat Pochai, (2021). A Numerical Model of Carbon Dioxide Concentration Measurement in a Room with an Opened Ventilation System. Environment and Ecology Research, 9(3), 107-113. DOI: 10.13189/eer.2021.090302

Abstract A vast number of patients visit the facility every day, causing a major air pollution issue that may pose a risk of exposure of respiratory infectious diseases in outpatient rooms and harm human health. TB, COVID-19, MERS, and SARS are dangerous communicable diseases that transmit from person to person through the air or aerosol in a variety of forms, such as coughing, spitting, sneezing, speaking, or through wounds. COVID-19, TB, MERS and SARS are risks and the chances of success toward lethal infection make more patients ill in the hospital. We should also be notified of the care and control of these diseases. As a result, effective air quality monitoring is needed to monitor and reduce the potential for infected air, such as carbon dioxide (CO2) concentrations. Measuring and controlling carbon dioxide in a hospital with a ventilation system where the number of patients in each room varies in time is challenging. In this research, the numerical model of carbon dioxide concentration measurement in a space with an opened ventilation system is proposed. The model sets the concentration of carbon dioxide at any point when the number of people and the rate of ventilation varies. The classical fourth-order Runge-Kutta method is employed to approximate the model solution. There are many cases of scenarios for improving air quality in the proposed simulations. In the air quality management process, the proposed model provides a balance between the number of persons allowed to stay in the room and the capacity of the air ventilation system.

Keywords Airborne, Infectious, Diseases, Ventilation System

1 Introduction

In [1],[2],[3],[4], and [5], they proposed that infectious disease of airborne such as tuberculosis (TB) spread in several gathering locate areas with infectors and poor ventilation per person rates, [1],[2],[3],[4], and [5]. In [6],[7],[8], and [4], they proposed infectors could be dangerous if there no is a high concentration of indoor rebreathed air because it could contain infector-borne infectious particles, which could lead to the spread of airborne infectious diseases like tuberculosis. In [6], and [9], they proposed carbon dioxide be used as an indicator of air quality indoor, built on the notion that people release carbon dioxide at a rate dictated by their body weight and bodily movement, and that levels of carbon dioxide indoor are measured by fresh air clearance. In [6],[10], and [9], they propose carbon dioxide concentration in the air of approximately 400 ppm in a room, but when but people enter it, exhaled air concentration begins to rise, depending on the rate of ventilation per person, the length of the room, and the number of persons who are present in the room, because of their oxygen intake, respiratory quotient, and bodily movement, person in the room add to the rise in rebreathed air. In [4], and [2], they proposed that as the exhaled air concentration in a room rises in the presence of infectors, the probability of vulnerable individuals contracting infectious diseases transmitted by the air, this is because contaminated people's exhaled air also contains con-

tagious airborne particles inside the nuclei with droplets that can stay airborne for extended periods and infect a susceptible person when inhaled. In [2],[11], and [12], they proposed the immune system's condition of the host, host physiology, and the virulence of the Mycobacterium tuberculosis (Mtb) infectious strain are all important factors in the advancement of infection to TB disease.

In [13],they proposed that respiratory activities including talking, coughing, sneezing, and singing may contribute to the formation of respiratory particles. In [14], and [15], they proposed that when a susceptible individual inhales airborne infectious particles, only a proportion of the infectious particles inhaled successfully infiltrate the target region of respiratory tract infection. In [16], they proposed a numerical model that may be used to explain the dynamic dispersion of airborne infectious illnesses in an outpatient room. In [17], and [12], they proposed that infectious particles with a key size range of 1 Mm to 5 Mm had a higher possibility of reaching and depositing on the alveolar area than those with sizes greater than 5 Mm, which are confined in the upper respiratory tract. This means that not all infectious particles absorbed from the air will reach or be kept at the site of infection. As a result, while evaluating the risk of airborne infectious illness, the respiratory deposition fraction of airborne infectious particles must be included. In [19], the main route is a droplet or an airborne transmission, the risk of infection is known to be much lower outside where ventilation is better. As winter approaches in the northern hemisphere, opportunities for socialization and outdoor exercise are becoming more challenging and concerns about the increased risk of COVID-19 transmission are growing. In [20], They proposed that about the efficacy of ventilation systems for human thermal comfort in terms of ceiling height, which contributes to green building architectures. Other advantages of ventilation, which we gain in high-ceilinged dwellings, cannot be overlooked. This would also assist to minimize moisture, smoke, odor, heat, dust, and germs. In this research, several numerical models of carbon dioxide concentration measurement in a room with an opened ventilation system is introduced.

2 The amount of rebreathed air inhaled in the room induce to cause infection.

In general, the rate of exhaled air generation and ventilation per person determine the raised concentration of indoor carbon dioxide [6],[8], and [9]. Because an infected individual's exhaled air contains airborne infectious particles, carbon dioxide levels can be employed as an exhaled air surrogate [6],[7],[9],[4], and [18]. Exhaled air contains approximately 40,000 ppm of carbon dioxide, compared to 400 ppm of carbon dioxide in ambient air [6],[4], and [3].

We assume that an indoor space, such as a room with a volume of V, begins the day with a carbon dioxide concentration of C_E of about 400 ppm and is occupied by a number of people, n. Given the presence of infectors, the concentration of exhaled air that may contain airborne contagious particles may tend to rise in the room, based on the rate of ventilation, Q, and the number of people in the room. We simply assume that persons in the room contribute substantially to the production of carbon dioxide, which serves as an exhaled air marker. The fundamental equation of the accumulation rate exhaled air concentration in a room with carbon dioxide environmental, is equal to the exhaled air rate generated by inhabitants plus the rate of carbon dioxide environmental, minus ventilation rate removes exhaled air:

$$V\frac{dC}{dt} = npC_a + QC_E - QC, \tag{1}$$

where C is the concentration of indoor air exhaled (ppm), p is the rate of breathing(L/s) for each person in the room and C_a is the carbon dioxide fraction included in inbreathed air. t is the duration time and T is the stationery simulation time. Initial condition $C(0) = C_0$ where C_0 is the latent carbon dioxide concentration.

If the value of Q assumed by Q_{in} and Q_{out}, then these values are named the inlet ventilation rate and the outlet ventilation respectively and in a simple scenario, a number of people are unstable then a number of people depend on the time assumed by $n(t)$. In this study preferred to use Eq.(1) as follow:

$$V\frac{dC}{dt} = n(t)pC_a + Q_{in}C_E - Q_{out}C, \tag{2}$$

for all $0 \leq t \leq T$.

3 Numerical technique

A continuous approximation to the solution $C(t)$ will not be obtained; instead, approximations to C will be generated at various values, called mush points, in the interval $[0, T]$.

Once the approximate solution is obtained at the points, the approximate solution at other points in the interval can be found by interpolation. We first make the stipulation that the mesh points are equally distributed throughout the interval $[0, T]$. This condition is ensured by choosing a positive integer N and selecting the mesh points $t_i = a + ih$, for each $i = 0, 1, 2, ..., N$. The common distance between the points $h = (T-0)/N = t_{i+1} - t_i$ is called the step size.

3.1 the classical fourth-order Runge-Kutta method

$$C \cong C_i \tag{3}$$

$$C_{i+1} = C_i + \frac{1}{6}(k_1 + 2k_2 + 2k3 + k_4)h \tag{4}$$

$$k_1 = f(t_i, C_i) \tag{5}$$

$$k_2 = f(t_i + \frac{1}{2}h, C_i + \frac{1}{2}k_1h) \tag{6}$$

$$k_3 = f(t_i + \frac{1}{2}h, C_i + \frac{1}{2}k_2h) \tag{7}$$

$$k_4 = f(t_i + h, C_i + k_3h) \tag{8}$$

from Eq.(2), we get the classical fourth-order RK method

$$\frac{dC}{dt} = f(t_i, C_i) \tag{9}$$

$$f(t_i, C_i) = \frac{1}{V}(n(t)pC_a + Q_{in}C_E - Q_{out}C_i) \tag{10}$$

4 Numerical experiments and results

Assuming that the class room of volume $V = 75\ (m^3)$, each person's breathing rate in the room assumed by $p = 0.12\ (L/s)$ and the carbon dioxide fraction included in inbreathed air $C_a = 0.04$.

4.1 Simulation 1: an ideal carbon dioxide concentration measurement.

Table 1 lists the model's physical parameters. $C_0 = 0.01$ is the ambient carbon dioxide concentration (ppm). The analytical solution for this case can be obtained by [21] such as,

$$C(t) = C_E + \frac{npC_a}{Q}[1 - e^{-Qt/V}]. \tag{11}$$

Table 2 presents the approximated solution's maximum errors. As seen in Fig 1. the approximated solutions are compared to the analytical solution.

Table 1. Physical parameters.

$n(t)$	C_E	Q
50	0.004	8

Table 2. The maximum l_2 norm error of the RK4 solution with the analytical solution.

$\triangle t$	Maximum error
0.100	0.1660×10^{-10}
0.050	0.0146×10^{-10}
0.025	0.0013×10^{-10}

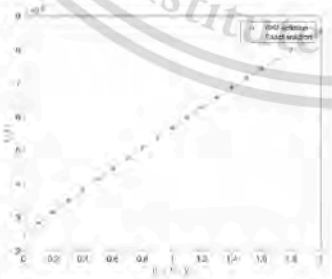

Figure 1. The comparison of the RK4 solution and the analytical solution in a room with a ventilation system $\triangle t = 0.1\ T = 180$.

4.2 Simulation 2: a small number of people in the room carbon dioxide concentration measurement.

Table 3 lists the physical parameters. $C_0 = 0.01$, 0.005, and 0.0025 are the initial carbon dioxide concentrations. We achieve the approximated solutions illustrated in Fig 2 by using the RK4 method Eqs.(3)-(10).

Table 3. Physical parameters.

$n(t)$	C_E	Q_{in}	Q_{out}
5	0.004	8	4

Figure 2. The approximated carbon dioxide concentration in a room with a ventilation system $\triangle t = 0.1\ T = 180$.

4.3 Simulation 3: a large number of people in the room carbon dioxide concentration measurement.

Table 4 lists the physical parameters. $C_0 = 0.01$, 0.005, and 0.0025 are the initial carbon dioxide concentrations. We achieve the approximated solutions illustrated in Fig 3 by using the RK4 method Eqs.(3)-(10).

Table 4. Physical parameters.

$n(t)$	C_E	Q_{in}	Q_{out}
50	0.004	8	4

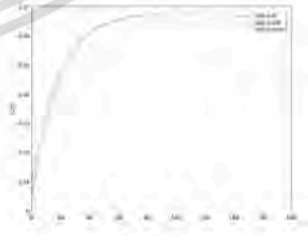

Figure 3. The approximated carbon dioxide concentration in a room with a ventilation system $\triangle t = 0.1\ T = 180$.

4.4 Simulation 4: a different number of people in the room carbon dioxide concentration measurement.

Table 5 lists the physical parameters. $n(t) = 5, 25$ and 50 are a number of people. We achieve the approximated solutions illustrated in Figs 4-6 by using the RK4 method Eqs.(3)-(10).

Table 5. Physical parameters.

C_0	C_E	Q_{in}	Q_{out}
0.01	0.004	4	8

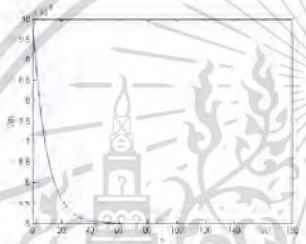

Figure 4. The approximated carbon dioxide concentration in a room with a ventilation system $\triangle t = 0.1$ $T = 180$.

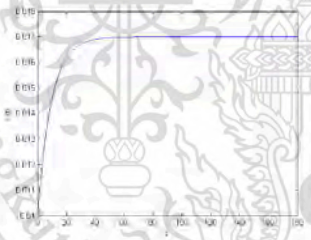

Figure 5. The approximated carbon dioxide concentration in a room with a ventilation system $\triangle t = 0.1$ $T = 180$.

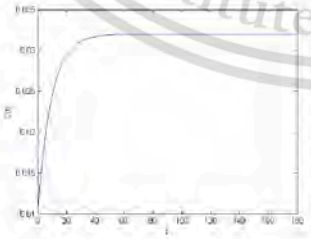

Figure 6. The approximated carbon dioxide concentration in a room with a ventilation system $\triangle t = 0.1$ $T = 180$.

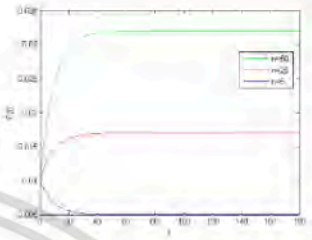

Figure 7. The comparison of RK4 solutions.

4.5 Simulation 5: varying number of people in the room carbon dioxide concentration measurement.

Table 6 lists the physical parameters. A number of people are unstable as show in table 7. We achieve the approximated solutions illustrated in Fig 8 by using the RK4 method Eqs.(3)-(10).

Table 6. Physical parameters.

C_0	C_E	Q_{in}	Q_{out}
0.0025	0.004	8	4

Table 7. A number of people $n(t)$.

t	0	20	40	60	80	100	120	140	160	180
$n(t)$	5	10	15	30	45	50	45	30	20	10

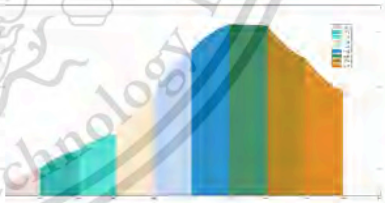

Figure 8. The approximated carbon dioxide concentration in a room with a ventilation system when the number of people are unstable $\triangle t = 0.1$ $T = 180$.

4.6 Simulation 6: changing rate of ventilation in a room carbon dioxide concentration measurement.

Table 8 lists the physical parameters. The rate of ventilations are unstable as show in table 9. We achieve the approximated solutions illustrated in Fig 9 by using the RK4 method Eqs.(3)-(10).

Table 8. Physical parameters.

C_0	C_E	$n(t)$
0.0025	0.004	50

Table 9. The rate of ventilations.

t	0-60	61-140	141-180
$Q_{in}(t)$	8	4	8
$Q_{out}(t)$	4	8	4

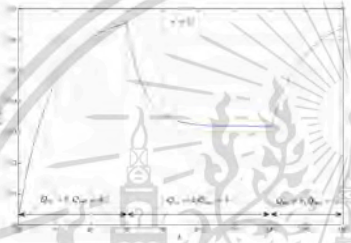

Figure 9. The approximated carbon dioxide concentration in a room with a ventilation system when $n(t)$ is unstable.

4.7 Simulation 7: the varying number of people when the outlet ventilation rate greater than inlet ventilation rate in the room carbon dioxide concentration measurement

Table 10 lists the physical parameters. A number of people are unstable as show in table 11. We achieve the approximated solutions illustrated in Fig 10 by using the RK4 method Eqs.(3)-(10).

Table 10. Physical parameters.

C_0	C_E	Q_{in}	Q_{out}
0.0025	0.004	4	8

Table 11. A number of people $n(t)$.

t	0	20	40	60	80	100	120	140	160	180
$n(t)$	5	10	15	30	45	50	45	30	20	10

Figure 10. The approximated carbon dioxide concentration in a room with a ventilation system when $n(t)$ is unstable.

4.8 Simulation 8: changing rate of ventilation which depends on the number of people in the room carbon dioxide concentration measurement.

Table 12 lists the physical parameters. A number of people and the rate of ventilations are unstable as show in table 12-14. We achieve the approximated solutions illustrated in Fig 11 by using the RK4 method Eqs.(3)-(10).

Table 12. Physical parameters.

C_0	C_E
0.0025	0.004

Table 13. A number of people $n(t)$.

t	0	20	40	60	80	100	120	140	160	180
$n(t)$	5	10	15	30	45	50	45	30	20	10

Table 14. The rate of ventilations.

t	0-60	61-140	141-180
$Q_{in}(t)$	8	4	8
$Q_{out}(t)$	4	8	4

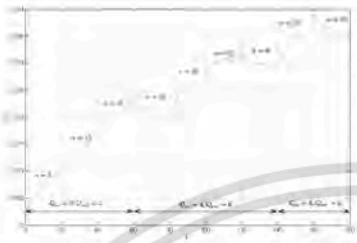

Figure 11. The approximated carbon dioxide concentration in a room with a ventilation system when $n(t)$, Q_{in} and Q_{out} are unstable.

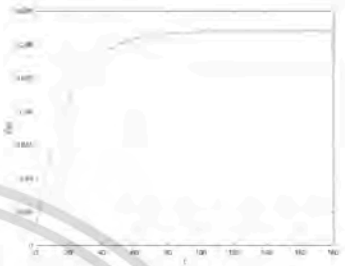

Figure 13. The approximated carbon dioxide concentration in a room with a ventilation system when $n(t) = 20 + 5\sin(\pi t)$.

4.9 Simulation 9: number of people is represented as a function in the room carbon dioxide concentration measurement.

Table 15 lists the physical parameters. A number of people assumed by $n(t) = 20 + 5\sin(\pi t)$ as show in Fig 12. We achieve the approximated solutions illustrated in Fig 13 by using the RK4 method Eqs.(3)-(10).

Table 15. Physical parameters.

C_0	C_E	Q_{in}	Q_{out}
0.0025	0.004	8	4

Figure 12. A number of people in a room $0 \leq n(t) \leq 20$

5 Discussion

In simulation 1, the RK4 solution and the analytical solution is used Eq.(1), The comparison of approximation techniques is illustrated in Fig 3. The RK4 method gives accurately approximated carbon dioxide concentration as show in Table 2.

In simulation 2, we can see that the carbon dioxide concentration along with the starting and the middle of the simulation depends on the potential concentration level. The carbon dioxide concentration for each case becomes close to 0.014 around 1.5 hours, the approximate RK4 solutions when $C(0)$ is divided by a half for each case and assume the number of people $n(t) = 5$ as show in Fig 2.

In simulation 3, we can see that the carbon dioxide concentration along with the starting and the middle of the simulation depends on the potential concentration level and the number of people. When the number of people increases the carbon dioxide concentration is increases. The carbon dioxide concentration for each case becomes close to 0.065 around 1.5 hours, the approximate RK4 solutions when $C(0)$ is divided by a half for each case and assume the number of people $n(t) = 50$ as show in Fig 3.

In simulation 4, when the inlet ventilation rate less than the outlet ventilation rate, the carbon dioxide concentration is reduced at $n(t) = 5$, in case $n(t) = 25$ and 50, the carbon dioxide concentration is increases. The carbon dioxide concentration for case 1 becomes close to 0.005 around 1 hours, The carbon dioxide concentration for case 2 becomes close to 0.017 around 1 hours, and The carbon dioxide concentration for case 3 becomes close to 0.033 around 1 hours. The approximate RK4 solutions when assume $n(t) = 5, 25$ and 50 in 3 case and the inlet ventilation rate less than the outlet ventilation as show in Figs 4-6 and the comparison of 3 cases are illustrated in Fig 7.

In simulation 5, when the number of people is varied, the carbon dioxide concentration of interval $0 - 2$ hours are increases, we can see that the maximum carbon dioxide concentration is 0.062, and the carbon dioxide concentration interval 2-3 hours is reduced, the carbon dioxide concentration in last time is 0.04. The approximate RK4 solutions when $n(t)$ is varied as shown in Fig 8 and the parameter of $n(t)$ as show in

Table 6.

In simulation 6, we can see that the carbon dioxide concentration is increases interval $0-1$ hours and $2.3-3$ hours, when the inlet ventilation rate more than the outlet ventilation rate, but the carbon dioxide concentration reduces interval $1-2.3$ hours when the inlet ventilation rate less than the outlet ventilation rate. The approximate RK4 solutions when the rate of ventilations are unstable as shown in Fig 9 and the parameter of the rate of ventilation as shown in Table 9.

In simulation 7, when the number of people is varied with the inlet ventilation rate less than the outlet ventilation, the carbon dioxide concentration around interval 0-2 hours are increases, we can see that the maximum carbon dioxide concentration is 0.032, and the carbon dioxide concentration around interval 2-3 hours reduces, the carbon dioxide concentration in last time is 0.015. the approximate RK4 solutions when $n(t)$ is varied and the inlet ventilation rate less than the outlet ventilations show in Fig 10 and the parameter of $n(t)$ as show in Table 11.

In simulation 8, the rate of ventilation and the number of people are varied. If the inlet ventilation rate is higher than the outlet ventilation rate, the carbon dioxide concentration will rise. However if the number of people is reduced, the concentration of carbon dioxide is also reduced. In the other hand, if the inlet ventilation rate is smaller than the outlet ventilation rate, the carbon dioxide concentration would decrease. On the other hand, if the inlet ventilation rate is less than the outlet ventilation rate, then the carbon dioxide concentration becomes reducing. However, if the number of people is increased, then the carbon dioxide concentration is also increasing. The approximated RK4 solutions of the simulation are shown in Fig 11 when their parameters are given in Tables 12-14 respectively.

In simulation 9, assume the number of people $n(t) = 20 + 5\sin(\pi t)$, we can see that the carbon dioxide concentration depends on the number of people. The approximate RK4 solutions when $n(t) = 20 + 5\sin(\pi t)$ as show in Fig 13 and the number of people in the room as show in Fig 12.

6 Conclusion

A computational model is used in this article to estimate the carbon dioxide concentration in a room with an open ventilation system. Because the number of persons in the room varies, a realistic carbon dioxide concentration measurement model is proposed. We can see that the concentration of carbon dioxide depends on the actual concentration level, the number of persons, and the rate of ventilation. We demonstrate that the proposed technique is applicable to real-world problems using the standard fourth order RK method. In an ideal scenario, the approximated solutions are compared to the analytical solution. It was determined that the numerical model produces good agreement findings. The proposed model in the air quality management process achieves a balance between the number of people allowed to remain in the room and the potential of the air ventilation system.

Acknowledgment

This paper is supported by the Centre of Excellence in Mathematics, the Commission on Higher Education, Thailand. The author greatly appreciates valuable comments received fro the referees.

REFERENCES

[1] J.R. Andrews, C. Morrow and R. Wood. Modeling the role of public transportation in sustaining tuberculosis transmission in South Africa Am. Vol.177, No.6, 556-561, 2012.

[2] W.F. Well, Airborne Contagion and Air Hygiene. An Ecological Study of Droplet infections, 1995.

[3] S.N. Rudnick, and D.K. Milton. Rick of indoor airborne infection transmission estimated from carbon dioxide concentration, Indoor Air. Vol.13, No.3, 237-245, 2003.

[4] E.T. Richardson, C.D. Morrow, D.B. Kalil, and L.G. Bekker. Shared air: a renewed focus on ventilation for the prevention of tuberculosis transmission, PloS One 9, No.5, e96334, 2014.

[5] L. Gammaitoni, and M.C. Nucci. Using a mathematical model to evaluate the efficacy of TB control measures, Emerg. Infect Dis, N0.3, 335-342, 1997.

[6] S.J. Emmerich, and A.K. Persily, State-Of-The-Art Review of Carbon Dioxide Demand Controlled Ventilation Technology an Application, NISTIR 6729, 2001.

[7] Y. Li, G.M. Leung, J.W. Tang, X. Yang, C.Y.H. Chao, J.Z. Lin, and P.L. Yuen. Role of ventilation in airborne transmission of infectious agents in the built environmental multidisciplinary systematic review, Am. Rev. Respir. Dis, Vol.95, No.3, 435-442, 2007.

[8] M. Murray, O. Oxlade, and H.H. Lin. Modeling social, environmental and biological determinants of tuberculosis, Int. J. Tuberc. Lsang Dis, Vol.15, No.6, S60-S70, 2011.

[9] A.K. Persily. Evaluating building IAQ and ventilation with indoor carbon dioxide, Trans. Am. Soc. Heat. Refrig. Air Cond. Eng. N0.103, 193-204, 1997.

[10] M. Lygizos, S.V. Shenoi, B.P. Brooks, A. Bhushan, J.C. Brust, D. Zeltenman, and G.H. Friedland. Natural ventilation reduces high tb transmission risk in traditional homes in rural Kwazulu-Natal, South Africa. BMC Infect. Dis, Vol.13, No.1, 300, 2013.

[11] H.L. Rieder. Socialization pattens are key to the transmission dynamics of tuberculosis, Int. J. Tuberc. Lung Dis, Vol.3, No.3, 177-178, 1999a.

[12] H.L. Rieder. Epidemiological Basis of Tuberculosis Control (No. Ed. 1), 1-162, 1999b.

[13] R.G. London, and R.M. Roberts. Droplet expulsion from the respiratory tract. Indoor Air, Vol.17, No.1, 2-18, 1967.

[14] C.B. Beggs, C.J. Noakes, P.A. Sleigh , L.A. Fletcher, and K. Siddiqi. the transmission of tuberculosis in confined spaces: an analytical review of alternative epidemiological models, Int. J. Tuberc. Lung Dis, Vol.7, No.11, 1015-1026, 2003.

[15] G.N. Sze To, and C.Y.H. Chao. Review and comparison between the wells-Riley and dose-response approaches to risk assessment of infections respiratory diseases, Indoor Air, Vol.20, No.1, 2-16, 2010.

[16] K. Suebyat, P. Oyjinda, S.A. Konglok, and N. Pochai. A mathematical model for the risk analysis of airborne infectious disease in an Outpatient room with personal classification factor, IAENG, V01.28, No.4, 2020.

[17] C.J. Noakes, and P.A. Sleigh. Mathematical models for assessing the role of airflow on the risk of airborne infection in hospital wards, J. R. Soc. Interface, Vol.6, No.6, S791-S800, 2009.

[18] R. Wood, C. Morrow, S. Ginsberg, E. Piccoli, D. Kalil, A. Sassi, and J.R. Andrews. Quantification of shared air: a social and environmental determinant of airborne disease transmission, PloS One 9, Vol.9, e106622, 2014.

[19] "COVID-19 transmission up in the air" Lancet Infect Dis 2020, late ed., September 2020, vol 8, issue 12, Editorial.

[20] S. Farooq, F. Zubair and M.A. Evaluation of ventilation system efficiency with reference to ceiling height in warm-humid climate of pakistan. Civil Engineering and Architecture Vol. 8(5), pp. 824 - 831, 2020.

[21] Chacha, M.I. Nicola, M. Robin, W. Modelling the risk of airborne infectious disease using exhaled air, Journal of Theoretical Biology, Vol 372, pp. 100-106, 2015.

Engineering Letters, 30:2, EL_30_2_56

A Mathematical Model of Risk Assessment on Airborne Infection in a Room with an Outlet Ventilation System

Wasu Timpitak, and Nopparat Pochai

Abstract—**The airborne infection is spread through the air, especially in indoor spaces. Indoor spaces present a significant risk of infection, although this may be reduced by employing all methodologies to prevent infection via aerosols. TB, COVID-19, MERS, and SARS are all hazardous communicable diseases that spread from person to person through air or aerosol in a variety of ways, including coughing, spitting, sneezing, speaking, or through wounds. COVID-19, TB, MERS, and SARS are all risks, and the elevated risk of a lethal infection leads more patients to become infected in indoor spaces. We should also be notified about the recognition and prevention of these diseases. As a result, proper air quality control, such as carbon dioxide (CO2) concentrations, is needed to monitor and reduce the potential for infected air. It is difficult to assess and monitor carbon dioxide in a room with a ventilation system where the number of people in each room changes frequently. In this research, the numerical model of carbon dioxide concentration measurement in a space with an opened ventilation system is proposed. The model is used to calculate the concentration of carbon dioxide at any time when the number of persons and the rate of ventilation vary. The standard fourth-order Runge-Kutta method is employed to approximate the model solution. There are many scenarios for improving air quality in the suggested simulations. The proposed model for the air quality control system achieves a balance between the number of persons permitted to remain in the room and the air ventilation system's efficiency.**

Index Terms—**airborne, infectious, diseases, ventilation system.**

I. Introduction

INFECTIOUS disease of airborne such as tuberculosis (TB) spread in several gathering locate areas with infectors and poor ventilation per person rates, [1],[2],[3],[4], and [5]. In [6],[7],[8], and [4], they proposed infectors could be dangerous if there no is high concentration of indoor rebreathed air because it could contain infector-borne infectious particles, which could lead to the spreading of airborne infectious illnesses like TB. In [6], and [9], they proposed carbon dioxide(CO_2) be used as an indicator of air quality indoor, built on the notion that people release CO_2 at a rate dictated by their body weight and bodily movement, and that levels of CO_2 indoor are measured by fresh air clearance. In [6],[10], and [9], they propose CO_2 concentration in the air of approximately 400 ppm in a area, but when people enter it, exhaled air concentration begins to rise, depending on the rate of ventilation each person, the length of the room, and the proportion of persons in the area, because of their oxygen intake, respiratory quotient, and bodily movement, the person in the area add to the rise in rebreathed air. In [4], and [2], they proposed that as the exhaled air concentration in a room rises in the presence of infectors, the probability of vulnerable individuals contracting infectious diseases transmitted by the air, this is because contaminated people's exhaled air also contains contagious airborne particles inside the nuclei with droplets that can stay airborne for extended periods and infect a susceptible person when inhaled. In [2] and [11], they proposed that the status of the immunological system of the host, host physiology, and the virulence of the Mycobacterium tuberculosis (Mtb) infectious strain are all important factors in the advancement of infection to TB disease.

In [12], they proposed that sneezing, laughing, singing, and crying would all contribute to the production of respiratory particles. In [13], and [14], they proposed when a susceptible person inhales airborne infectious particles, only a fraction of infective particles inhaled would successfully penetrate the respiratory tract infection's target site. In [15], they proposed a numerical model that can be used to describe the dynamic dispersion of airborne infectious diseases in an outpatient room. In [16], and [17], they proposed a critical scale range of infective particles of 1 Mm to 5 Mm, have a better risk of touching and deposition on the region of the alveoli than those with sizes larger than 5 Mm, which are stuck in the system of upper respiratory, according to the researchers. The respiratory concentration fraction airborne infective particles must also be considered when determining the possibility of airborne infectious disease. In [18], the main route is a droplet or an airborne transmission. Outside, where there is better ventilation, the risk of infection is considered to be much lower. As the northern hemisphere faces winter, opportunities for socialization and outdoor exercise are becoming more challenging and concerns about the increased risk of COVID-19 transmission are growing. In [19], they proposed developing a model for superspreading episodes of infectious diseases based on the SARS epidemic. In [20], they proposed the random forest method to fuse the WRF model, using the atmospheric pollutant concentration and fundamental meteorological parameters training model, and add the atmospheric thermal stability factor as an extra element to model and forecast the municipal PM2.5 concentration. In [21], they proposed that more secure indoor surroundings are required not simply to protect the unvaccinated and those for whom

Manuscript received December 31, 2020; revised May 3, 2022.

This paper is supported by Centre of Excellence in Mathematics, Ministry of Higher Education, Science, Research and Innovation Bangkok, Thailand.

N. Pochai is an Assistant Professor of Department of Mathematics, Faculty of Science, King Mongkut's Institute of Technology Ladkrabang, Bangkok, 10520, Thailand (corresponding author to provide phone: 662329-8400; fax: 662-329-8400; e-mail: nop_math@yahoo.com).

W. Timpitak is a PhD candidate of Mathematics Department, Faculty of Science, King Mongkut's Institute of Technology Ladkrabang, Bangkok, 10520, Thailand (e-mail: zienws@gmail.com).

vaccines have failed but to prevent vaccine-resistant variations or novel airborne dangers from emerging anywhere at a time. Improved interior ventilation and air quality, especially in health, work, and educational institutions, would help us all stay healthy in the present and future. In this research, a mathematical model of risk assessment on airborne infection in a room with outlet ventilation system is introduced.

II. GOVERNING EQUATION

In general, the exhaled air output rate and ventilation per person determine the elevated concentration of indoor CO_2 [6],[8], and [9]. Since particles of infection are found in exhaled air from an infected human, exhaled air can be substituted with CO_2 levels [6],[7],[9],[4], and [22]. Exhaled air comprises around 40,000 ppm of CO_2, equivalent to about 400 ppm of CO_2 in the air of the environment [6],[4], and [3].

We suppose that an indoor area, such as a room with a volume of V, begins the day with an environment CO_2 concentration of C_E roughly 400 ppm and is inhabited by the number of people(n). Given the presence of infectors, the concentration of exhaled air that may include airborne contagious particles may tend to rise in the room, determined by the rate of ventilation (Q) and n. We simply assume that persons in the room make a significant contribution to the production of CO_2, which serves as an exhaled air marker. The general equation of the accumulation rate exhaled air concentration in a room with C_E, is equivalent to the exhaled air rate generated by inhabitants plus the rate of C_E, minus Q removes exhaled air:

$$V\frac{dC}{dt} = np C_a + QC_E - QC, \tag{1}$$

In this research, we focus on airborne infections generated by inhabitants. The fundamental equation of the accumulation rate exhaled air concentration in a room, is equivalent to the exhaled air rate generated by inhabitants minus ventilation rate removes exhaled air is introduced. If the value of Q is assumed by Q_{out}, then this value is named the outlet ventilation rate. In a simple scenario, a number of people are unstable and depend on the time assumed by $n(t)$. This study preferred to use Eq.(1) as follow:

$$V\frac{dC}{dt} = n(t)pC_a - Q_{out}C, \tag{2}$$

for all $0 \leq t \leq T$. Where C is the concentration of air exhaled indoors (ppm), p is the rate of respiration in the room (L/s) for each person and C_a is a fraction of the airborne infection concentration contained inbreathed air. t is the duration time and T is the stationery simulation time. Initial condition $C(0) = C_0$ where C_0 is the latent airborne infection concentration.

A. the volume fraction of exhaled air under unsteady-state

In Eq.(2), calculation of the volume fraction of exhaled air in a room with an outlet ventilation system under unsteady state conditions, we get

$$f(t) = \frac{C(t)}{C_a}. \tag{3}$$

B. The airborne infectious particles concentration

Any infectious particles that become lodged in the upper respiratory tract or other regions of the body may be impacted, even if the probability of infection is virtually nil. Assume that β is the infector's production rate of total released airborne infectious particles and μ is the rate of infectious particles death in the air caused by the infector that cannot be embedded in the alveoli layer. As a result, the rate of survival of airborne infectious particles generated by the infector that reaches its target the infected area of the person who is vulnerable to infection at a threshold value $(\beta - \mu)$ (particles per second) as illustrated in Figure 1.

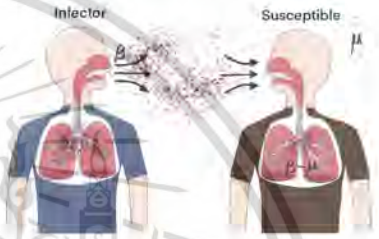

Fig. 1. Movement of airborne infectious particles.

The infection-causing concentration of infectious particles in the air, $N(t)$, is expressed as [23]:

$$N(t) = \frac{If(t)(\beta - \mu)}{np}, \tag{4}$$

where I is the number of people infected inside the room. So, the airborne infectious particles concentration that cause airborne infection unsteady-state conditions are derived by replacing Eq.(3) into Eq.(4):

$$N(t) = \frac{IC(t)(\beta - \mu)}{npC_a}. \tag{5}$$

C. The number of airborne infectious particles

Not that all infected particles can reach the alveolar cavity and deposit there; let θ be the proportion of airborne infected particles that penetrate and deposit at the host's location of the infected area. As a result, the number of airborne infectious particles(λ), inhaled by a susceptible individual and resulting in infection is expressed as [23]:

$$\lambda(t) = pt\theta N(t), \tag{6}$$

where t is the time consumed in the room got to the moment of infection in the room and $(0 < \theta < 1)$.

D. The probability of airborne infectors

In [2],[3] and [23], they proposed tuberculosis transmission follows a Poisson distribution, the probability of airborne infectors is expressed as:

$$P(T \leq t | I, Q, V, p, \theta, \mu, \beta) = 1 - e^{-\lambda(t)}, \tag{7}$$

where P is the probability of susceptible individuals with airborne infectors risk and $T \leq t$ are the random parameters that represent the infection risk for susceptible individuals up to around the time lived in a restricted location during an infected environment.

III. Numerical technique

There will be no continuous approximation to the solution $C(t)$; instead, approximations to C will be constructed at various values as in interval $[0, T]$, known as mush points.

Once the estimated solution at the points is determined, an approximation can be used to find the approximate solution at other points in the interval. We first make the stipulation that the mesh points are distributed equally over the interval $[0, T]$.

This condition is achieved by selecting a positive integer N and the mesh points $t_i = a+ih$, for each $i = 0, 1, 2, ..., N$. The general distance between the points $h = (T-0)/N = t_{i+1} - t_i$ is called the step size.

A. Fourth-Order Runge-Kutta Method

The classical fourth-order Runge-Kutta method is expressed as [24]:

$$C \cong C_i \tag{8}$$

$$C_{i+1} = C_i + \frac{1}{6}(k_1 + 2k_2 + 2k3 + k_4)h \tag{9}$$

$$k_1 = f(t_i, C_i) \tag{10}$$

$$k_2 = f(t_i + \frac{1}{2}h, C_i + \frac{1}{2}k_1 h) \tag{11}$$

$$k_3 = f(t_i + \frac{1}{2}h, C_i + \frac{1}{2}k_2 h) \tag{12}$$

$$k_4 = f(t_i + h, C_i + k_3 h) \tag{13}$$

from Eq.(2), we get the classical fourth-order RK method

$$\frac{dC}{dt} = f(t_i, C_i) \tag{14}$$

$$f(t_i, C_i) = \frac{1}{V}(n(t)pC_a - Q_{out}C_i) \tag{15}$$

IV. Numerical experiments and results

Assuming that the respiration rate assumed by $p = 0.12$ (L/s) and a fraction of the Covid-19 concentration contained inbreathed air $C_a = 0.04$. By employing the classical fourth-order Runge-Kutta method Eqs.8-15.

A. Simulation 1 : The concentration measurement of exhaled air with difference number of people in a room.

The parameters are assumed in Table I. The number of people in the room is assumed in three cases by $n(t) = 5, 25$, and 50. The approximated solutions are illustrated in Figure 2.

TABLE I
PARAMETER

C_E	C_0	V	Q_{out}
0.004	0.0025	75	4

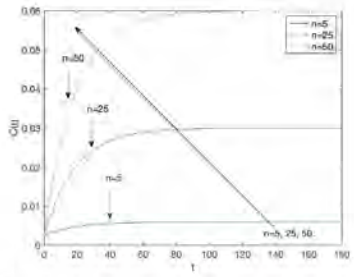

Fig. 2. The approximated air exhaled indoors concentration in a room with difference number of people in a room $\triangle t = 0.05$ $T = 180$.

B. Simulation 2 : The concentration measurement of exhaled air with difference primitive levels.

The parameters are assumed in Table II. The initial condition is assumed in three cases by $C_0 = 0.01, 0.005$ and 0.0025. The approximated solutions are illustrated in Figure 3.

TABLE II
PARAMETER

C_E	$n(t)$	V	Q_{out}
0.004	50	75	4

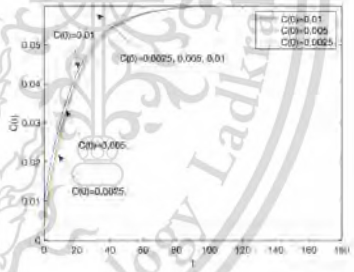

Fig. 3. The approximated air exhaled indoors concentration in a room with difference primitive levels $\triangle t = 0.05$ $T = 180$.

C. Simulation 3 : The concentration measurement of exhaled air when difference outlet ventilation levels.

The parameters are assumed in Table III. The outlet ventilation is assumed in three cases by $Q_{out} = 1, 4$, and 8. The approximated solutions are illustrated in Figure 4.

TABLE III
PARAMETER

C_E	$n(t)$	V	C_0
0.004	50	75	0.0025

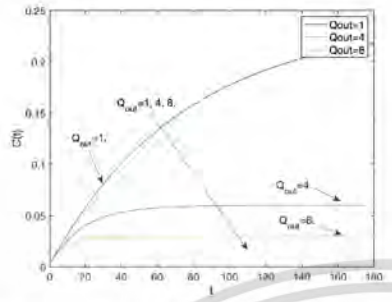

Fig. 4. The approximated air exhaled indoors concentration in a room when difference outlet ventilation levels $\triangle t = 0.05$ $T = 180$.

D. Simulation 4 : The concentration measurement of exhaled air with difference room sizes.

The parameters are assumed in Table IV. The class room of volume is assumed in three cases by $V = 50, 75$, and 100. The approximated solutions are illustrated in Figure 5.

TABLE IV
PARAMETER

C_E	$n(t)$	Q_{out}	C_0
0.004	50	4	0.0025

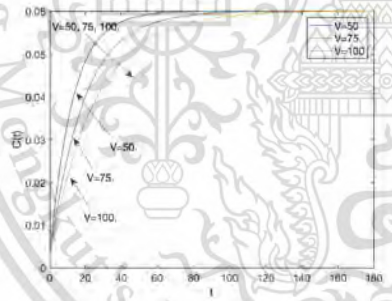

Fig. 5. The approximated air exhaled indoors concentration in a room with difference room sizes $\triangle t = 0.05$ $T = 180$.

E. Simulation 5 : The concentration measurement of exhaled air with varied numbers of people.

The parameters are assumed in Table V. As assumed in Table VI, the number of people changes over time. The approximated solutions are illustrated in Figure 6.

TABLE V
PARAMETER

C_E	V	Q_{out}	C_0
0.004	50	8	0.0025

TABLE VI
A NUMBER OF PEOPLE $n(t)$

t	0	20	40	60	80	100	120	140	160	180
$n(t)$	5	10	15	30	45	50	45	30	20	10

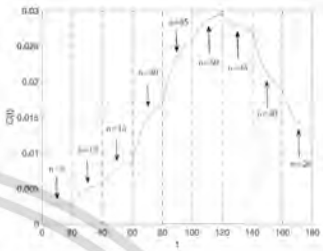

Fig. 6. The approximated air exhaled indoors concentration in a room with varied numbers of people $\triangle t = 0.05$ $T = 180$.

F. Simulation 6 : The concentration measurement of exhaled air when the outlet ventilation levels depend on the stayed number of people.

The parameters are assumed in Table VII. As asumed in Tables VIII-IX, the number of people and the rate of ventilation change over time. The approximated solutions are illustrated in Figure 7.

TABLE VII
PARAMETER

C_E	Q_{out}	C_0
0.004	8	0.0025

TABLE VIII
A NUMBER OF PEOPLE $n(t)$

t	0	20	40	60	80	100	120	140	160	180
$n(t)$	5	10	15	30	45	50	45	30	20	10

TABLE IX
THE RATE OF VENTILATIONS

t	0-60	61-140	141-180
$Q_{out}(t)$	4	8	4

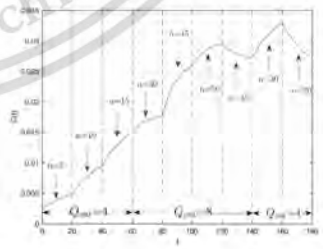

Fig. 7. The approximated air exhaled indoors concentration in a room when the outlet ventilation levels depend on the stayed number of people $\triangle t = 0.05$ $T = 180$.

G. Simulation 7 : The risk of normal peoples who staying in a room with infectors.

The parameters are assumed in Table X. The number of infected people in the room is assumed in three cases by $I = 1, 2,$ and 4. The probability of normal people being infected is illustrated in Figure 8.

TABLE X
PARAMETER

C_E	$n(t)$	Q_{out}	C_0	V	β	μ
0.004	50	4	0.0025	50	30	20

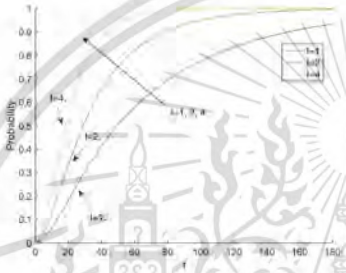

Fig. 8. The risk of normal peoples who staying in a room with infectors $\triangle t = 0.05$ $T = 180$.

H. Simulation 8 : The risk of vaccinated peoples who constantly staying in a room with an infectors.

The parameters are assumed in Table XI. The survival rate of airborne infectious particles is assumed in three cases by $\beta - \mu = 20, 10,$ and 2. The probability of normal people being infected is illustrated in Figure 9.

TABLE XI
PARAMETER

C_E	$n(t)$	Q_{out}	C_0	V	I
0.004	50	4	0.0025	50	1

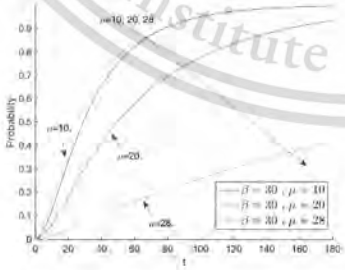

Fig. 9. The risk of vaccinated peoples who constantly staying in a room with an infectors $\triangle t = 0.05$ $T = 180$.

I. Simulation 9 : The risk of vaccinated peoples who varied staying in a room with infectors.

The parameters are assumed in Table XII. As assumed in Table XIII, the number of people changes over time. The probability of normal people being infected is illustrated in Figure 10.

TABLE XII
PARAMETER

C_E	Q_{out}	C_0	V	β	μ	I
0.004	4	0.0025	50	30	20	1

TABLE XIII
A NUMBER OF PEOPLE $n(t)$

t	0	20	40	60	80	100	120	140	160	180
$n(t)$	5	10	15	30	45	50	45	30	20	10

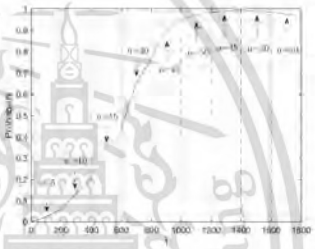

Fig. 10. The risk of vaccinated peoples who varied staying in a room with infectors $\triangle t = 0.05$ $T = 180$.

V. Discussion

In simulation 1. the exhaled air concentration the simulation depends on the number of persons in a room. If the number of persons in the room increases, the exhaled air concentration will increases. Figure 2 illustrates the approximate RK4 solutions when the number of persons is different.

In simulation 2, the exhaled air concentration along with the starting and the middle of the simulation depends on the potential concentration level. The exhaled air concentration for each case becomes close to 0.060 around 1.5 hours.Figure 3 illustrates the approximate RK4 solutions when $C(0)$ is divided by half for each case.

In simulation 3. the exhaled air concentration the simulation depends on the outlet ventilation level. If the outlet ventilation level is increased, the exhaled air concentration is reduced. Figure 4 illustrates the approximate RK4 solutions when the outlet ventilation level is different.

In simulation 4, the exhaled air concentration along with the starting and the middle of the simulation depends on the room sizes. If the room sizes are increased, the exhaled air concentration is reduced. Figure 5 illustrates the approximate RK4 solutions when the different room sizes.

In simulation 5. the exhaled air concentration of the simulation depends on the various number of persons in time. The exhaled air concentration of interval $0 - 2$ hours

is increased and the exhaled air concentration interval $2-3$ hours are reduced. Figure 6 illustrates the approximate RK4 solutions when $n(t)$ is varied in time.

In simulation 6, the exhaled air concentration when the number of persons is varied with the out ventilation level depends on the staying number of persons in the room. If we change the outlet ventilation level varies on the number of persons, the exhaled air concentration values will change. Figure 7 illustrates the approximate RK4 solutions when $n(t)$ is varied with the out ventilation level.

In simulation 7, the risk of infectors depends on the number of infectors in the room. If we change the number of infectors in the room, the risk of infection will change. We can see that the more time spent in the room, the greater the risk of infection. Figure 8 illustrates the risk of normal people staying in a room with infectors.

In simulation 8, the risk of infectors depends on the number of vaccinated persons constantly staying in a room. In case $\beta-\mu=2$, the risk of infection is very low, when compared to cases $\beta-\mu=20$ and $\beta-\mu=10$. When a person gets an effective vaccine, the risk of infection is low. Figure 9 illustrates the risk of vaccinated people who constantly stay in a room with infectors.

In simulation 9, the risk of vaccinated people remaining in a room containing infectors is related to the number of persons staying. If we change the number of vaccinated persons in the room, the risk of infection will change. At intervals of 2.4 – 3.0 hours, the number of vaccinated persons is reduced, and the risk of infection is reduced. Figure 10 illustrates the risk of vaccinated persons who vary their time in a room containing infectors.

VI. Conclusion

This research can use mathematical analysis to simulate the exhaled air concentration in a space with an outlet ventilation system and the risk of infection while normal people and vaccinated people remain in the same room as infectors. As a result, the exhaled air concentration and infection risk are affected by the actual concentration level, the number of users, and the rate of ventilation. Using the classical fourth-order RK method, we show that the proposed method applies to real-world situations. In the air quality management process, the proposed model achieves a balance between the number of people permitted to stay in the room and the potential of the air ventilation system.

References

[1] J. R. Andrews, C. Morrow, and R. Wood, "Modeling the role of public transportation in sustaining tuberculosis transmission in south africa am," *American journal of epidemiology*, vol. 177, no. 6, pp. 556–561, 2013.

[2] W. F. Well, "Airborne contagion and air hygiene. an ecological study of droplet infections," *Airborne Contagion and Air Hygiene. An Ecological Study of Droplet Infections*, 1955.

[3] S. N. Rudnick and D. K. Milton, "Rick of indoor airborne infection transmission estimated from carbon dioxide concentration," *Indoor Air*, vol. 13, no. 3, pp. 237–245, 2003.

[4] E. T. Richardson, C. D. Morrow, D. B. Kalil, and L. G. Bekker, "Shared air: a renewed focus on ventilation for the prevention of tuberculosis transmission," *PLoS One*, vol. 9, no. 5, 2014.

[5] L. Gammaitioni and M. C. Nucci, "Using a mathematical model to evaluate the efficacy of tb control measures," *Emerging infectious diseases*, vol. 3, no. 3, 1997.

[6] S. J. Emmerich and A. K. Persily, "State-of-the-art review of carbon dioxide bemand controlled ventilation technology an application," *NISTIR 6729*, 2001.

[7] Y. Li, G. Leung, J. W. Tang, X. Yang, C. Y. H. Chao, J. Z. Lin, and P. L. Yuen, "Role of ventilation in airborne transmission of infectious agents in the built environmental multidisciplinary systematic review," *Indoor air*, vol. 17, no. 1, pp. 2–18, 2007.

[8] M. Murray, O. Oxlade, and H. H. Lin, "Modeling social, environmental and biological determinants of tuberculosis," *The International Journal of Tuberculosis and Lung Disease*, vol. 15, no. 6, pp. S64–S70, 2011.

[9] A. K. Persily, "Evaluating building iaq and ventilation with indoor carbon dioxide," *Transactions-American society of heating refrigerating and air conditioning engineers*, no. 103, pp. 193–204, 1997.

[10] M. Lygizos, S. V. Shenoi, B. P. Brooks, A. Bhushan, J. C. Brust, D. Zeltenman, and G. H. Friedland, "Natural ventilation reduces high tb transmission risk in traditional homes in rural kwazulu-natal," *BMC infectious diseases*, vol. 13, no. 1, pp. 1–8, 2013.

[11] H. L. Rieder, "Socialization pattens are key to the transmission dynamics of tuberculosis," *The International Journal of Tuberculosis and Lung Disease*, vol. 3, no. 3, pp. 177–178, 1999.

[12] R. G. London and R. M. Roberts, "Droplet expulsion from the respiratory tract," *Indoor Air*, vol. 95, no. 3, pp. 435–442, 1967.

[13] C. B. Beggs, C. Noakes, P. A. Sleigh, L. A. Fletcher, and K. Siddiqi, "the transmission of tuberculosis in confined spaces: an analytical review of alternative epidemiological models," *The international journal of tuberculosis and lung disease*, vol. 7, no. 11, pp. 1015–1026, 2003.

[14] G. N. S. To and C. Y. H. Chao, "Review and comparison between the wells-riley and dose-response approaches to risk assessment of infections respiratory diseases," *Indoor Air*, vol. 20, no. 1, pp. 2–16, 2010.

[15] K. Suebyat, P. Oyjinda, S. A. Konglok, and N. Pochai, "A mathematical model for the risk analysis of airborne infectious disease in an outpatient room with personal classification factor," *Engineering Letters*, vol. 28, no. 4, pp1331-1337, 2020.

[16] C. J. Noakes and P. A. Sleigh, "Mathematical models for assessing the role of airflow on the risk of airborne infection in hospital wards," *Journal of the Royal Society Interface*, vol. 6, no. suppl_6, pp. S791–S800, 2009.

[17] H. L. Rieder, *Epidemiologic Basis of Tuberculosis Control*, one ed. International Union Against Tuberculosis and Lung Disease Paris, 1999.

[18] T. L. R. Medicine, "Covid-19 transmission—up in the air," *The Lancet. Respiratory Medicine*, vol. 8, no. 12, 2020.

[19] T. Mkhatshwa and A. Mummert, "Modeling super-spreading events for infectious diseases: case study sars," *IAENG International Journal of Applied Mathematics*, vol. 41, no. 2, pp82-88, 2010.

[20] N. Jiang, F. Fu, H. Zuo, X. Zheng, and Q. Zheng, "A municipal pm2.5 forecasting method based on random forest and wrf model," *Engineering Letters*, vol. 28, no. 2, pp312-321, 2020.

[21] J. W. Tang, L. C. Marr, Y. Li, and S. J. Dancer, "Covid-19 has redefined airborne transmission," 2021.

[22] R. Wood, C. D. Morrow, S. Ginsberg, E. Piccoli, D. Kalil, A. Sassi, and J. R. Andrews, "Quantification of shared air: a social and environmental determinant of airborne disease transmission," *PloS One 9*, vol. 9, no. 9, 2014.

[23] M. I. Chacha, M. Nicola, and W. Robin, "Modelling the risk of airborne infectious disease using exhaled air," *Journal of theoretical biology*, no. 372, pp. 100–106, 2015.

[24] R. Burden and J. Faires, *Numerical Analysis*. Cengage learning, 2015.

N. Pochai is a researcher of Centre of Excellence in Mathematics, MHESI, Bangkok 10400, Thailand.

W. Timpitak is an assistant researcher of Centre of Excellence in Mathematics, MHESI, Bangkok 10400, Thailand.

IAENG International Journal of Applied Mathematics, 52:4, IJAM_52_4_04

A Risk Assessment Model for Airborne Infection in a Ventilated Room using the Adaptive Runge-Kutta Method with Cubic Spline Interpolation

Wasu Timpitak, and Nopparat Pochai

Abstract—**Bacteria or viruses that are spread by tiny respiratory droplets are known as airborne infections. These infectious vehicles can move along air currents, stay in the air, or stick to surfaces before being inhaled by another person. Airborne transmission may happen across long ranges and time periods. Increased infection rates or clusters of airborne infections are linked to a lack of ventilation or low ventilation rates. While normal people remain in the same room as infectors, this research will utilize a mathematical model for estimating the concentration of exhaled air in a space with an outlet ventilation system, as well as the risk of infection. As a result, the exhaled air concentration and infection risk are affected by the actual concentration level, the number of users, and the rate of ventilation. The adaptive Runge-Kutta technique and the standard fourth-order Runge-Kutta technique are used to estimate the model solution. Because the number of individuals who stay in the space varies over time, the Lagrange interpolating polynomial and cubic splines interpolation are employed to represent the number of individuals in the space. A good agreement solution is obtained using the adaptive Runge-Kutta method with cubic spline interpolation. The proposed strategy represents the balance in the air quality management process between the number of individuals allowed to stay in the space and the performance of the air ventilation system. For the optimal outcomes, the proposed technique was capable of converting field data from a the number of individuals using cubic splines and adaptive RK methods. The model can also be utilized as a part of an internet of things (IoT) system to develop new approaches to controlling infection-free zones. We demonstrate that the proposed strategy works in real-world scenarios.**

Index Terms—**airborne, infectious, diseases, ventilation system.**

I. Introduction

BACTERIA or viruses that are spread by tiny respiratory droplets are known as airborne infections. These infectious vehicles can move along air currents, stay in the air, or stick to surfaces before being inhaled by another person. Airborne transmission may happen across long ranges and time periods. Increased infection rates or clusters of airborne infections are linked to a lack of ventilation or low ventilation rates. TB, COVID-19, MERS, and SARS are all dangerous infectious illnesses that transmit through the air or aerosol in a multitude of ways, including coughing, spitting, sneezing, speaking, or through wounds.

In [1], they proposed the risk of inhalation of indoor airborne infection by using the probability transmission dynamic modeling method. Three examples were estimated using Wells-Riley mathematical models: (1) CO2 exposure concentrations in indoor settings based on epidemiological data, (2) baseline reproduction numbers, and (3) local air variability. The risk of infection in susceptible populations under a variety of scenarios of exposure. Improved indoor ventilation has been demonstrated to minimize the risk of infection in studies. In [2], they proposed the Wells-Riley mathematical model for predicting the risk of influenza infection during train transportation. The marginal incidence of infection rises as the number of people using public transportation rises. Improving ventilation is an efficient method of preventing influenza infection. In [3], they proposed an assessment of the feasibility of using natural ventilation to control infection in naturally ventilated hospital wards in Hong Kong. A high rate of natural ventilation can reduce cross-infection of airborne diseases. In [4], they proposed to develop multilevel IAQ control strategies to reduce the risk of infection in buildings and transport areas. A multi-level IAQ control technique is evaluated for indoor environments, including long-term care facilities such as schools, universities, retail stores, hospitals, and transport areas. Assessing the effectiveness of IAQ control strategies can be used to help address the current challenges of COVID-19. In [5], [6], they proposed that as the exhaled air concentration in a room rises in the presence of infectors, the probability of vulnerable individuals contracting infectious diseases transmitted by the air, this is because contaminated people's exhaled air also contains contagious airborne particles inside the nuclei with droplets that can stay airborne for extended periods and infect a susceptible person when inhaled. In [7], they propose a mathematical model to estimate the risk of transmissible diseases in the air. The calculations revealed that the probability of infection increased when the numeral of ill people and airborne viral infections increased.

In [8], they proposed a numerical model that can be used to describe the dynamic dispersion of airborne infectious diseases in an outpatient room. In [9], they proposed developing a model for superspreading episodes of infectious diseases based on the SARS epidemic. In [10], they proposed the random forest method to fuse the WRF model, using the atmospheric pollutant concentration and fundamental meteo-

Manuscript received March 8, 2022; revised August 8, 2022.

This paper is supported by Centre of Excellence in Mathematics, Ministry of Higher Education, Science, Research and Innovation Bangkok, Thailand.

N. Pochai is an Assistant Professor of Department of Mathematics, Faculty of Science, King Mongkut's Institute of Technology Ladkrabang, Bangkok, 10520, Thailand (corresponding author to provide phone: 662329-8400; fax: 662-329-8400; e-mail: nop_math@yahoo.com).

W. Timpitak is a PhD candidate of Mathematics Department, Faculty of Science, King Mongkut's Institute of Technology Ladkrabang, Bangkok, 10520, Thailand (e-mail: zienws@gmail.com).

rological parameters training model, and add the atmospheric thermal stability factor as an extra element to model and forecast the municipal PM2.5 concentration. While normal people do remain in the same room as infectors, this research will utilize a mathematical model for estimating the concentration of exhaled air in a space with an outlet ventilation system, as well as the risk of infection.

II. GOVERNING EQUATION

CO_2 concentration in the air of approximately 400 ppm in a area, but when people enter it, exhaled air concentration begins to rise, depending on the rate of ventilation each person, the length of the room, and the proportion of persons in the area [11],[12], and [13].

We suppose that an indoor area, such as a room with a volume of V, begins the day with an environment CO_2 concentration of C_E roughly 400 ppm and is inhabited by the number of individuals(n). Given the presence of infectors, the exhale air concentration that may include airborne contagious particles may tend to rise in the room, determined by the rate of ventilation (Q) and n. We simply assume that persons in the room make a significant contribution to the production of CO_2, which serves as an exhaled air marker. The general equation of the accumulation rate exhaled air concentration in a room with C_E, is equivalent to the exhaled air rate generated by inhabitants plus the rate of C_E, minus Q removes exhaled air:

$$V\frac{dC}{dt} = npC_a + QC_E - QC, \tag{1}$$

where C is the exhale air concentration indoor(ppm), C_a is a fraction of the CO_2 contained in inbreathed air and p is the rate of respiration in the room for each person(L/s). t is the duration time and T is the stationery simulation time. Initial condition $C(0) = C_0$ where C_0 is the latent CO_2 concentration.

In this paper, we consider airborne infections generated by inhabitants, and the value of Q is assumed by Q_{out}, then this value is named the outlet ventilation rate. In a simple scenario, the number of people is varied and depends on the time are assumed by $n(t)$. The general equation of the accumulation rate exhaled air concentration in a room with C_E in Eq.(1) can be written as:

$$V\frac{dC}{dt} = n(t)pC_a - Q_{out}C, \tag{2}$$

for all $0 \le t \le T$.

A. The percentage of exhaled air in an unstable state

In Eq.(2), calculation of the percentage of exhaled air in a room with an outlet ventilation system under unsteady state conditions, we get

$$f(t) = \frac{C(t)}{C_a}. \tag{3}$$

B. The airborne infection particles concentration

In [14], [15], they proposed when a susceptible individual inhales the infected particle, a limited amount of contaminated particles may reach the location of the respiratory ailment. This is because the infected particle has varied sizes and deposition percentages in different parts of the respiratory system. In determining the risk of airborne infection the accumulation proportion of airborne infection particles in the airways must also be considered.

Given $(\beta - \mu)$ is the rate of survival of airborne infection particles generated by the infector that reaches its target the infected area of the person who is vulnerable to infection at a threshold value (particles per second) as illustrated in Figure 1,

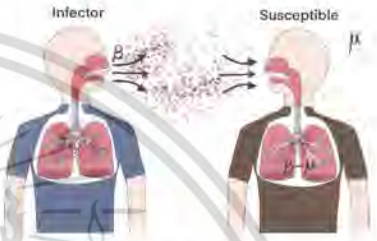

Fig. 1. Movement of airborne infectious particles.

where β is the infector's production rate of total released airborne infection particles and μ is the rate of infected particles death in the air caused by the infector that cannot be embedded in the alveoli layer.

The infection-causing concentration of airborne infection particle, $N(t)$, is expressed as [7]:

$$N(t) = \frac{If(t)(\beta - \mu)}{np}, \tag{4}$$

where I is the number of people infected inside the room. Substituting Eq.(3) into Eq.(4), we obtain the concentration of infectious airborne particles under unstable conditions.

$$N(t) = \frac{IC(t)(\beta - \mu)}{npC_a}. \tag{5}$$

C. The number of airborne infection particle

Not that all infected particles can reach the alveolar cavity and deposit there, let θ be the proportion of airborne infection particles that penetrate and deposit at the host's location of the infected area. As a result, the number of airborne infection particles(λ), inhaled by an individual susceptible and resulting in infection is expressed as [7],

$$\lambda = pt\theta N, \tag{6}$$

where the time consumed (t) in the room got to the moment of infection in the room and $(0 < \theta < 1)$.

D. The probability of airborne infectors

In [7],[6] and [16], they proposed that TB transmission is governed by a Poisson distribution, the probability of airborne infectors is expressed as:

$$P(t) = 1 - e^{-\lambda(t)}, \tag{7}$$

where the probability (P) of susceptible individuals with airborne infectors risk.

III. Numerical technique

There will be no continuous approximation to the solution $C(t)$; instead, approximations to C will be constructed at various values as in interval $[0, T]$, known as mush points.

Once the estimated solution at the points is determined, an approximation can be used to find the approximate solution at other points in the interval. We first make the stipulation that the mesh points are distributed equally over the interval $[0, T]$.

This condition is achieved by selecting a positive integer N and the mesh points $t_i = a+ih$, for each $i = 0, 1, 2, ..., N$. The general distance between the points $h = (T - 0)/N = t_{i+1} - t_i$ is called the step size.

A. The classical fourth-order Runge-Kutta method

The classical fourth-order Runge-Kutta method is expressed as [17],

$$C \cong C_i, \tag{8}$$

$$C_{i+1} = C_i + \frac{1}{6}(k_1 + 2k_2 + 2k3 + k_4)h, \tag{9}$$

$$k_1 = f(t_i, C_i), \tag{10}$$

$$k_2 = f(t_i + \frac{1}{2}h, C_i + \frac{1}{2}k_1h), \tag{11}$$

$$k_3 = f(t_i + \frac{1}{2}h, C_i + \frac{1}{2}k_2h), \tag{12}$$

$$k_4 = f(t_i + h, C_i + k_3h), \tag{13}$$

from Eq.(2), we get the classical fourth-order RK method

$$\frac{dC}{dt} = f(t_i, C_i), \tag{14}$$

$$f(t_i, C_i) = \frac{1}{V}(n(t)pC_a - Q_{out}C_i). \tag{15}$$

B. Adaptive Runge-Kutta method

This technique uses a Runge-Kutta method with local truncation error of order five. The Adaptive Runge-Kutta method is expressed as, [17],

$$\tilde{C}_{i+1} = C_i + \frac{16}{135}k_1 + \frac{6656}{12825}k_3 + \frac{28561}{56430}k_4 - \frac{9}{50}k_5 + \frac{2}{55}k_6, \tag{16}$$

to calculate the local error in a four-order Runge-Kutta technique given by

$$C_{i+1} = C_i + \frac{25}{216}k_1 + \frac{1408}{2565}k_3 + \frac{2197}{4140}k_4 - \frac{1}{5}k_5, \tag{17}$$

where the coefficient equations are

$$C \cong C_i, \tag{18}$$

$$k_1 = hf(t_i, C_i), \tag{19}$$

$$k_2 = hf(t_i + \frac{h}{4}, C_i + \frac{1}{4}k_1), \tag{20}$$

$$k_3 = hf(t_i + \frac{3h}{8}, C_i + \frac{3}{32}k_1 + \frac{9}{32}k_2), \tag{21}$$

$$k_4 = hf(t_i + \frac{12h}{13}, C_i + \frac{1932}{2197}k_1 - \frac{7200}{2197}k_2 + \frac{7296}{2197}k_3), \tag{22}$$

$$k_5 = hf(t_i + h, C_i + \frac{439}{216}k_1 - 8k_2 + \frac{3680}{513}k_3 - \frac{845}{4104}k_4), \tag{23}$$

$$k_6 = hf(t_i + \frac{h}{2}, C_i - \frac{8}{27}k_1 + 2k_2 - \frac{3544}{2565}k_3 + \frac{1859}{4104}k_4 - \frac{11}{40}k_5), \tag{24}$$

from Eq.(2), we get the Adaptive Runge-Kutta method method

$$\frac{dC}{dt} = f(t_i, C_i), \tag{25}$$

$$f(t_i, C_i) = \frac{1}{V}(n(t)pC_a - Q_{out}C_i). \tag{26}$$

C. Lagrange interpolating polynomial

Suppose we formulate a linear interpolating polynomial as the weighted average of the two values that we are connecting by a straight line [18]:

$$f(x) = L_1 f(x_1) + L_2 f(x_2), \tag{27}$$

where the L_1 and L_2 are the weighting coefficients. It is logical that the first weighting coefficient is the straight line that is equal to 1 at x_1 and 0 at x_2:

$$L_1 = \frac{x - x_2}{x_1 - x_2}. \tag{28}$$

Similarly, the second coefficient is the straight line that is equal to 1 at x_2 and 0 at x_1:

$$L_2 = \frac{x - x_1}{x_2 - x_1}. \tag{29}$$

Substituting these coefficients into Eq. (27),

$$f_1(x) = \frac{x - x_2}{x_1 - x_2}f(x_1) + \frac{x - x_1}{x_2 - x_1}f(x_2), \tag{30}$$

where the nomernclature $f_1(x)$ designates that this is a first-order polynomial. Eq. (30) is referred to as the linear lagrange interpolating polynomial. Such a second-order Lagrange interpolating polynomial can be written as

$$f_2(x) = \frac{(x - x_2)(x - x_3)}{(x_1 - x_2)(x_1 - x_3)}f(x_1) + \frac{(x - x_1)(x - x_3)}{(x_2 - x_1)(x_2 - x_3)}f(x_2) + \frac{(x - x_1)(x - x_2)}{(x_3 - x_1)(x_3 - x_2)}f(x_3). \tag{31}$$

Notice how the first term is equal to $f(x_1)$ at x_1 and is equal to zero at x_2 and x_3. The other terms work in a similar fashion. Both the first-order and second-order versions as well as higher-order Lagrange polynomials can be represented concisely as,

$$f_{n-1}(x) = \sum_{i=1}^{n} L_i(x)f(x_i). \tag{32}$$

D. Cubic splines interpolation

As the preceding example demonstrates, a spline defined on an interval that is divided into n subintervals will require determining $4n$ constants. To generate the cubic spline interpolation for a given function f, the definition's conditions are applied to cubic polynomials [17],

$$S_j(x) = a_j + b_j(x - x_j) + c_j(x - x_j)^2 + d_j(x - x_j)^3, \tag{33}$$

for each $j = 0, 1, \ldots, n-1$. Since $S_j(x_j) = a_j = f(x_j)$, condition (c) can be applied to obtain,

$$a_{j+1} = S_{j+1}(x_{j+1}) = a_j + b_j(x_{j+1} - x_j) + c_j(x_{j+1} - x_j)^2 + d_j(x_{j+1} - x_j), \tag{34}$$

for $j = 0, 1, \ldots, n-2$.

As the terms $x_{j+1} - x_j$ appear several times in this progression, it is more comfortable to utilize the simplified notation.

$$h_j = x_{j+1} + x_j,$$

for each $j = 0, 1, \ldots, n-1$. If we also define $a_n = f(x_n)$, then the equation

$$a_{j+1} = a_j + b_j h_j + c_j h_j^2 + d_j h_j^3, \tag{35}$$

holds for each $j = 0, 1, \ldots, n-1$. Similarly, define $b_n = S'(x_n)$ and observe that

$$S'_j(x) = b_j + 2c_j(x - x_j) + 3d_j(x - x_j)^2.$$

Implies $S'_j(x) = b_j$, for each $j = 0, 1, \ldots, n-1$. Using condition (d), we get

$$b_{j+1} = b_j + 2c_j h_j + 3d_j h_j^2, \tag{36}$$

for each $j = 0, 1, \ldots, n-1$. The additional connection here between coefficients of S_j is derived by defining $c_n = S''(x_n)/2$ and applying condition (e). Then, for each $j = 0, 1, \ldots, n-1$,

$$c_{j+1} = c_j + 3d_j h_j. \tag{37}$$

Solving for d_j in Eq.(37) and substituting this value into Eqs.(35) and (36) gives, for each $j = 0, 1, \ldots, n-1$, the new equations

$$a_{j+1} = a_j + b_j h_j + \frac{h_j^2}{3}(2c_j + c_{j+1}), \tag{38}$$

and

$$b_{j+1} = b_j + h_j(c_j + c_{j+1}). \tag{39}$$

The concluding coefficient relation is achieved by first calculating the relevant equation in the formula of equation (38), for b_j,

$$b_{j+1} = \frac{1}{h_j}(a_{j+1} - a_j) - \frac{h_j}{3}(2c_j + c_{j+1}), \tag{40}$$

and then, with a decrease in the index, for b_{j-1}. This gives

$$b_{j-1} = \frac{1}{h_{j-1}}(a_j - a_{j-1}) - \frac{h_{j-1}}{3}(2c_{j-1} + c_j).$$

Substituting these values into the equation derived from Eq.(39), with the index reduced by one, gives the linear system of equations,

$$h_{j-1}c_{j-1} + 2(h_{j-1} + h_j)c_j + h_j c_{j+1} = \frac{3}{h_j}(a_{j+1} - a_j) - \frac{3}{h_{j-1}}(a_j - a_{j-1}) - \frac{3}{h_{j-1}}(a_j - a_{j-1}), \tag{41}$$

for each $j = 0, 1, \ldots, n-1$.

This system involves only the $\{c_j\}_{j=0}^{n}$ as unknowns. The values of $\{h_j\}_{j=0}^{n-1}$ and $\{a_j\}_{j=0}^{n}$ are given, respectively, by the spacing of the nodes $\{x_j\}_{j=0}^{n}$ and the values of f at the nodes. So once the values of $\{c_j\}_{j=0}^{n}$ are determined, it is a straightforward affair to find the reminder of the constant $\{b_j\}_{j=0}^{n-1}$ from Eq.(40) and $\{d_j\}_{j=0}^{n-1}$ from Eq.(37). Then we can construct the cubic polynomials $\{S_j(x)\}_{j=0}^{n-1}$.

IV. Numerical Experiments and Results

Assuming that the respiration rate assumed by $p = 0.12$ (L/s) and a fraction of the Covid-19 concentration contained inbreathed air $C_a = 0.04$. By employing the classical fourth-order Runge-Kutta method Eqs.8-15 and the adaptive fourth-order Runge-Kutta method Eqs.16-26.

The number of people in the room is represented using the Lagrange interpolating polynomial and the cubic splines interpolation since the number of people who stay in the room varies over time.

A. Simulation 1: an ideal carbon dioxide concentration measurement.

Table I, lists the model's physical parameters. $C_0 = 0.01$ is the ambient carbon dioxide concentration (ppm). The analytical solution for this case can be obtained by [7] such as,

$$C(t) = C_E + \frac{npC_a}{Q}[1 - e^{-Qt/V}]. \tag{42}$$

Table II presents the maximum error of the fourth-order Runge-Kutta solution and the adaptive fourth-order Runge-Kutta solution with the analytical solution. As seen in Figure 2, the adaptive fourth-order Runge-Kutta solution and the fourth-order Runge-Kutta solution are compared to the analytical solution.

TABLE I
PHYSICAL PARAMETERS.

$n(t)$	C_E	V	Q
50	0.004	75	8

TABLE II
THE MAXIMUM ERROR OF THE RK4 SOLUTION AND THE ADRK4 SOLUTION WITH THE ANALYTICAL SOLUTION.

$\triangle t$	Maximum error RK4	Maximum error ADRK4
0.100	9.6097×10^{-13}	1.1102×10^{-15}
0.050	5.9789×10^{-14}	1.3184×10^{-16}
0.025	3.7192×10^{-15}	1.3878×10^{-16}

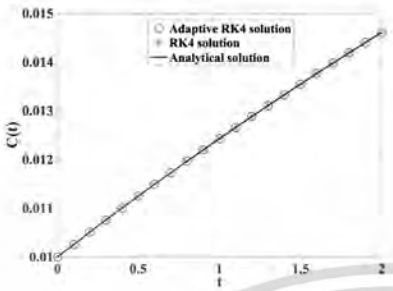

Fig. 2. The approximated air exhaled indoor concentration in a room $T = 180$.

B. Simulation 2 : The concentration measurement of exhaled air with $n(t)$ is function.

The parameters are assumed in Table III. A number of people are assumed by $n(t) = 45 + 5\sin(\pi t)$ is illustrated in Figure 3. Figure 4 shows the approximated solution.

TABLE III
PARAMETERS

C_E	V	Q_{out}	C_0
0.004	75	4	0.01

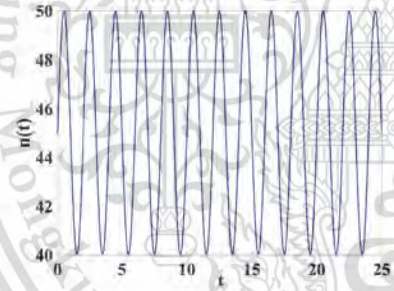

Fig. 3. A number of people in a room $0 \leq t \leq 25$.

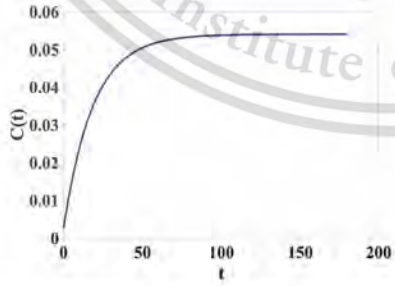

Fig. 4. The approximated air exhaled indoor concentration in a room with $n(t)$ is function $\triangle t = 0.025$ $T = 180$.

C. Simulation 3 : The concentration measurement of exhaled air with cubic splines interpolation of function $n(t)$.

The parameters are assumed in Table IV. A number of people are assumed by $n(t) = 45 + 5\sin(\pi t)$. As seen in Figure 5, the cubic spline interpolation is compared to the function of $n(t)$. Figure 6 shows the approximated solution.

TABLE IV
PARAMETER

C_E	V	Q_{out}	C_0
0.004	75	4	0.01

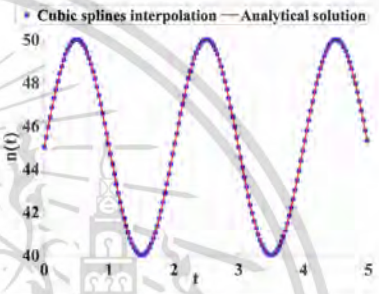

Fig. 5. The cubic splines interpolation is compared to the function of $n(t)$

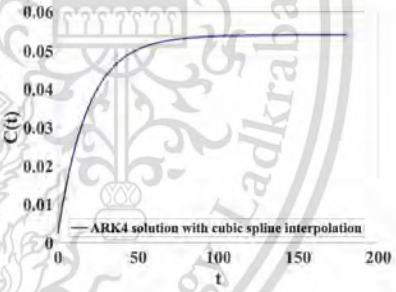

Fig. 6. The approximated air exhaled indoor concentration in a room with cubic splines interpolation of function $n(t)$ $\triangle t = 0.025$ $T = 180$.

D. Simulation 4 : The concentration measurement of exhaled air with lagrange interpolation of function $n(t)$.

The parameters are assumed in Table V. A number of people are assumed by $n(t) = 45 + 5\sin(\pi t)$. As seen in Figure 7, the lagrange interpolation is compared to the function of $n(t)$. Figure 8 shows the approximated solution.

TABLE V
PARAMETER

C_E	V	Q_{out}	C_0
0.004	75	4	0.01

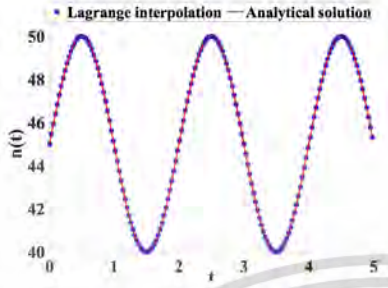

Fig. 7. The lagrange interpolation is compared to the function of $n(t)$

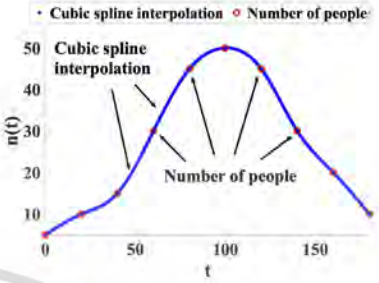

Fig. 9. The cubic spline interpolation is compared to the number of people

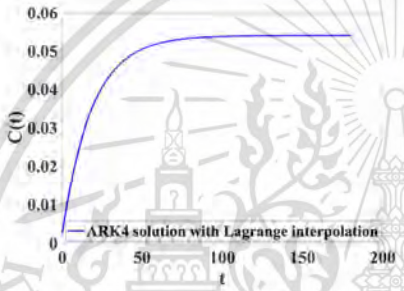

Fig. 8. The approximated air exhaled indoor concentration in a room with lagrange interpolation of function $n(t)$ $\triangle t = 0.025$ $T = 180$.

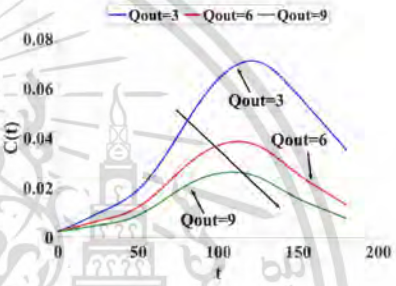

Fig. 10. The approximated air exhaled indoor concentration in a room with cubic spline interpolation $\triangle t = 0.025$ $T = 180$.

TABLE VI
THE ROOT MEAN SQUARE ERROR OF THE CUBIC SPLINES INTERPOLATION AND THE LAGRANGE INTERPOLATION ARE COMPARED TO THE FUNCTION OF $n(t)$

RMSE of the lagrange polynomial	RMSE of the cubic splines
3.8748×10^{-5}	1.0157×10^{-7}

E. Simulation 5 : The risk of normal peoples who staying in a room with infectors.

The initial condition is assumed by $C_0 = 0.01$ and the environmental carbon dioxide concentration(CE) is 0.004. The size of the room is 75 (m^3) and ventilation fan levels are assumed in three cases by 0.18, 0.36, and 0.54 (m^3/min). As assumed in Table VII, the number of people changes over time.

As seen in Figure 9, the cubic splines interpolation is compared to the number of people. Figure 10 shows the approximated air exhaled indoor concentration in a room with cubic spline interpolation. Table VIII presents the approximated air exhaled indoor concentration in a room when ventilation fan levels are assumed in three cases.

TABLE VII
A NUMBER OF PEOPLE $n(t)$

t	0	20	40	60	80	100	120	140	160	180
$n(t)$	5	10	15	30	45	50	45	30	20	10

TABLE VIII
THE APPROXIMATED AIR EXHALED INDOOR CONCENTRATION IN A ROOM

t	C		
	$Q_{out} = 3$	$Q_{out} = 6$	$Q_{out} = 9$
20	0.0082	0.0058	0.0044
40	0.0145	0.0092	0.0067
60	0.0267	0.0171	0.0126
80	0.0464	0.0290	0.0209
100	0.0637	0.0371	0.0258
120	0.0711	0.0380	0.0254
140	0.0642	0.0305	0.0192
160	0.0500	0.0241	0.0128
180	0.0352	0.0131	0.0076

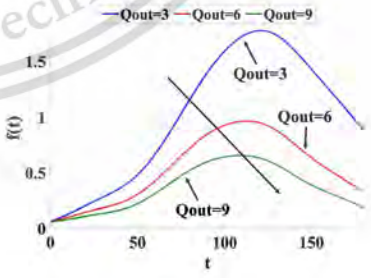

Fig. 11. The perceniage of exhaled air

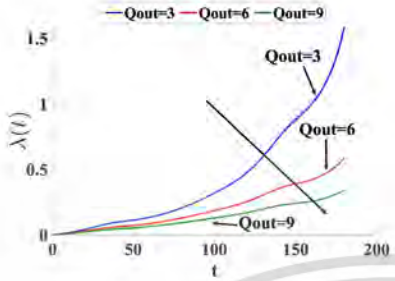

Fig. 12. The number of airborne infection particles

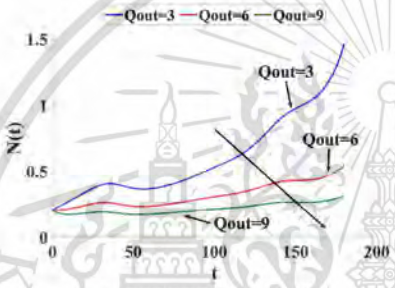

Fig. 13. The airborne infection particles concentration

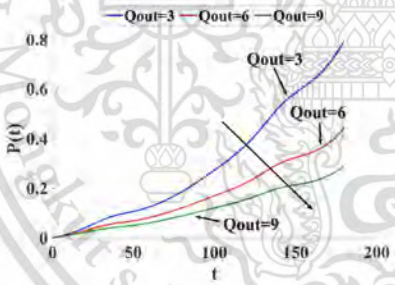

Fig. 14. The probability of airborne infector

V. Discussion

Simulation 1 compares the analytical solution with the classical fourth-order Runge-Kutta method and the Adaptive Runge-Kutta method. In Table II, the maximum error of the classical fourth-order Runge-Kutta method is more than the Adaptive Runge-Kutta method. Figure 2 shows the comparison of both approximation techniques.

Simulation 2, in reality, people were constantly entering and leaving our room, implying that $n(t)$ is a function. Figure 3 shows the number of individuals in the room is between 40 and 50. The approximated air exhaled indoor concentration in a room with $n(t)$ is function as illustrated in Figure 4.

Simulation 3, the cubic spline interpolation is used to interpolate the function $n(t)$. Figure 5 shows the comparison of the cubic spline interpolation and the exact solution. Figure 6 shows the approximated air exhaled indoor concentration in a room with cubic spline interpolation of the function $n(t)$.

Simulation 4, the Lagrange interpolation is used to interpolate the function $n(t)$. Figure 7 shows the comparison of the Lagrange interpolation and the exact solution. Figure 8 shows the approximated air exhaled indoor concentration in a room with the Lagrange interpolation of the function $n(t)$. Table VI shows the root mean square error of both interpolation techniques.

Simulation 5, the number of people as illustrated in Table VII and interpolated by the cubic spline interpolation. Figure 9 shows the comparison of the cubic spline interpolation and the number of people. Figure 10 shows the approximated air exhaled indoor concentration has reduced when outlet ventilation has increased. Figures 11-14 shows the percentage of exhaled air, the number of airborne infection particles, the airborne infection particles concentration, and the probability of airborne infector.

VI. Conclusion

This study will use a mathematical model to predict the concentration of exhaled air in a space with an outlet ventilation system and the risk of infections when healthy people remain in the same room as infected people. As a result, the actual concentration level, the number of users, and the ventilation rate all impact the exhaled air concentration and infection risk. The adaptive Runge-Kutta approach and the classic fourth-order Runge-Kutta method are all used to estimate the model solution. The number of people in the room is represented using the Lagrange interpolating polynomial and the cubic splines interpolation since the number of individuals who stay in the room varies over time. The adaptive Runge-Kutta technique with cubic splines interpolation turns out to be a good agreement solution. The proposed strategy represents the balance in the air quality management process between the number of individuals allowed to stay in the space and the performance of the air ventilation system. For the optimal outcomes, the proposed technique was capable of converting field data from a number of people using cubic splines and adaptive RK methods. The model can also be utilized as a part of an internet of things (IoT) system to develop new approaches to controlling infection-free zones. Due to the proposed numerical enhancement of the adaptive Runge-Kutta technique with cubic spline interpolation, we show that the suggested strategy is effective in real-world scenarios.

References

[1] C. M. Liao, C. F. Chang, and H. M. Liang, "A probabilistic transmission dynamic model to assess indoor airborne infection risks," *Risk Analysis: An International Journal*, vol. 25, no. 5, pp. 1097–1107, 2005.

[2] H. Furuya, "Risk of transmission of airborne infection during train commute based on mathematical model," *Environmental health and preventive medicine*, vol. 12, no. 2, pp. 78–83, 2007.

[3] H. Qian, Y. Li, W. H. Seto, P. Ching, W. H.Ching, and H. Q. Sun, "Natural ventilation for reducing airborne infection in hospitals," *Building and Environment*, vol. 45, no. 3, pp. 559–565, 2010.

[4] J. Shen, M. Kong, B. Dong, M. J. Birnkrant, and J. Zhang, "A systematic approach to estimating the effectiveness of multi-scale iaq strategies for reducing the risk of airborne infection of sars-cov-2," *Building and environment*, vol. 200, p. 107926, 2021.

[5] E. T. Richardson, C. D. Morrow, D. B. Kalil, and L. G. Bekker, "Shared air: a renewed focus on ventilation for the prevention of tuberculosis transmission." *PloS One 9*, no. 5, p. e96334, 2014.
[6] W. F. Well, "Airborne contagion and air hygiene. an ecological study of droplet infections," 1995.
[7] M. Chacha, M. Nicola, and W. Robin, "Modelling the risk of airborne infectious disease using exhaled air." *Journal of Theoretical Biology*, no. 372, pp. 100–106, 2015.
[8] K. Suebyat, P. Oyjinda, S. A. Konglok, and N. Pochai, "A mathematical model for the risk analysis of airborne infectious disease in an outpatient room with personal classification factor," *Engineering Letters*, vol. 28, no. 4, pp1331-1337, 2020.
[9] T. Mkhatshwa and A. Mummert, "Modeling super-spreading events for infectious diseases: case study sars," *IAENG International Journal of Applied Mathematics*, vol. 41, no. 2, pp82-88, 2010.
[10] N. Jiang, F. Fu, H. Zuo, X. Zheng, and Q. Zheng, "A municipal pm2.5 forecasting method based on random forest and wrf model," *Engineering Letters*, vol. 28, no. 2, pp312-321, 2020.
[11] S. J. Emmerich and A. K. Persily, "State-of-the-art review of carbon dioxide bemand controlled ventilation technology an application." *NISTIR 6729*, 2001.
[12] A. K. Persily, "Evaluating building iaq and ventilation with indoor carbon dioxide." *Trans. Am. Soc. Heat. Refrig. Air. Cond. Eng.*, no. 103, pp. 193–204, 1997.
[13] M. Lygizos, S. V. Shenoi, B. P. Brooks, A. Bhushan, J. C. Brust, D. Zeltenman, and G. H. Friedland, "Natural ventilation reduces high tb transmission risk in traditional homes in rural kwazulu-natal," *South Africa. BMC Infect. Dis.*, vol. 13, no. 1, p. 300, 2013.
[14] C. B. Beggs, C. Noakes, P. A. Sleigh, L. A. Fletcher, and K. Siddiqi, "the transmission of tuberculosis in confined spaces: an analytical review of alternative epidemiological models." *Int. J. Tuberc. Lung Dis*, vol. 7, no. 11, pp. 1015–1026, 2003.
[15] G. N. S. To and C. Y. H. Chao, "Review and comparison between the wells-riley and dose-response approaches to risk assessment of infections respiratory diseases." *Indoor Air*, vol. 20, no. 1, pp. 2–16, 2010.
[16] S. N. Rudnick and D. K. Milton, "Rick of indoor airborne infection transmission estimated from carbon dioxide concentration." *Indoor Air*, vol. 13, no. 3, pp. 237–245, 2003.
[17] R. Burden and J. Faires, *Numerical Analysis*, nine ed. Richard Strtton.
[18] S. C. Chapra, *Applied Numerical Methods with MATLAB for Engineers and Scientists*, 3rd ed. McGraw Hill.

N. Pochai is a researcher of Centre of Excellence in Mathematics, MHESI, Bangkok 10400, Thailand.

W. Timpitak is an assistant researcher of Centre of Excellence in Mathematics, MHESI, Bangkok 10400, Thailand.

Author Biography

Name	Mr. Wasu Timpitak
Date of Birth	27 June 1995
Address	9, Samut Songkhram Province, Amphawa District, 75110
Education	2016 Bachelor of Science in Applied Mathematics GPA 3.29
	Kasetsart University Sriracha Campus
	2019 Master of Science in Applied Mathematics GPA 3.79
	King Mongkut's Institute of Technology Ladkrabang
	2022 Doctoral of Science in Applied Mathematics GPA 3.8x
	King Mongkut's Institute of Technology Ladkrabang
Scholarship(s)	Assistant Researcher by Centre of Excellence
	in Mathematics(CEM) Mahidol university.

Academic Publication(s)

Wasu Timpitak and Nopparat Pochai, "A Numerical Model of Carbon Dioxide Concentration Measurement in a room with an Opened Ventilation System", Environment and Ecology Research, Vol.9, issue 3, pp. 107-113, 2021.

Wasu Timpitak and Nopparat Pochai, "A Mathematical Model of Risk Assessment on Airborne Infection in a Room with an Outlet Ventilation System." Engineering Letters, Vol.30, issue 2, pp898-903, 2022.

Wasu Timpitak and Nopparat Pochai, "A Risk Assessment Model for Airborne Infection in a Ventilated Room using the Adaptive Runge-Kutta Method with Cubic Spline Interpolation." IAENG International Journal of Applied Mathematics, Vol.52, issue 4, pp791-798, 2022.